[American Journal of Science, Vol. 318, June, 2018, P. 684–725, DOI 10.2475/06.2018.03]

DETRITAL ZIRCON GEOCHRONOLOGY OF THE FREDERICTON TROUGH, NEW BRUNSWICK, CANADA: CONSTRAINTS ON THE SILURIAN CLOSURE OF REMNANT IAPETUS OCEAN

ROBERT J. DOKKEN*, JOHN W.F. WALDRON*,†, and S. ANDREW DUFRANE*

ABSTRACT. The Fredericton Trough in the Appalachians of southwestern New Brunswick is filled by the Silurian Kingsclear Group, consisting mainly of turbidites, deposited during convergence of Laurentia with components of the peri-Gondwanan domain Ganderia. Its tectonic setting has been interpreted as a successor basin, trench, foredeep or foreland basin. We present new detrital zircon U-Pb data from four formations of the Kingsclear Group, collected north and south of the Fredericton Fault, which bisects the trough. South of the Fredericton Fault, detrital zircon ages from an early Silurian (Llandovery) unit show a late Neoproterozoic peak, typical of peri-Gondwanan provenance. Detrital zircons from a younger Silurian unit (Wenlock - Ludlow, intruded by the Pocomoonshine pluton, 422.7 ± 3 Ma) display a distinctive asymmetric peak at ~1.0 Ga with a tail of older Proterozoic zircons, suggesting Laurentian provenance. North of the Fredericton Fault, a Llandovery sample also shows a signature consistent with Laurentian sources. In a mid-Silurian (Wenlock) unit zircon peaks indicate mixed Laurentian and peri-Gondwanan sources, consistent with exhumation of the Miramichi terrane to the north. The absence of Laurentian material in Llandovery strata south of the fault, contrasted with a strong Laurentian signature in rocks to the north, suggests that a remnant of the Iapetus Ocean, in which turbidites of the Kingsclear Group were deposited, persisted until at least the mid-Silurian. The timing of its closure is constrained by the arrival of Laurentian detritus south of the Fredericton Fault before 422.7 ± 3 Ma, and probably by the mid-Wenlock.

Keywords: Iapetus, detrital zircon, Appalachian, Laurentia, Ganderia, Fredericton Trough, geochronology, provenance, Silurian, Salinic, New Brunswick, suture

INTRODUCTION

Sedimentary basins within orogens carry a sedimentary record of tectonic activity that can constrain tectonic models. For example, terrane accretion at a convergent plate boundary is typically accompanied by an influx of sediment from the upper plate onto the lower plate. Therefore, in convergent tectonic settings, analyzing the provenance of selected sedimentary rocks can constrain the timing of terrane juxtaposition (for example, Phillips and others, 2003; Waldron and others, 2008, 2012, 2014a; Pothier and others, 2015).

The Appalachian orogen of eastern Canada records a complex history of orogenesis, resulting from the convergence of Gondwanan elements with Laurentia, the ancestral core of North America, during the closure of the Iapetus Ocean. Previous work has divided the orogen into distinct lithotectonic domains based on their Laurentian or Gondwanan origin (fig. 1; Williams, 1979; Hibbard and others, 2006; Hibbard and others, 2007). Ganderia (van Staal and others, 1998; Hibbard and others, 2006, 2007; Pollock and others, 2012) is a peri-Gondwanan microcontinental domain, which probably rifted from the margin of Amazonia (van Staal and others, 1996, 1998) in the mid-Cambrian (van Staal and others, 2012). Avalonia (Kerr and others, 1995; Landing, 1996; O'Brien and others, 1996; van Staal and others, 1998; Hibbard and others, 2007; Pollock and others, 2012) is a peri-Gondwanan domain that probably separated from West Africa or Amazonia (van Staal and others, 1996; McNamara and

* Department of Earth and Atmospheric Sciences, University of Alberta, Edmonton, Alberta, T6G 2E3, Canada
† Corresponding author: john.waldron@ualberta.ca

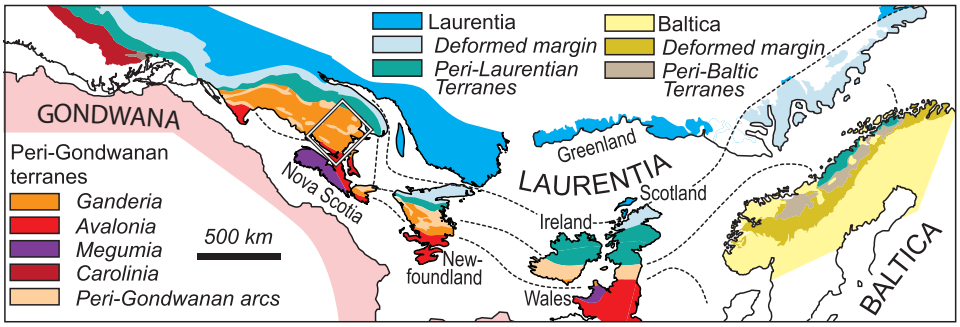

Fig. 1. Lithotectonic divisions of the Appalachian-Caledonide orogen. Pangean (pre-Mesozoic) reconstruction after Waldron and others (2014b) and references therein. Box encloses figure 2. Lithotectonic divisions after van Staal and others (1998) and Hibbard and others (2006, 2007).

others, 2001; Murphy and others, 2002) in the Early Ordovician (Prigmore and others, 1997; van Staal and others, 1998; Murphy and others, 2004b) and was accreted to the southern margin of Ganderia. Multiple positions and timings, between Early Ordovician and Early Devonian, have been proposed for sutures associated with Iapetus Ocean closure between Laurentia, Ganderia and Avalonia (for example, McKerrow and Ziegler, 1971; McKerrow, 1982; Bluck and others, 1992; van Staal and others, 1998; Macdonald and others, 2014). In this paper, we use detrital zircon geochronology to provide new evidence for the timing of amalgamation between Laurentia and peri-Gondwanan terranes in New Brunswick during early Paleozoic orogenesis. The results show that the Fredericton Trough, in southern New Brunswick, conceals a remnant of the Iapetus Ocean that closed during the Silurian, and that Ganderia was accreted to Laurentia in more than one stage.

GEOLOGIC SETTING

Tectonic Overview

Laurentia developed during the late Neoproterozoic break-up of Rodinia (Li and others, 2008). The Iapetus Ocean opened between Laurentia, Baltica, and Amazonia by *ca.* 570 to 550 Ma (Williams and Hiscott, 1987; Cawood and others, 2001; timescale of Peng and others, 2012). Ganderia separated from Gondwana by about 505 Ma (White and others, 1994; Schulz and others, 2008; van Staal and others, 2009, 2012), though the mechanism of separation is uncertain; van Staal and others (2012) propose back-arc basin opening, whereas Waldron and others (2014b) propose oblique separation. Ganderia underwent a complex history of arc formation and rifting before and during its accretion to Laurentia (van Staal and others, 2009). Components of Ganderia (see below) collided with Laurentia beginning in the Early Ordovician in New England (Macdonald and others, 2014), and Late Ordovician in Newfoundland (van Staal and others, 2009). Silurian accretion of Ganderian material has been interpreted as the cause of Salinic orogenesis (Dunning and others, 1990; van Staal and others, 2008, 2009), defined by multiple diachronous unconformities in New Brunswick (van Staal and de Roo, 1995; Fyffe and others, 2011; Wilson and others, 2015) some of which continue into adjacent New England (for example, Wilson and others, 2015; Bradley and O'Sullivan, 2017). Avalonia separated from Gondwana by the Early Ordovician (Nance and others, 2002) and is interpreted to have collided with Laurentia during late Silurian to mid-Devonian Acadian orogenesis (van Staal and others, 2009).

In New Brunswick, Ganderia is represented by several terranes (fig. 2; Fyffe and others, 2011). North of the Fredericton Trough these include the Popelogan and Miramichi terranes (fig. 2). The Popelogan terrane (Wilson, 2000, 2003; van Staal and others, 2016) is correlated with the Victoria Arc of Newfoundland and the Ammonoosuc Arc exposed in the Bronson Hill belt in New England (van Staal and others, 1998). It is interpreted to have been accreted to Laurentia during the Late Ordovician (van Staal and others, 2009). Volcanic and sedimentary rocks of the Miramichi terrane characterize the Brunswick subduction complex (van Staal, 1994; van Staal and others, 2008), recording the accretion of Ganderian microcontinental material, accompanied by deformation and high-pressure/low-temperature metamorphism (van Staal and others, 2008), to Laurentia from the Late Ordovician to early Silurian.

The Annidale and New River terranes (fig. 2) include rocks similar to the Miramichi terrane (Johnson and McLeod, 1996; Johnson and others, 2009; Fyffe and others, 2011; Johnson and others, 2012), but located south of the Fredericton Trough. Along strike to the southwest, the St. Croix terrane is characterized by the Cambrian to Upper Ordovician Cookson Group (Ludman, 1987; Fyffe and Riva, 1990; Ludman, 1991), interpreted by Fyffe and others (2011) to have been deposited on a Ganderian passive margin.

The Fredericton Trough obscures the contact between the Miramichi terrane to the north and the St. Croix terrane to the south (fig. 2); it is filled by the Silurian Kingsclear Group, consisting mainly of turbiditic sandstone, siltstone, and shale, which sit unconformably upon the Cookson Group of the St. Croix terrane along the southern boundary of the trough (Fyffe and others, 2011; Reusch and van Staal, 2012). The trough is divided by the northeast-striking Fredericton Fault (Park and Whitehead, 2003). To the north of the fault, the Kingsclear Group is in contact with rocks of the Miramichi terrane along the Bamford Brook - Hainesville Fault; its basement is unexposed. The trough was interpreted as the floor of the "Proto-Atlantic" or Iapetus Ocean by McKerrow and Ziegler (1971; see also McKerrow, 1982) but reinterpreted by Williams (1979) as a successor basin. More recent interpretations have suggested it is a marine foredeep or foreland basin (van Staal and others, 1990; van Staal and de Roo, 1995; van Staal and others 1998) formed by tectonic loading of the Brunswick subduction complex upon the subducting Ganderian margin during Salinic orogenesis (Fyffe and others, 2011). The clastic sedimentary fill of the Fredericton Trough contrasts dramatically with Silurian volcanic successions that characterize the Mascarene Basin and the Kingston belt farther south in New Brunswick.

To the south of all these Silurian basins, the Brookville terrane (fig. 2) (Barr and White, 1996; White and Barr, 1996; Barr and others, 2003; Fyffe and others, 2011) has similarities with the New River terrane (Johnson and McLeod, 1996), allowing it to be assigned to Ganderia (Fyffe and others, 2009, 2011), though some previous workers (for example, Williams, 1979) assigned the Brookville Terrane to Avalonia. The Caledonia terrane (fig. 2) includes Ediacaran tuffaceous rock, comagmatic plutons and a Cambrian to Early Ordovician platformal sedimentary succession consistent with Avalonia elsewhere in the northern Appalachians (Barr and White, 1996; Barr and others, 2003; Fyffe and others, 2011).

Interpretations of the Ganderian domain variously regard it as a coherent microcontinent or a domain of many distinct slivers of lithosphere (Waldron and others, 2014a, 2014b; Pothier and others, 2015). Whereas the timing of accretion of the Popelogan and Miramichi terranes of Ganderia to the Laurentian margin has been relatively well constrained (for example, van Staal, 1994; van Staal and others, 1998, 2008, 2016), the accretion of southern Ganderian components, particularly the St. Croix terrane (and its assumed New River basement) is less well known. Central to these issues is the timing of closure of the Iapetus Ocean. In the earliest tectonic

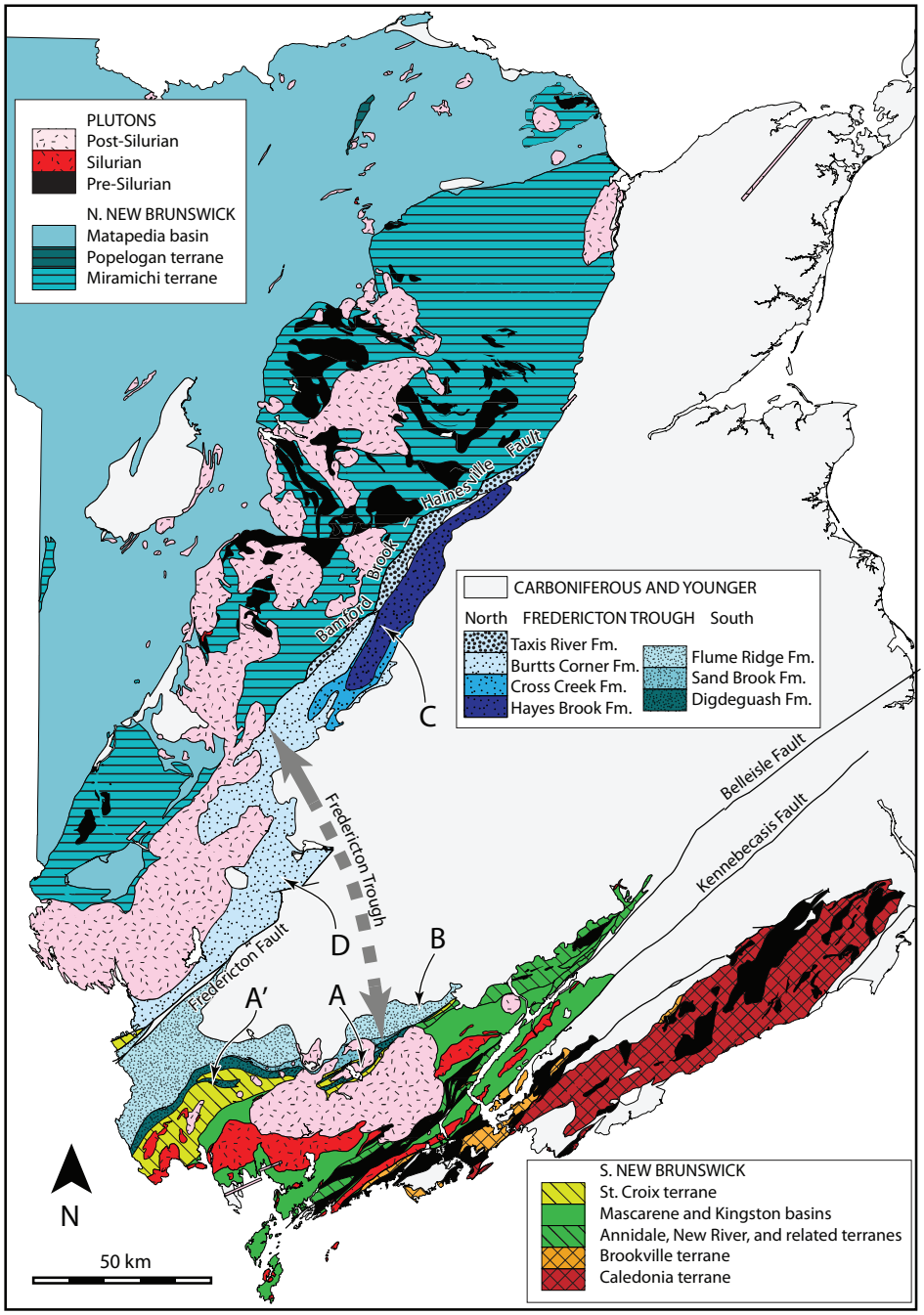

Fig. 2. New Brunswick terranes and cover successions. Map units after Smith (2005) and Smith and Fyffe (2006); see also Fyffe and others (2011). Locations reported in this paper are shown. A: Digdeguash Formation sample; A': Digdeguash Formation type section. B: Flume Ridge Formation sample. C: Hayes Brook Formation sample. D: Burtts Corner Formation sample.

models (for example, McKerrow and Ziegler, 1971; McKerrow, 1982) the Fredericton Trough was regarded as marking a Silurian Iapetus suture correlative with that identified in the British Isles (Phillips and others, 1976; Leggett and others, 1983; Bluck and others, 1992). However, Williams (1979) interpreted Iapetus closure in the Appalachians as Middle Ordovician; Late Ordovician and Silurian rocks including the Fredericton Trough were regarded as successor basins deposited across the accreted terranes. Later work (for example, van Staal and others, 1998) in New Brunswick demonstrated the peri-Gondwanan affinities of the Popelogan and Miramichi terranes, suggesting that the Iapetus Ocean closed in the Late Ordovician with the accretion of the Ganderian Popelogan-Victoria arc to Laurentia (figs. 1 and 2; van Staal and others, 1998). However, prior to this collision, Early Ordovician separation of this arc from the remainder of Ganderia had opened a wide Tetagouche-Exploits backarc basin (van Staal and others, 2009, 2012); this basin closed over the Late Ordovician to mid-Silurian (Williams and others, 1993; van Staal and others, 2009; Reusch and van Staal, 2012), ending with the accretion of the trailing Gander margin (including the St. Croix terrane and other southern components – *sensu* Reusch and van Staal, 2012), in the terminal event of Salinic orogenesis. In this model, the Fredericton Trough is interpreted as a marine foredeep basin built upon a Ganderian microcontinent and filled during the closure of the Tetagouche-Exploits backarc basin. In the remainder of this paper we examine the provenance of sedimentary rocks in the Fredericton Trough to determine when a sedimentary connection was established across the trough and to shed light on the separation and collision of Ganderian fragments as remnants of the Iapetus Ocean closed.

Stratigraphy

The Fredericton Trough (fig. 2) is filled by the Silurian Kingsclear Group (fig. 3). At its southern margin, it sits unconformably upon rocks of the Late Ordovician Kendall Mountain Formation, belonging to the Cookson Group of the St. Croix terrane. The Kendall Mountain Formation bears Sandbian (*ca.* 455–453 Ma: timescale of Cooper and Sadler, 2012) graptolites of the *Climacograptus wilsoni* zone (Fyffe and Riva, 1990). To the north, the Fredericton Trough is in contact with rocks of the Miramichi terrane, separated from them by the Bamford Brook – Hainesville fault. The Fredericton Trough itself is divided by the Fredericton Fault (fig. 2), correlated with a segment of the Norumbega Fault Zone in Maine (Ludman and West, 1999; Ludman and others, 1999).

To the south of the fault, the Kingsclear Group includes the Digdeguash Formation, comprising medium-grained lithic and feldspathic wacke, quartz wacke, granule conglomerate, and gray to black shale, with commonly well-graded beds exhibiting Bouma sequences (Ruitenberg and Ludman, 1978). Fyffe and Riva (2001) recovered graptolites of the *Coronograptus cyphus* zone of the upper Rhuddanian stage (early Llandovery), corresponding to a numerical age of *ca.* 441.6 to 440.8 Ma in the timescale of Melchin and others (2012), as shown in figure 3.

The Sand Brook Formation conformably overlies the Digdeguash Formation, and pinches out to the west. It consists of green-gray feldspathic wacke interlayered with green siltstone and mudstone (Fyffe, 1991). The age of the Sand Brook Formation is constrained as late Rhuddanian to Pridoli by its stratigraphic location above the Digdeguash and below the Flume Ridge Formation.

The highest unit south of the fault, the Flume Ridge Formation, sits with apparent conformity upon both older units. It includes gray-green calcareous and argillaceous sandstone, siltstone, and shale (Ruitenberg and Ludman, 1978). The Pocomoonshine pluton intrudes the Flume Ridge Formation in Maine, and has been dated by West and others (1992) at 422.7 ± 3 Ma, near the Ludlow-Pridoli boundary (Melchin and others, 2012).

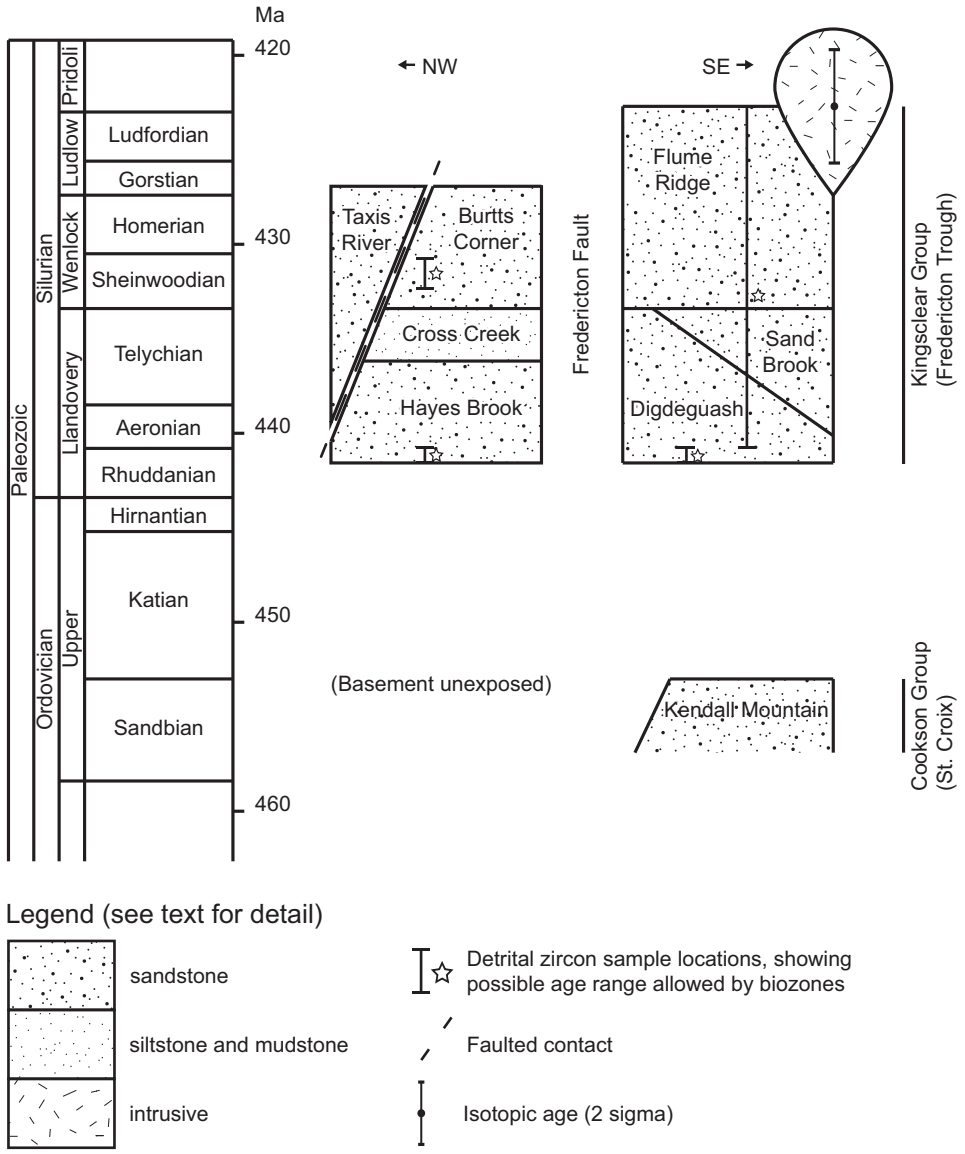

Fig. 3. Simplified stratigraphic chart for the Kingsclear Group. Timescale from Cooper and Sadler (2012) and Melchin and others (2012); Pocomoonshine pluton age from West and others (1992).

North of the Fredericton Fault, the lowest unit in the Kingsclear Group is the Hayes Brook Formation, medium to thickly bedded gray quartz wacke interlayered with thin gray-black shale (Poole, 1963). Its depositional age is constrained by upper Rhuddanian graptolites of the *Coronograptus cyphus* zone (formerly *Monograptus cyphus*; Cumming, 1960; Fyffe, 1995; Zalasiewicz and others, 2003), identical in age to those from the Digdeguash Formation to the south.

The Hayes Brook Formation is conformably overlain by green siltstone and shale of the Cross Creek Formation (Poole, 1963). Its depositional age is constrained by its

stratigraphic position between the Hayes Brook and the conformably overlying Burtts Corner Formation.

The Burtts Corner Formation includes gray lithic wacke interlayed with dark gray siltstone and shale. Beds are well-graded with Bouma sequences, and show flute casts, climbing ripples, and soft-sediment deformation structures such as flames and convolute bedding (Fyffe, 1995; Park and Whitehead, 2003). Mid-Wenlock (*ca.* 432.4–430.5 Ma: timescale of Melchin and others, 2012) to early Ludlow (*ca.* 427.4–426.9 Ma) graptolites (*Cyrtograptus linnarssoni* and *M. nilssoni* zones, now respectively the *Cyrtograptus rigidus* and *Neodiversograptus nilssoni* zones; Zalasiewicz and others, 2009) have been recovered from the Burtts Corner Formation (Fyffe, 1995).

The Taxis River Formation, comprising gray lithic wacke and shale, was previously interpreted (Poole, 1963) to rest conformably upon the Burtts Corner Formation, but recent mapping (Smith and Fyffe, 2006 and references therein) suggests faulted contacts with bounding formations; its depositional age has not been determined, and it is not further considered here.

Structure

The northeast-trending belt of rocks comprising the Fredericton Trough shows multiple stages of deformation (for example, Smith, 2005; Smith and Fyffe, 2006), and only a few studies (for example, Park and Whitehead, 2003) have examined their structural characteristics in detail. Structural characteristics of individual formations at their sampled locations are described later in this paper (see also Fyffe, 1995; Fyffe and others, 2011 and references therein). Rocks of the Fredericton Trough are interpreted by Park and Whitehead (2003) to record southeast-vergent Silurian thrusting and folding, documenting Salinic orogenesis, in which a low-angle, northwest-dipping thrust, a precursor to the Fredericton Fault, divided adjacent slices of the Kingsclear Group. Later dextral transpressive deformation may have resulted either in the steepening of this thrust (Park and Whitehead, 2003), or may have produced a new structure which reactivated or cut it. Ludman and others (1999; see also Ludman and West, 1999) have documented an extensive history of activity on the correlative Norumbega Fault Zone to the southwest; the earliest dateable activity of this system is at *ca.* 380 Ma, and at present it has been interpreted to display up to 135 km of dextral offset, although Ghanem and others (2016) have documented earlier cleavage development in the Central Maine Trough farther to the NW. Additional work in correlating the New Brunswick Fredericton Trough with equivalents in Maine is in part hindered by an increasing Acadian metamorphic overprint (Ludman and others, 1999) to the southwest, and a paucity of fossils to provide depositional age constraint (Ludman and others, 1993, 2017).

METHODS

Detrital zircon geochronology has been successfully applied in the Appalachian-Caledonide orogen to determining provenance and correlating terranes (Cawood and Nemchin, 2001; Cawood and others, 2003, 2004; Murphy and others, 2004b; Wintsch and others, 2007; Dorais and others, 2009; McWilliams and others, 2010; Dorais and others, 2012; Waldron and others, 2012; Macdonald and others, 2014; Waldron and others, 2014a). Previous work (for example, Cawood and Nemchin, 2001; Waldron and others, 2014a) has demonstrated that Laurentian provenance is marked by an asymmetric peak at 1.0 to 1.1 Ga, with a tail of zircons typically extending to *ca.* 2.0 Ga, and a scarcity of zircons in the 2.0 to 2.4 Ga range. The population at 1.0 to 1.1 Ga is attributed to the Grenville orogen, which dominates the provenance of the Laurentian margin (Cawood and Nemchin, 2001; Waldron and others, 2014a). Peri-Gondwanan zircon signatures lack this distinctive asymmetric peak, and are distinguished by one or more large late Neoproterozoic populations, in the 550 to 650 Ma range. Within this

range, peri-Gondwanan terranes of Avalonia and Ganderia may be distinguished by slightly older or younger peaks respectively (Murphy and others, 2004a; Fyffe and others, 2009; Pollock and others, 2009). Additionally, peri-Gondwanan detritus is frequently distinguished by zircon peaks from 2.0 to 2.2 Ga, often interpreted as representing derivation from the Eburnian orogen of West Africa or the Trans-Amazonian orogen of Amazonia (Pollock and others, 2007; Waldron and others, 2009, 2011, 2014a). These distinguishing characteristics enable the differentiation between sources in Laurentia and the Ganderian terranes which converged with it during Salinic orogenesis (Waldron and others, 2014a). By examining the fill of the Fredericton Trough for these distinctive detrital zircon signatures, we can determine when southern components of Ganderia were juxtaposed with Laurentia, and investigate whether they were separated by a seaway, a possible remnant of the Iapetus Ocean.

Four samples from the Kingsclear Group were chosen, where possible, from known fossil localities to constrain depositional age. Samples of ~10 kg mass were selected from the coarser-grained sandstones representative of each formation, while avoiding any obvious weathering, alteration, or mineralization. A polished thin-section was made from each sample, for optical and electron microprobe examination. Each sample was then disaggregated by crushing and milling, and dense minerals concentrated using a Wilfley table. The heavy mineral concentrate was sieved with a standard 70 size nylon mesh (approx. 210 μm) to remove remnant aggregate particles, and further processed with Frantz Isodynamic and Barrier separators (for example, Rosenblum and Brownfield, 2000) to remove magnetic minerals. A final zircon concentrate was obtained by gravity separation with methylene iodide (specific gravity of 3.32). Obvious non-zircons (for example, pyrite) were removed and the remaining portion then mounted in epoxy for LA-MC-ICP-MS (laser ablation multi-collector inductively coupled plasma mass spectrometry) U-Pb analysis. Zircons were not selected individually for analysis, to avoid bias towards easily recognizable zircon morphologies. Each zircon mount was polished to expose sections through the grains, and imaged to reveal internal structure (for example, zonation, inherited cores, altered rims) by backscattered electron and cathodoluminescence imaging utilizing a Zeiss EVO scanning electron microscope. Separated and analyzed zircon grains were classified according to their morphology, from euhedral to anhedral, as shown in tables 1, 2, 3, and 4.

Representative selections of 132 to 152 grains from each sample were analyzed at the Canadian Centre for Isotopic Microanalysis (CCIM) at the University of Alberta, using procedures modified from Simonetti and others (2005) for measuring U-Pb isotopic ratios by LA-MC-ICP-MS. Each zircon is typically represented by a single spot analysis, as restricted by physical grain size. When discrete cores and rims of different age can be distinguished, they are represented by separate analyses (for example, 001A and 001B within grain 001). Instrumentation consisted of a New Wave UP-213 laser ablation system interfaced with a Nu Plasma MC-ICP-MS, with three ion counters to measure Pb isotopes and twelve Faraday buckets measuring ^{238}U, ^{235}U, ^{205}Tl and ^{203}Tl. The laser was operated with a beam diameter of 30 microns, 4 Hz pulse frequency and fluence of ~3 J/cm^2. A He atmosphere was maintained in the ablation cell at a flow rate of 1 L/min. Output from this cell was combined with that from a standard Nu Instruments desolvating nebulizer (DSN). Unknowns from each sample were analyzed in groups of 10, with data collected statically in thirty 1 s integrations. Separating each set of analyses, on peak gas + acid blanks were measured over a duration of 30 s, and two zircon reference materials were analyzed to monitor U-Pb fractionation, reproducibility, and instrumental drift: LH94-15 (1830 ± 1 Ma; Ashton and others, 1999; Simonetti and others, 2005; Heaman, unpublished data) and GJ1-32 (606 Ma; Jackson and others, 2004; Elhlou and others, 2006; Heaman, unpublished data). Mass bias for Pb isotopes was corrected for by concurrently measuring $^{205}Tl/^{203}Tl$ from an aspirated

TABLE 1

Laser ablation U/Pb isotopic data for sample NA003A, Digdeguash Formation

Digdeguash Fm. (NA003A)	Morph.	Isotopic ratios									Ages (Ma)						disc.	Reported age	
sample name		^{206}Pb (cps)	^{204}Pb (cps)	$\frac{^{207}Pb}{^{206}Pb}$	2σ	$\frac{^{207}Pb}{^{235}U}$	2σ	$\frac{^{206}Pb}{^{238}U}$	2 σ	ρ	$\frac{^{207}Pb}{^{206}Pb}$	2 σ	$\frac{^{207}Pb}{^{235}U}$	2 σ	$\frac{^{206}Pb}{^{238}U}$	2 σ	%	(Ma)	2 σ
NA003A-001	2	152041	172	0.06127	0.00065	0.84231	0.05621	0.09970	0.00657	0.987	649	23	620	31	613	38	5.8	613	38
NA003A-002	2	63385	160	0.06189	0.00081	0.84860	0.05749	0.09944	0.00661	0.981	670	28	624	31	611	39	9.3	611	39
NA003A-003	2	80685	212	0.06147	0.00076	0.83114	0.05464	0.09806	0.00633	0.982	656	26	614	30	603	37	8.4	603	37
NA003A-004	2	61206	204	0.06202	0.00089	0.84203	0.05750	0.09847	0.00658	0.978	675	30	620	31	605	38	10.8	605	38
NA003A-005	1	148125	218	0.06118	0.00066	0.88302	0.05796	0.10468	0.00678	0.986	646	23	643	31	642	39	0.6	642	39
NA003A-006	2	27213	204	0.05834	0.00098	0.62358	0.04214	0.07752	0.00508	0.969	543	36	492	26	481	30	11.7	481	30
NA003A-007	2	328550	250	0.06264	0.00067	0.97817	0.06566	0.11326	0.00751	0.987	696	23	693	33	692	43	0.7	692	43
NA003A-008	2	49145	240	0.05824	0.00078	0.64972	0.04376	0.08091	0.00534	0.980	539	29	508	27	502	32	7.2	502	32
NA003A-009	2	71682	240	0.06194	0.00068	0.86299	0.05645	0.10105	0.00652	0.986	672	23	632	30	621	38	8.0	621	38
NA003A-010	2	234641	269	0.06206	0.00067	0.99482	0.06800	0.11625	0.00785	0.987	676	23	701	34	709	45	-5.1	709	45
NA003A-011	1	120447	250	0.06156	0.00067	0.85131	0.05710	0.10030	0.00664	0.987	659	23	625	31	616	39	6.8	616	39
NA003A-012	2	303091	284	0.06101	0.00067	0.87067	0.05913	0.10350	0.00694	0.987	640	24	636	32	635	40	0.8	635	40
NA003A-013	2	117635	240	0.06279	0.00068	0.97647	0.06816	0.11279	0.00778	0.988	701	23	692	34	689	45	1.8	689	45
NA003A-014	2	90638	275	0.05772	0.00063	0.61844	0.04072	0.07771	0.00504	0.986	519	24	489	25	482	30	7.3	482	30
NA003A-015	2	23862	231	0.06322	0.00091	0.83073	0.05444	0.09531	0.00609	0.976	716	30	614	30	587	36	18.8	587	36
NA003A-016	2	63223	237	0.06176	0.00075	0.83793	0.05675	0.09839	0.00656	0.984	666	26	618	31	605	38	9.6	605	38
NA003A-017	2	155856	247	0.06128	0.00067	0.82690	0.05460	0.09786	0.00637	0.986	649	23	612	30	602	37	7.6	602	37
NA003A-018	2	408306	235	0.09884	0.00109	3.51590	0.22963	0.25800	0.01661	0.986	1602	20	1531	50	1480	85	8.6	1602	20
NA003A-019	2	40057	218	0.06151	0.00080	0.83577	0.05584	0.09855	0.00646	0.981	657	28	617	30	606	38	8.1	606	38
NA003A-020	2	122989	469	0.05966	0.00122	0.63874	0.04429	0.07765	0.00515	0.956	591	44	502	27	482	31	19.2	482	31
NA003A-02I	2	44875	163	0.06426	0.00085	0.94358	0.06583	0.10649	0.00729	0.982	750	28	675	34	652	42	13.7	652	42
NA003A-022	3	63599	166	0.06178	0.00072	0.84645	0.05631	0.09937	0.00651	0.984	667	25	623	31	611	38	8.8	611	38
NA003A-023	2	24598	182	0.06165	0.00097	0.82667	0.05548	0.09726	0.00634	0.972	662	33	612	30	598	37	10.1	598	37
NA003A-024	3	99376	155	0.09561	0.00111	3.28920	0.21552	0.24952	0.01609	0.984	1540	22	1479	50	1436	82	7.5	1540	22
NA003A-025	2	94578	162	0.06142	0.00070	0.86444	0.05655	0.10208	0.00658	0.985	654	24	633	30	627	38	4.4	627	38
NA003A-026	2	178097	179	0.05998	0.00227	0.80632	0.06373	0.09750	0.00676	0.878	603	80	600	35	600	40	0.5	600	40
NA003A-027	2	61501	190	0.05812	0.00075	0.65003	0.04580	0.08112	0.00562	0.983	534	28	508	28	503	33	6.1	503	33
NA003A-028	2	60817	150	0.10797	0.00126	4.24516	0.28747	0.28515	0.01902	0.985	1766	21	1683	54	1617	95	9.5	1766	21
NA003A-029	2	81445	150	0.06142	0.00070	0.84802	0.05944	0.10014	0.00693	0.987	654	24	624	32	615	40	6.2	615	40
NA003A-030	2	104738	159	0.06351	0.00076	0.96798	0.06378	0.11054	0.00716	0.983	725	25	687	32	676	41	7.2	676	41
NA003A-031	2	98621	202	0.06424	0.00135	0.85763	0.05716	0.09683	0.00613	0.949	749	44	629	31	596	36	21.5	596	36
NA003A-032	1	83595	179	0.06142	0.00074	0.85603	0.05844	0.10108	0.00679	0.984	654	26	628	31	621	40	5.3	621	40
NA003A-033	1	226627	172	0.06178	0.00082	0.86638	0.05827	0.10171	0.00671	0.980	666	28	634	31	624	39	6.6	624	39
NA003A-034	2	47271	180	0.06518	0.00084	1.02469	0.06818	0.11402	0.00744	0.981	780	27	716	34	696	43	11.4	696	43
NA003A-035	2	59059	166	0.06194	0.00079	0.83831	0.05546	0.09816	0.00637	0.981	672	27	618	30	604	37	10.7	604	37

TABLE 1
(continued)

Digdeguash Fm. (NA003A)	Morph.	Isotopic ratios									Ages (Ma)						disc.	Reported age	
sample name		^{206}Pb (cps)	^{204}Pb (cps)	$\frac{^{207}Pb}{^{206}Pb}$	2σ	$\frac{^{207}Pb}{^{235}U}$	2σ	$\frac{^{206}Pb}{^{238}U}$	2 σ	ρ	$\frac{^{207}Pb}{^{206}Pb}$	2 σ	$\frac{^{207}Pb}{^{235}U}$	2 σ	$\frac{^{206}Pb}{^{238}U}$	2 σ	%	(Ma)	2 σ
NA003A-036	2	58099	134	0.05794	0.00070	0.61386	0.04075	0.07684	0.00501	0.983	528	26	486	25	477	30	9.9	477	30
NA003A-037	2	235240	175	0.06073	0.00064	0.84934	0.05632	0.10143	0.00664	0.987	630	23	624	30	623	39	1.2	623	39
NA003A-038	2	153738	203	0.06058	0.00067	0.85208	0.05625	0.10200	0.00664	0.986	625	24	626	30	626	39	-0.3	626	39
NA003A-039	2	145991	215	0.07785	0.00090	2.01546	0.13386	0.18775	0.01228	0.985	1143	23	1121	44	1109	66	3.2	1143	23
NA003A-040	2	79343	234	0.06063	0.00069	0.84164	0.05582	0.10068	0.00658	0.985	626	24	620	30	618	38	I.3	618	38
NA003A-041	2	40106	253	0.06222	0.00084	0.81859	0.05425	0.09541	0.00619	0.979	682	29	607	30	587	36	14.5	587	36
NA003A-042	2	38025	270	0.05877	0.00078	0.62977	0.04246	0.07772	0.00514	0.980	559	29	496	26	483	31	14.1	483	31
NA003A-043	2	305408	257	0.08171	0.00093	2.35999	0.15000	0.20947	0.01310	0.984	1239	22	1231	44	1226	69	1.1	1239	22
NA003A-044	2	68242	261	0.06136	0.00073	0.85690	0.05782	0.10129	0.00673	0.984	652	25	628	31	622	39	4.8	622	39
NA003A-045	2	96521	290	0.06134	0.00078	0.86584	0.05890	0.10238	0.00684	0.982	651	27	633	32	628	40	3.7	628	40
NA003A-046	2	163930	307	0.06098	0.00069	0.83558	0.05549	0.09939	0.00650	0.985	638	24	617	30	611	38	4.5	611	38
NA003A-047	2	46162	298	0.06411	0.00085	0.96817	0.06444	0.10953	0.00714	0.980	745	28	688	33	670	41	10.6	670	41
NA003A-048	2	65107	294	0.05854	0.00072	0.60520	0.04050	0.07498	0.00493	0.983	550	26	481	25	466	30	15.8	466	30
NA003A-049	2	46580	279	0.06492	0.00077	0.93058	0.06052	0.10397	0.00665	0.983	772	25	668	31	638	39	18.2	638	39
NA003A-050	2	19874	301	0.06903	0.00148	1.06212	0.07296	0.11160	0.00728	0.950	900	44	735	35	682	42	25.5	900	44
NA003A-051	2	157625	293	0.10529	0.00119	4.23078	0.28192	0.29142	0.01914	0.986	1719	21	1680	53	1649	95	4.7	1719	21
NA003A-052	2	23256	299	0.05945	0.00096	0.61741	0.04354	0.07533	0.00517	0.973	583	35	488	27	468	31	20.5	468	31
NA003A-053	2	39093	261	0.06200	0.00091	0.81540	0.05619	0.09539	0.00642	0.977	674	31	605	31	587	38	13.5	587	38
NA003A-054	2	58228	294	0.06244	0.00075	0.84968	0.05777	0.09870	0.00660	0.984	689	25	624	31	607	39	12.5	607	39
NA003A-055	1	77699	266	0.06071	0.00071	0.78857	0.05444	0.09421	0.00641	0.986	629	25	590	30	580	38	8.1	580	38
NA003A-056	2	56030	265	0.06245	0.00090	0.83062	0.05669	0.09646	0.00644	0.978	690	30	614	31	594	38	14.6	594	38
NA003A-057	2	51623	271	0.06138	0.00079	0.81356	0.05379	0.09613	0.00624	0.981	653	27	604	30	592	37	9.8	592	37
NA003A-058	2	151152	284	0.06090	0.00070	0.82253	0.05530	0.09796	0.00649	0.985	636	24	609	30	602	38	5.5	602	38
NA003A-059	2	81060	259	0.06129	0.00073	0.87312	0.05769	0.10332	0.00672	0.984	649	25	637	31	634	39	2.5	634	39
NA003A-060	2	30839	274	0.06415	0.00087	0.95298	0.06540	0.10774	0.00725	0.980	747	28	680	33	660	42	12.3	660	42
NA003A-061	2	611397	548	0.06895	0.00118	1.04132	0.06918	0.10954	0.00703	0.966	897	35	725	34	670	41	26.6	897	35
NA003A-062	3	100830	235	0.06240	0.00117	0.85759	0.05815	0.09968	0.00650	0.961	688	39	629	31	613	38	11.5	613	38
NA003A-063	2	55523	204	0.06195	0.00086	0.84769	0.05802	0.09924	0.00665	0.979	672	30	623	31	610	39	9.7	610	39
NA003A-064	2	89135	218	0.06333	0.00079	0.98990	0.06732	0.11336	0.00758	0.983	719	26	699	34	692	44	4.0	692	44
NA003A-065	2	151224	228	0.06127	0.00069	0.87458	0.05952	0.10353	0.00695	0.986	649	24	638	32	635	40	2.2	635	40
NA003A-066	2	153322	240	0.06100	0.00067	0.87286	0.05918	0.10378	0.00694	0.987	639	24	637	32	637	40	0.4	637	40
NA003A-067	2	91156	194	0.06099	0.00069	0.86636	0.05850	0.10303	0.00686	0.986	639	24	634	31	632	40	1.1	632	40
NA003A-068	2	117027	209	0.06137	0.00075	0.82412	0.06051	0.09739	0.00705	0.986	652	26	610	33	599	41	8.5	599	41
NA003A-069	2	60802	212	0.05754	0.00068	0.63805	0.04261	0.08043	0.00529	0.984	512	26	501	26	499	31	2.7	499	31
NA003A-070	2	35987	496	0.16258	0.00734	2.34008	0.18880	0.10439	0.00698	0.829	2483	74	1225	56	640	41	77.8	2483	74
NA003A-071	2	123229	255	0.06337	0.00080	0.77435	0.05660	0.08863	0.00638	0.985	721	27	582	32	547	38	25.1	547	38
NA003A-072	2	23036	186	0.06415	0.00106	0.85743	0.05881	0.09694	0.00645	0.971	747	34	629	32	596	38	21.1	596	38

TABLE 1
(continued)

Digdeguash Fm. (NA003A)	Morph.	Isotopic ratios									Ages (Ma)						disc.	Reported age	
sample name		^{206}Pb (cps)	^{204}Pb (cps)	$\frac{^{207}Pb}{^{206}Pb}$	2σ	$\frac{^{207}Pb}{^{235}U}$	2σ	$\frac{^{206}Pb}{^{238}U}$	2 σ	ρ	$\frac{^{207}Pb}{^{206}Pb}$	2 σ	$\frac{^{207}Pb}{^{235}U}$	2 σ	$\frac{^{206}Pb}{^{238}U}$	2 σ	%	(Ma)	2 σ
NA003A-073	2	81591	207	0.06157	0.00076	0.83208	0.05941	0.09802	0.00689	0.985	659	26	615	32	603	40	9.0	603	40
NA003A-074	2	46481	208	0.06132	0.00079	0.84684	0.05845	0.10016	0.00679	0.983	650	27	623	32	615	40	5.7	615	40
NA003A-075	1	145090	242	0.06124	0.00071	0.88466	0.06114	0.10478	0.00714	0.986	648	25	643	32	642	42	0.8	642	42
NA003A-076	2	679810	290	0.06071	0.00063	0.92995	0.06172	0.11110	0.00728	0.988	629	22	668	32	679	42	-8.4	679	42
NA003A-077	2	77245	268	0.06064	0.00161	0.79873	0.07367	0.09554	0.00844	0.958	626	56	596	41	588	49	6.4	588	49
NA003A-078	2	112356	250	0.06111	0.00066	0.84685	0.05626	0.10051	0.00659	0.987	643	23	623	30	617	38	4.2	617	38
NA003A-079	2	327175	317	0.06276	0.00090	0.88392	0.05869	0.10215	0.00662	0.976	700	30	643	31	627	39	11.0	627	39
NA003A-080	2	74316	247	0.06079	0.00071	0.85448	0.05805	0.10195	0.00682	0.985	632	25	627	31	626	40	1.0	626	40
NA003A-081	2	369766	256	0.06238	0.00067	1.05751	0.06872	0.12295	0.00788	0.986	687	23	733	33	748	45	-9.3	748	45
NA003A-082	2	278691	283	0.11752	0.00133	4.66815	0.34057	0.28809	0.02076	0.988	1919	20	1762	59	1632	103	16.9	1919	20
NA003A-083	2	95952	250	0.06128	0.00070	0.87315	0.05804	0.10334	0.00677	0.985	649	24	637	31	634	39	2.5	634	39
NA003A-084	2	47942	232	0.06108	0.00074	0.84678	0.05662	0.10054	0.00661	0.984	642	26	623	31	618	39	4.0	618	39
NA003A-085	2	38660	223	0.06124	0.00081	0.84915	0.05725	0.10057	0.00665	0.981	648	28	624	31	618	39	4.8	618	39
NA003A-086	2	188426	236	0.06081	0.00066	0.84321	0.05493	0.10057	0.00646	0.986	633	23	621	30	618	38	2.5	618	38
NA003A-087	3	180309	244	0.10797	0.00122	4.61577	0.30031	0.31005	0.01986	0.985	1765	21	1752	53	1741	97	1.6	1765	21
NA003A-088	1	198763	262	0.06034	0.00063	0.84693	0.05540	0.10180	0.00657	0.987	616	22	623	30	625	38	-1.5	625	38
NA003A-089	2	14432	256	0.06239	0.00118	0.90972	0.06282	0.10575	0.00702	0.962	688	40	657	33	648	41	6.0	648	41
NA003A-090	2	86179	255	0.06490	0.00123	0.88854	0.05986	0.09930	0.00642	0.960	771	39	646	32	610	38	21.8	610	38
NA003A-091	2	20425	325	0.05936	0.00093	0.63582	0.04339	0.07768	0.00516	0.973	580	34	500	27	482	31	17.5	482	31
NA003A-092	1	116516	278	0.06159	0.00074	0.87273	0.05885	0.10278	0.00682	0.984	660	26	637	31	631	40	4.6	631	40
NA003A-093	2	93148	325	0.06787	0.00111	1.00936	0.06663	0.10786	0.00690	0.969	865	34	709	33	660	40	24.8	865	34
NA003A-094	2	49368	259	0.05827	0.00077	0.62801	0.04250	0.07817	0.00519	0.981	540	29	495	26	485	31	10.5	485	31
NA003A-095	1	37083	261	0.06569	0.00103	0.85981	0.05573	0.09493	0.00597	0.970	797	32	630	30	585	35	27.8	585	35
NA003A-096	2	191240	257	0.08224	0.00092	2.27265	0.14728	0.20043	0.01279	0.985	1251	22	1204	45	1178	68	6.4	1251	22
NA003A-097	2	145828	238	0.08415	0.00143	1.83455	0.12841	0.15812	0.01074	0.970	1296	33	1058	45	946	59	29.0	1296	33
NA003A-098	2	92300	252	0.06323	0.00072	0.97838	0.06437	0.11223	0.00727	0.985	716	24	693	33	686	42	4.4	686	42
NA003A-099	2	70917	227	0.06170	0.00069	0.82008	0.05533	0.09640	0.00641	0.986	664	24	608	30	593	38	II.I	593	38
NA003A-100	3	713322	261	0.11667	0.00127	5.55441	0.35745	0.34529	0.02190	0.986	1906	19	1909	54	1912	104	-0.4	1906	19
NA003A-101	2	49789	202	0.05874	0.00068	0.62323	0.04085	0.07695	0.00496	0.984	558	25	492	25	478	30	14.8	478	30
NA003A-102	3	199868	175	0.06302	0.00067	0.98048	0.06490	0.11284	0.00737	0.987	709	22	694	33	689	43	2.9	689	43
NA003A-103	2	172265	164	0.06088	0.00091	0.82467	0.06616	0.09825	0.00775	0.983	635	32	611	36	604	45	5.1	604	45
NA003A-104	2	100248	159	0.06299	0.00071	0.95439	0.06357	0.10989	0.00721	0.986	708	24	680	32	672	42	5.3	672	42
NA003A-105	2	89250	176	0.06189	0.00101	0.83384	0.05782	0.09771	0.00658	0.972	670	35	616	32	601	39	10.9	601	39
NA003A-106	2	339357	142	0.06033	0.00065	0.83336	0.05558	0.10019	0.00659	0.987	615	23	615	30	616	39	0.0	616	39
NA003A-107	2	349441	139	0.06065	0.00063	0.86819	0.05641	0.10382	0.00666	0.987	627	22	635	30	637	39	-1.6	637	39
NA003A-108	2	131760	130	0.06252	0.00066	0.96927	0.06367	0.11245	0.00729	0.987	692	22	688	32	687	42	0.7	687	42
NA003A-109	2	127939	134	0.10911	0.00124	4.62671	0.29486	0.30755	0.01929	0.984	1785	21	1754	52	1729	94	3.6	1785	21

TABLE 1

(continued)

Digdeguash Fm. (NA003A)	Morph.	Isotopic ratios									Ages (Ma)						disc.	Reported age	
sample name		^{206}Pb (cps)	^{204}Pb (cps)	$\frac{^{207}Pb}{^{206}Pb}$	2σ	$\frac{^{207}Pb}{^{235}U}$	2σ	$\frac{^{206}Pb}{^{238}U}$	2 σ	ρ	$\frac{^{207}Pb}{^{206}Pb}$	2 σ	$\frac{^{207}Pb}{^{235}U}$	2 σ	$\frac{^{206}Pb}{^{238}U}$	2 σ	%	(Ma)	2 σ
NA003A-110	2	89113	133	0.06100	0.00070	0.82451	0.05410	0.09803	0.00633	0.985	639	24	611	30	603	37	5.9	603	37
NA003A-111	2	35286	109	0.06256	0.00098	0.84250	0.05600	0.09767	0.00631	0.972	693	33	621	30	601	37	14.0	601	37
NA003A-112	2	21810	120	0.05898	0.00094	0.59676	0.04033	0.07338	0.00482	0.972	566	34	475	25	457	29	20.1	457	29
NA003A-113	2	61207	127	0.06019	0.00080	0.71744	0.04895	0.08644	0.00578	0.981	611	29	549	29	534	34	13.0	534	34
NA003A-114	2	34932	136	0.06184	0.00083	0.81508	0.05457	0.09560	0.00627	0.980	669	28	605	30	589	37	12.5	589	37
NA003A-115	2	173119	146	0.06466	0.00073	1.04859	0.07221	0.11762	0.00799	0.987	763	24	728	35	717	46	6.4	717	46
NA003A-116	2	453545	178	0.11142	0.00123	4.50817	0.28597	0.29345	0.01833	0.985	1823	20	1732	51	1659	91	10.2	1823	20
NA003A-117	2	23072	172	0.05886	0.00124	0.61152	0.04289	0.07535	0.00504	0.954	562	45	485	27	468	30	17.3	468	30
NA003A-118	2	56094	139	0.05788	0.00071	0.61078	0.04034	0.07654	0.00497	0.983	525	26	484	25	475	30	9.8	475	30
NA003A-119	2	3120	316	0.82957	0.01841	198.75024	237.86663	1.73760	2.07923	1.000	4973	31	5379	796	6492	3642	-49.4	4973	31
NA003A-120	2	37465	156	0.06124	0.00083	0.72319	0.04953	0.08565	0.00575	0.980	648	29	553	29	530	34	18.9	530	34
NA003A-121	2	82582	200	0.06165	0.00070	0.83726	0.05449	0.09850	0.00631	0.985	662	24	618	30	606	37	8.9	606	37
NA003A-122	2	78381	197	0.06179	0.00069	0.83665	0.05543	0.09821	0.00641	0.986	667	24	617	30	604	38	9.9	604	38
NA003A-123	2	63835	230	0.05781	0.00079	0.60161	0.03993	0.07548	0.00490	0.978	522	30	478	25	469	29	10.6	469	29
NA003A-124	2	72141	197	0.06047	0.00075	0.74402	0.05061	0.08924	0.00597	0.983	620	26	565	29	551	35	11.6	551	35
NA003A-125	2	98609	223	0.06223	0.00075	0.79794	0.05307	0.09300	0.00608	0.984	682	25	596	30	573	36	16.7	573	36
NA003A-126	2	145145	220	0.06149	0.00066	0.87271	0.05664	0.10293	0.00659	0.986	656	23	637	30	632	38	4.0	632	38
NA003A-127	1	180680	220	0.06110	0.00071	0.84276	0.05753	0.10003	0.00673	0.985	643	25	621	31	615	39	4.6	615	39
NA003A-128	2	1978019	401	0.11294	0.00155	4.67464	0.31329	0.30019	0.01969	0.979	1847	25	1763	55	1692	97	9.5	1847	25
NA003A-129	2	100204	241	0.06062	0.00076	0.83884	0.05510	0.10036	0.00647	0.982	626	27	619	30	617	38	1.6	617	38
NA003A-130	2	29500	231	0.05851	0.00102	0.62009	0.04299	0.07687	0.00516	0.968	549	38	490	27	477	31	13.5	477	31
NA003A-131	2	113112	5520	0.29999	0.02079	8.79306	5.08967	0.21258	0.12216	0.993	3470	103	2317	425	1243	619	70.2	3470	103
NA003A-132	2	43447	194	0.06166	0.00108	0.82523	0.05540	0.09707	0.00629	0.965	662	37	611	30	597	37	10.3	597	37
NA003A-133	2	55301	181	0.06146	0.00084	0.83897	0.05674	0.09901	0.00656	0.979	655	29	619	31	609	38	7.5	609	38
NA003A-134	2	30301	161	0.06247	0.00104	0.84320	0.05720	0.09789	0.00644	0.969	690	35	621	31	602	38	13.4	602	38
NA003A-135	I	206336	171	0.08810	0.00118	2.21343	0.15726	0.18222	0.01272	0.982	1385	25	1185	49	1079	69	24.0	1385	25
NA003A-136	2	11170	146	0.05942	0.00116	0.68185	0.04729	0.08322	0.00554	0.959	583	42	528	28	515	33	12.0	515	33
NA003A-137	1	47224	122	0.06155	0.00074	0.81034	0.05405	0.09549	0.00627	0.984	658	25	603	30	588	37	11.2	588	37
NA003A-138	2	535352	137	0.09581	0.00106	3.44132	0.22217	0.26051	0.01657	0.985	1544	21	1514	50	1492	84	3.7	1544	21
NA003A-139	2	152170	117	0.09397	0.00104	3.24202	0.20904	0.25022	0.01589	0.985	1508	21	1467	49	1440	81	5.0	1508	21
NA003A-140	2	69197	104	0.06110	0.00077	0.79570	0.05437	0.09445	0.00634	0.983	643	27	594	30	582	37	9.9	582	37
NA003A-141	2	189740	111	0.06102	0.00065	0.85444	0.05827	0.10156	0.00684	0.988	640	23	627	31	624	40	2.7	624	40
NA003A-142-X	2	42112	87	0.05852	0.00081	0.59353	0.03986	0.07356	0.00484	0.979	549	30	473	25	458	29	17.3	458	29
NA003A-143	2	169443	103	0.09325	0.00106	2.89983	0.19893	0.22555	0.01526	0.986	1493	21	1382	51	1311	80	13.4	1493	21
NA003A-144	2	95791	562	0.10041	0.00584	1.32920	0.11913	0.09601	0.00655	0.761	1632	104	859	51	591	38	66.7	1632	104

TABLE 1
(continued)

Digdeguash Fm. (NA003A)	Morph.	Isotopic ratios									Ages (Ma)						disc.	Reported age	
sample name		^{206}Pb (cps)	^{204}Pb (cps)	$\frac{^{207}Pb}{^{206}Pb}$	2σ	$\frac{^{207}Pb}{^{235}U}$	2σ	$\frac{^{206}Pb}{^{238}U}$	2 σ	ρ	$\frac{^{207}Pb}{^{206}Pb}$	2 σ	$\frac{^{207}Pb}{^{235}U}$	2 σ	$\frac{^{206}Pb}{^{238}U}$	2 σ	%	(Ma)	2 σ
NA003A-145	2	55511	81	0.07437	0.00101	1.64734	0.11558	0.16066	0.01106	0.981	1051	27	989	43	960	61	9.3	1051	27
NA003A-146	2	132491	746	0.06662	0.00275	0.82817	0.06519	0.09016	0.00605	0.852	826	84	613	36	556	36	34.0	826	84
NA003A-147	2	74521	75	0.06074	0.00074	0.82775	0.05828	0.09883	0.00685	0.985	630	26	612	32	608	40	3.8	608	40
NA003A-148	2	535862	73	0.10848	0.00126	3.84526	0.24955	0.25709	0.01641	0.984	1774	21	1602	51	1475	84	18.8	1774	21
NA003A-149	1	59325	62	0.06079	0.00076	0.81439	0.05483	0.09717	0.00643	0.982	632	27	605	30	598	38	5.6	598	38

$^{207}Pb/^{235}U$ ratios are calculated as $137.88 \times {}^{206}Pb/^{238}U \times {}^{207}Pb/^{206}Pb$. Samples in *italics* are corrected for common lead. Correlation coefficients (ρ) calculated by the following formula:

$$\rho = \frac{\left(\frac{2\sigma_{^{207}Pb/^{235}U}}{^{207}Pb/^{235}U}\right)^2 + \left(\frac{2\sigma_{^{206}Pb/^{238}U}}{^{206}Pb/^{238}U}\right)^2 - \left(\frac{2\sigma_{^{207}Pb/^{206}Pb}}{^{207}Pb/^{206}Pb}\right)^2}{2\left(\frac{2\sigma_{^{207}Pb/^{235}U}}{^{207}Pb/^{235}U}\right)\left(\frac{2\sigma_{^{206}Pb/^{238}U}}{^{206}Pb/^{238}U}\right)}$$

Percent discordance between $^{206}Pb/^{238}U$ and $^{207}Pb/^{206}Pb$ is determined by the formula:

$$discordance = 100\left[(e^{0.000155125 \times (^{207}Pb/^{206}Pb\ age)} - 1) - \frac{^{206}Pb}{^{238}PU}\right] / [e^{0.000155125 \times (^{207}Pb/^{206}Pb\ age)} - 1]$$

A discordance cutoff of 10% is applied: analyses which fall outside the −10% to +10% range are greyed out.

$^{207}Pb/^{206}Pb$ ages are reported for $^{207}Pb/^{206}Pb$ ratios greater than 0.0658 (800 Ma); $^{206}Pb/^{238}U$ ages reported otherwise.

Zircon morphologies are designated as 1 (euhedral), 2 (subhedral), and 3 (anhedral).

TABLE 2

Laser ablation U/Pb isotopic data for sample NA010A, Flume Ridge Formation. Notes and calculations as Table 1

Flume Ridge Fm.(Na010A)	Morph.	Isotopic ratios									Ages (Ma)						disc.	Reported age	
sample name		^{206}Pb (cps)	^{204}Pb (cps)	$\frac{^{207}Pb}{^{206}Pb}$	2σ	$\frac{^{207}Pb}{^{235}U}$	2σ	$\frac{^{206}Pb}{^{238}U}$	2 σ	ρ	$\frac{^{207}Pb}{^{206}Pb}$	2 σ	$\frac{^{207}Pb}{^{235}U}$	2 σ	$\frac{^{206}Pb}{^{238}U}$	2 σ	%	(Ma)	2 σ
NA010A-001	2	58406	173	0.05982	0.00113	0.63832	0.05359	0.07739	0.00633	0.974	597	40	501	33	480	38	20.3	480	38
NA010A-002	1	209441	171	0.05683	0.00093	0.58408	0.04815	0.07454	0.00602	0.980	485	36	467	30	463	36	4.6	463	36
NA010A-003	2	169222	233	0.07662	0.00122	1.97887	0.13808	0.18730	0.01272	0.973	1111	32	1108	46	1107	69	0.5	1111	32
NA010A-004	2	676632	207	0.08781	0.00102	2.95579	0.20113	0.24413	0.01637	0.985	1378	22	1396	50	1408	84	-2.4	1378	22
NA010A-005	3	153568	194	0.09477	0.00113	3.66860	0.24441	0.28076	0.01840	0.984	1524	22	1565	52	1595	92	-5.3	1524	22
NA010A-006	2	574423	230	0.07499	0.00091	1.91600	0.12651	0.18531	0.01203	0.983	1068	24	1087	43	1096	65	-2.8	1068	24
NA010A-007	2	341912	184	0.10386	0.00123	4.45781	0.30387	0.31128	0.02090	0.985	1694	22	1723	55	1747	102	-3.6	1694	22
NA010A-008	3	860846	185	0.07711	0.00088	2.11434	0.14975	0.19886	0.01390	0.987	1124	22	1153	48	1169	74	-4.4	1124	22
NA010A-009	2	123001	205	0.05789	0.00098	0.63248	0.05404	0.07924	0.00663	0.980	526	37	498	33	492	40	6.8	492	40
NA010A-010	2	209413	204	0.05823	0.00148	0.58611	0.05057	0.07300	0.00602	0.956	539	54	468	32	454	36	16.2	454	36
NA010A-011	2	469855	34	0.10092	0.00117	4.14868	0.27624	0.29816	0.01955	0.985	1641	21	1664	53	1682	96	-2.9	1641	21
NA010A-012	2	784461	49	0.10089	0.00115	4.20521	0.27774	0.30229	0.01967	0.985	1641	21	1675	53	1703	97	-4.3	1641	21
NA010A-013	2	298487	43	0.05569	0.00090	0.59272	0.04962	0.07719	0.00634	0.981	440	35	473	31	479	38	-9.3	479	38
NA010A-014	3	369203	35	0.10438	0.00121	4.62223	0.31226	0.32117	0.02138	0.985	1703	21	1753	55	1795	103	-6.2	1703	21
NA010A-015	2	509581	34	0.05619	0.00090	0.59334	0.04919	0.07659	0.00623	0.981	460	35	473	31	476	37	-3.6	476	37
NA010A-016	2	123213	39	0.09001	0.00106	3.30887	0.22320	0.26661	0.01771	0.985	1426	22	1483	51	1524	89	-7.7	1426	22
NA010A-017	2	532208	101	0.08519	0.00102	2.75165	0.18992	0.23426	0.01592	0.985	1320	23	1343	50	1357	83	-3.1	1320	23
NA010A-018	3	1076743	67	0.07032	0.00081	1.56292	0.10185	0.16119	0.01034	0.984	938	23	956	40	963	57	-2.9	938	23
NA010A-019	2	391752	207	0.06361	0.00107	0.75680	0.06414	0.08629	0.00717	0.980	729	35	572	36	534	42	27.9	534	42
NA010A-020	2	767424	41	0.09336	0.00113	3.27865	0.25894	0.25470	0.01988	0.988	1495	23	1476	60	1463	101	2.4	1495	23
NA010A-021	2	102972	19	0.09726	0.00121	3.73370	0.25459	0.27843	0.01867	0.983	1572	23	1579	53	1583	93	-0.8	1572	23
NA010A-022	2	292835	16	0.06983	0.00082	1.60933	0.10561	0.16714	0.01079	0.984	923	24	974	40	996	59	-8.5	923	24
NA010A-023	2	97875	60	0.06092	0.00171	0.63114	0.05538	0.07514	0.00625	0.948	636	59	497	34	467	37	27.6	467	37
NA010A-024	2	128819	52	0.06011	0.00121	0.67637	0.05971	0.08161	0.00701	0.974	607	43	525	36	506	42	17.4	506	42
NA010A-025	3	298383	35	0.13033	0.00151	7.07077	0.48335	0.39349	0.02651	0.986	2102	20	2120	59	2139	121	-2.0	2102	20
NA010A-026	2	24673	17	0.05805	0.00184	0.60957	0.05584	0.07616	0.00655	0.938	532	68	483	35	473	39	11.4	473	39
NA010A-027	2	96724	64	0.07373	0.00145	1.84522	0.12619	0.18151	0.01189	0.958	1034	39	1062	44	1075	65	-4.3	1034	39
NA010A-028	2	220568	20	0.08407	0.00099	2.68798	0.17791	0.23190	0.01510	0.984	1294	23	1325	48	1344	79	-4.3	1294	23
NA010A-029	3	673018	39	0.11306	0.00132	5.37922	0.39185	0.34508	0.02481	0.987	1849	21	1882	61	1911	118	-3.9	1849	21
NA010A-030	2	691175	41	0.08645	0.00108	2.89062	0.19473	0.24250	0.01605	0.983	1348	24	1379	50	1400	83	-4.2	1348	24
NA010A-031A	2	271952	40	0.07726	0.00092	2.05218	0.13975	0.19264	0.01292	0.985	1128	24	1133	45	1136	69	-0.8	1128	24
NA010A-031B	2	24741	40	0.05292	0.00102	0.58263	0.04965	0.07985	0.00663	0.974	325	43	466	31	495	39	-54.3	495	39
NA010A-032	2	251095	89	0.05650	0.00104	0.56691	0.04790	0.07277	0.00600	0.976	472	40	456	31	453	36	4.2	453	36
NA010A-033	3	573501	76	0.08544	0.00098	2.87017	0.22354	0.24363	0.01877	0.989	1326	22	1374	57	1406	97	-6.7	1326	22
NA010A-034	2	198464	46	0.08525	0.00101	2.81584	0.19881	0.23956	0.01667	0.986	1321	23	1360	52	1384	86	-5.3	1321	23
NA010A-035	2	385078	210	0.06010	0.00112	0.62234	0.05192	0.07510	0.00611	0.975	607	40	491	32	467	37	24.0	467	37
NA010A-036	2	521755	90	0.08778	0.00104	2.97575	0.19890	0.24588	0.01618	0.984	1378	23	1401	50	1417	83	-3.2	1378	23

TABLE 2
(continued)

Flume Ridge Fm.(Na010A)	Morph.	Isotopic ratios									Ages (Ma)						disc.	Reported age	
sample name		^{206}Pb (cps)	^{204}Pb (cps)	$\frac{^{207}Pb}{^{206}Pb}$	2σ	$\frac{^{207}Pb}{^{235}U}$	2σ	$\frac{^{206}Pb}{^{238}U}$	2 σ	ρ	$\frac{^{207}Pb}{^{206}Pb}$	2 σ	$\frac{^{207}Pb}{^{235}U}$	2 σ	$\frac{^{206}Pb}{^{238}U}$	2 σ	%	(Ma)	2 σ
NA010A-037	2	67478	80	0.05465	0.00105	0.54468	0.04704	0.07228	0.00609	0.975	398	43	442	30	450	36	-13.5	450	36
NA010A-038	2	181364	64	0.08422	0.00102	2.62626	0.17577	0.22616	0.01489	0.984	1298	23	1308	48	1314	78	-1.4	1298	23
NA010A-039	2	188375	78	0.05520	0.00092	0.54104	0.04600	0.07109	0.00593	0.981	420	37	439	30	443	36	-5.6	443	36
NA010A-040	2	279802	102	0.05533	0.00094	0.53147	0.04478	0.06967	0.00575	0.979	425	38	433	29	434	35	-2.1	434	35
NA010A-041	3	205646	38	0.05748	0.00094	0.59698	0.05182	0.07533	0.00642	0.982	510	36	475	32	468	38	8.5	468	38
NA010A-042	3	71252	27	0.09717	0.00124	3.87954	0.25931	0.28956	0.01900	0.982	1571	24	1609	53	1639	94	-5.0	1571	24
NA010A-043	2	22140	30	0.09494	0.00251	3.92280	0.30943	0.29969	0.02227	0.942	1527	49	1618	62	1690	110	-12.1	1527	49
NA010A-044	2	445648	53	0.05735	0.00110	0.60189	0.05279	0.07612	0.00651	0.976	505	42	478	33	473	39	6.6	473	39
NA010A-045	2	187399	19	0.05641	0.00091	0.58141	0.04856	0.07476	0.00612	0.981	468	35	465	31	465	37	0.8	465	37
NA010A-046	2	149015	32	0.05589	0.00111	0.57370	0.04868	0.07444	0.00614	0.972	448	44	460	31	463	37	-3.4	463	37
NA010A-047	3	287449	30	0.11277	0.00130	5.23678	0.36034	0.33681	0.02285	0.986	1844	21	1859	57	1871	109	-1.7	1844	21
NA010A-048	*3*	*336835*	*1121*	*0.05665*	*0.00451*	*0.55797*	*0.06147*	*0.07144*	*0.00544*	*0.692*	*478*	*167*	*450*	*39*	*445*	*33*	*7.1*	*478*	*167*
NA010A-049	2	1228633	63	0.10137	0.00114	4.18650	0.28025	0.29952	0.01976	0.986	1649	21	1671	53	1689	97	-2.7	1649	21
NA010A-050	2	409657	38	0.07450	0.00086	1.89883	0.12598	0.18485	0.01207	0.985	1055	23	1081	43	1093	65	-3.9	1055	23
NA010A-051A	2	219644	71	0.08977	0.00103	3.12038	0.22160	0.25209	0.01767	0.987	1421	22	1438	53	1449	90	-2.2	1421	22
NA010A-051B	2	223249	95	0.07913	0.00175	2.20649	0.19220	0.20222	0.01704	0.967	1176	43	1183	59	1187	91	-1.1	1176	43
NA010A-052	2	114108	107	0.05547	0.00103	0.57266	0.04883	0.07487	0.00623	0.976	431	41	460	31	465	37	-8.2	465	37
NA010A-054	*2*	*669649*	*319*	*0.10226*	*0.00172*	*4.04861*	*0.37314*	*0.28715*	*0.02602*	*0.983*	*1666*	*31*	*1644*	*72*	*1627*	*129*	*2.6*	*1666*	*31*
NA010A-055A	2	96842	104	0.05580	0.00103	0.59674	0.05257	0.07757	0.00668	0.978	444	40	475	33	482	40	-8.7	482	40
NA010A-055B	2	43694	106	0.05472	0.00109	0.57588	0.05031	0.07634	0.00649	0.974	401	44	462	32	474	39	-19.1	474	39
NA010A-055C	2	171513	113	0.05621	0.00096	0.59860	0.05129	0.07724	0.00649	0.980	461	37	476	32	480	39	-4.3	480	39
NA010A-056	2	197317	118	0.05559	0.00093	0.56126	0.05030	0.07323	0.00645	0.982	436	37	452	32	456	39	-4.7	456	39
NA010A-057	*2*	*136412*	*399*	*0.08887*	*0.00569*	*3.63907*	*0.35163*	*0.29698*	*0.02149*	*0.749*	*1401*	*118*	*1558*	*74*	*1676*	*106*	*-22.3*	*1401*	*118*
NA010A-058	2	31682	134	0.06313	0.00279	0.68562	0.06359	0.07877	0.00642	0.879	713	91	530	38	489	38	32.6	489	38
NA010A-059	2	107872	123	0.05459	0.00095	0.51006	0.04464	0.06777	0.00581	0.980	395	39	418	30	423	35	-7.2	423	35
NA010A-060	1	176294	141	0.07902	0.00094	2.32780	0.15683	0.21364	0.01417	0.984	1173	23	1221	47	1248	75	-7.1	1173	23
NA010A-061	3	260911	27	0.10093	0.00116	3.85117	0.25888	0.27674	0.01833	0.985	1641	21	1604	53	1575	92	4.6	1641	21
NA010A-062	1	154972	43	0.06029	0.00147	0.59260	0.05283	0.07129	0.00611	0.962	614	52	473	33	444	37	28.6	444	37
NA010A-063	2	181015	20	0.08674	0.00105	2.78688	0.19585	0.23303	0.01613	0.985	1355	23	1352	51	1350	84	0.3	1355	23
NA010A-064	3	266796	12	0.10163	0.00121	4.16874	0.29483	0.29749	0.02074	0.986	1654	22	1668	56	1679	102	-1.7	1654	22
NA010A-065	2	230707	12	0.09302	0.00108	3.42692	0.22678	0.26718	0.01741	0.984	1488	22	1511	51	1526	88	-2.9	1488	22
NA010A-066	1	107770	12	0.05677	0.00093	0.56892	0.04895	0.07268	0.00614	0.982	483	36	457	31	452	37	6.5	452	37
NA010A-067	3	658274	36	0.10218	0.00117	4.18497	0.30742	0.29705	0.02156	0.988	1664	21	1671	58	1677	106	-0.9	1664	21
NA010A-068	2	508331	7	0.10561	0.00120	4.49465	0.32515	0.30867	0.02205	0.988	1725	21	1730	58	1734	108	-0.6	1725	21
NA010A-069	3	220996	14	0.09285	0.00112	3.22104	0.22523	0.25160	0.01733	0.985	1485	23	1462	53	1447	89	2.9	1485	23
NA010A-070	3	421382	23	0.07792	0.00090	2.15030	0.15693	0.20014	0.01442	0.987	1145	23	1165	49	1176	77	-3.0	1145	23
NA010A-071	*2*	*1136140*	*578*	*0.07670*	*0.00129*	*1.86435*	*0.13724*	*0.17628*	*0.01263*	*0.973*	*1114*	*33*	*1069*	*48*	*1047*	*69*	*6.5*	*1114*	*33*

TABLE 2
(continued)

Flume Ridge Fm.(Na010A)	Morph.	Isotopic ratios									Ages (Ma)						disc.	Reported age	
sample name		^{206}Pb (cps)	^{204}Pb (cps)	$\frac{^{207}Pb}{^{206}Pb}$	2σ	$\frac{^{207}Pb}{^{235}U}$	2σ	$\frac{^{206}Pb}{^{238}U}$	2 σ	ρ	$\frac{^{207}Pb}{^{206}Pb}$	2 σ	$\frac{^{207}Pb}{^{235}U}$	2 σ	$\frac{^{206}Pb}{^{238}U}$	2 σ	%	(Ma)	2 σ
NA010A-072	2	76768	7	0.07212	0.00107	1.63719	0.12435	0.16464	0.01226	0.981	989	30	985	47	982	68	0.8	989	30
NA010A-073	2	81856	7	0.07506	0.00095	1.84220	0.12068	0.17800	0.01144	0.981	1070	25	1061	42	1056	62	1.4	1070	25
NA010A-074	2	145132	7	0.16164	0.00194	10.47351	0.69930	0.46994	0.03087	0.984	2473	20	2478	60	2483	134	-0.5	2473	20
NA010A-075	2	91065	5	0.05684	0.00096	0.57501	0.04871	0.07337	0.00609	0.980	485	37	461	31	456	36	6.2	456	36
NA010A-076	2	45713	16	0.07761	0.00111	2.00267	0.13854	0.18715	0.01267	0.978	1137	28	1116	46	1106	68	3.0	1137	28
NA010A-077	3	759908	18	0.07508	0.00085	1.96054	0.13326	0.18939	0.01269	0.986	1071	23	1102	45	1118	68	-4.8	1071	23
NA010A-078	2	271056	12	0.09852	0.00114	3.92168	0.27489	0.28871	0.01996	0.986	1596	21	1618	55	1635	99	-2.8	1596	21
NA010A-079	2	727726	5	0.08459	0.00097	2.65919	0.18660	0.22800	0.01579	0.987	1306	22	1317	51	1324	82	-1.5	1306	22
NA010A-080	3	458380	8	0.07364	0.00085	1.76822	0.11897	0.17415	0.01155	0.985	1032	23	1034	43	1035	63	-0.3	1032	23
NA010A-081	2	405797	58	0.18810	0.00215	14.35581	0.98261	0.55351	0.03736	0.986	2726	19	2774	63	2840	153	-5.2	2726	19
NA010A-082	2	160549	54	0.07648	0.00098	1.91502	0.14463	0.18161	0.01352	0.986	1108	25	1086	49	1076	73	3.1	1108	25
NA010A-083	1	400800	200	0.06212	0.00155	0.58377	0.05180	0.06815	0.00580	0.959	678	53	467	33	425	35	38.6	425	35
NA010A-084	2	84366	22	0.05764	0.00153	0.58417	0.05014	0.07351	0.00600	0.951	516	57	467	32	457	36	11.8	457	36
NA010A-085	2	311680	86	0.10383	0.00122	4.13563	0.31080	0.28889	0.02144	0.988	1694	22	1661	60	1636	106	3.9	1694	22
NA010A-086	3	567456	39	0.08731	0.00099	2.86461	0.19375	0.23795	0.01587	0.986	1367	22	1373	50	1376	82	-0.7	1367	22
NA010A-087	2	45495	32	0.06223	0.00114	0.61544	0.05159	0.07173	0.00587	0.976	682	39	487	32	447	35	35.7	447	35
NA010A-088	3	368436	53	0.10692	0.00130	4.55783	0.31512	0.30917	0.02104	0.984	1748	22	1742	56	1737	103	0.7	1748	22
NA010A-089	3	571299	45	0.07309	0.00084	1.77808	0.12145	0.17644	0.01188	0.986	1016	23	1037	43	1048	65	-3.3	1016	23
NA010A-090	2	140134	41	0.05579	0.00092	0.54647	0.04587	0.07104	0.00585	0.981	444	36	443	30	442	35	0.4	442	35
NA010A-091	2	64110	75	0.06726	0.00101	1.07045	0.07112	0.11544	0.00747	0.974	846	31	739	34	704	43	17.7	846	31
NA010A-092	2	335259	80	0.05698	0.00091	0.59914	0.05135	0.07626	0.00642	0.982	491	35	477	32	474	38	3.6	474	38
NA010A-093	2	86927	107	0.07549	0.00109	1.73957	0.11949	0.16714	0.01122	0.978	1081	29	1023	43	996	62	8.5	1081	29
NA010A-094	2	64855	102	0.05713	0.00101	0.58182	0.04892	0.07386	0.00607	0.978	496	39	466	31	459	36	7.7	459	36
NA010A-095	2	321574	110	0.09020	0.00107	3.04674	0.20912	0.24498	0.01656	0.985	1430	23	1419	51	1413	85	1.3	1430	23
NA010A-096	2	403790	75	0.07407	0.00086	1.82049	0.12239	0.17826	0.01180	0.985	1043	23	1053	43	1057	64	-1.5	1043	23
NA010A-097	1	596225	2941	0.07710	0.00194	0.50132	0.04125	0.04716	0.00369	0.952	1124	49	413	28	297	23	75.2	1124	49
NA010A-098	1	52456	114	0.05887	0.00122	0.64906	0.05687	0.07996	0.00681	0.972	562	44	508	34	496	41	12.3	496	41
NA010A-099	1	71874	107	0.07348	0.00094	1.81303	0.12527	0.17895	0.01215	0.983	1027	26	1050	44	1061	66	-3.6	1027	26
NA010A-100	2	1052389	152	0.09249	0.00106	3.31455	0.22263	0.25992	0.01720	0.985	1477	22	1484	51	1489	87	-0.9	1477	22
NA010A-101	3	1128613	132	0.07364	0.00084	1.76794	0.11791	0.17413	0.01144	0.985	1032	23	1034	42	1035	63	-0.3	1032	23
NA010A-102	3	325004	101	0.09181	0.00106	3.18324	0.21944	0.25145	0.01709	0.986	1464	22	1453	52	1446	87	1.3	1464	22
NA010A-103	1	366760	99	0.05598	0.00090	0.56757	0.04766	0.07353	0.00606	0.982	452	35	456	30	457	36	-1.3	457	36
NA010A-104	2	182102	275	0.08838	0.00144	2.35943	0.16596	0.19362	0.01325	0.973	1391	31	1230	49	1141	71	19.6	1391	31
NA010A-105	2	528325	128	0.09134	0.00104	3.18240	0.23059	0.25270	0.01808	0.988	1454	22	1453	54	1452	92	0.1	1454	22
NA010A-106	2	200570	115	0.05664	0.00094	0.59597	0.05234	0.07632	0.00658	0.982	477	36	475	33	474	39	0.7	474	39
NA010A-107	3	357248	269	0.10291	0.00192	4.19795	0.30430	0.29584	0.02072	0.966	1677	34	1674	58	1671	102	0.5	1677	34
NA010A-108	2	39363	119	0.08225	0.00136	2.23322	0.16100	0.19693	0.01382	0.973	1251	32	1192	49	1159	74	8.1	1251	32

TABLE 2
(continued)

Flume Ridge Fm.(Na010A)	Morph.	Isotopic ratios									Ages (Ma)						disc.	Reported age	
sample name		^{206}Pb (cps)	^{204}Pb (cps)	$\frac{^{207}Pb}{^{206}Pb}$	2σ	$\frac{^{207}Pb}{^{235}U}$	2σ	$\frac{^{206}Pb}{^{238}U}$	2 σ	ρ	$\frac{^{207}Pb}{^{206}Pb}$	2 σ	$\frac{^{207}Pb}{^{235}U}$	2 σ	$\frac{^{206}Pb}{^{238}U}$	2 σ	%	(Ma)	2 σ
NA010A-109	2	124136	94	0.07282	0.00085	1.73467	0.11647	0.17277	0.01142	0.985	1009	23	1021	42	1027	62	-2.0	1009	23
NA010A-110	2	255222	118	0.09619	0.00113	3.49387	0.24613	0.26343	0.01830	0.986	1552	22	1526	54	1507	93	3.2	1552	22
NA010A-111	2	320881	88	0.08699	0.00102	2.49296	0.17064	0.20784	0.01402	0.985	1360	22	1270	48	1217	74	11.5	1360	22
NA010A-112	*2*	*717999*	*451*	*0.07321*	*0.00153*	*1.81507*	*0.13549*	*0.17980*	*0.01288*	*0.960*	*1020*	*42*	*1051*	*48*	*1066*	*70*	*-4.9*	*1020*	*42*
NA010A-113	2	690013	83	0.10000	0.00114	4.21923	0.32362	0.30600	0.02321	0.989	1624	21	1678	61	1721	114	-6.8	1624	21
NA010A-114	2	37879	40	0.05655	0.00137	0.62350	0.05459	0.07996	0.00673	0.961	474	53	492	34	496	40	-4.8	496	40
NA010A-115	2	109696	57	0.08436	0.00101	2.64982	0.18795	0.22780	0.01593	0.986	1301	23	1315	51	1323	83	-1.9	1301	23
NA010A-116	2	212134	31	0.10567	0.00124	4.78941	0.32796	0.32873	0.02218	0.985	1726	21	1783	56	1832	107	-7.1	1726	21
NA010A-117	2	1228135	39	0.07629	0.00088	2.01042	0.13809	0.19113	0.01294	0.986	1103	23	1119	46	1127	70	-2.5	1103	23
NA010A-118	2	158959	39	0.09165	0.00113	3.30210	0.23535	0.26130	0.01834	0.985	1460	23	1482	54	1496	93	-2.8	1460	23
NA010A-119	2	357175	55	0.05738	0.00096	0.59298	0.05083	0.07496	0.00630	0.981	506	36	473	32	466	38	8.2	466	38
NA010A-120	1	48906	18	0.05812	0.00114	0.60345	0.05101	0.07531	0.00619	0.972	534	43	479	32	468	37	12.8	468	37
NA010A-121	*1*	*441550*	*167*	*0.05777*	*0.00154*	*0.63080*	*0.05704*	*0.07919*	*0.00684*	*0.956*	*521*	*57*	*497*	*35*	*491*	*41*	*5.9*	*491*	*41*
NA010A-122	2	130937	16	0.07256	0.00085	1.71648	0.11660	0.17156	0.01148	0.985	1002	24	1015	43	1021	63	-2.0	1002	24
NA010A-123	1	382736	15	0.05658	0.00090	0.60159	0.05028	0.07711	0.00633	0.982	475	35	478	31	479	38	-0.8	479	38
NA010A-124	2	272613	20	0.11593	0.00151	5.60035	0.38939	0.35037	0.02393	0.982	1894	23	1916	58	1936	113	-2.6	1894	23
NA010A-125	2	119116	15	0.05577	0.00093	0.54828	0.04589	0.07130	0.00585	0.980	443	37	444	30	444	35	-0.1	444	35
NA010A-126	3	364513	42	0.10207	0.00135	3.97524	0.26925	0.28246	0.01876	0.981	1662	24	1629	54	1604	94	4.0	1662	24
NA010A-127	2	415090	16	0.07631	0.00087	1.98367	0.14108	0.18854	0.01323	0.987	1103	23	1110	47	1113	71	-1.0	1103	23
NA010A-128	2	603303	3	0.07305	0.00083	1.77311	0.12137	0.17605	0.01188	0.986	1015	23	1036	43	1045	65	-3.2	1015	23
NA010A-129	2	366328	4	0.07178	0.00082	1.65077	0.10958	0.16680	0.01091	0.985	980	23	990	41	994	60	-1.6	980	23
NA010A-130	2	37642	19	0.05988	0.00116	0.78029	0.07031	0.09451	0.00832	0.977	599	41	586	39	582	49	3.0	582	49
NA010A-131	2	182869	120	0.10479	0.00302	3.71335	0.28423	0.25701	0.01823	0.926	1711	52	1574	59	1475	93	15.4	1711	52
NA010A-132	2	181505	2	0.09205	0.00107	3.07869	0.20485	0.24257	0.01589	0.985	1468	22	1427	50	1400	82	5.2	1468	22
NA010A-133	*2*	*2045756*	*1545*	*0.07496*	*0.00131*	*1.63224*	*0.13550*	*0.15793*	*0.01282*	*0.978*	*1067*	*35*	*983*	*51*	*945*	*71*	*12.3*	*1067*	*35*
NA010A-134	2	231033	9	0.05631	0.00091	0.53615	0.04441	0.06905	0.00561	0.981	465	36	436	29	430	34	7.6	430	34
NA010A-135	2	339390	2	0.09619	0.00116	3.40814	0.24465	0.25698	0.01819	0.986	1551	22	1506	55	1474	93	5.6	1551	22
NA010A-136	2	258132	0	0.07467	0.00087	1.65208	0.10903	0.16048	0.01042	0.984	1060	23	990	41	959	58	10.2	1060	23
NA010A-137	2	163348	5	0.09303	0.00115	2.68758	0.24350	0.20952	0.01880	0.991	1489	23	1325	65	1226	99	19.3	1489	23
NA010A-138	2	28403	0	0.07972	0.00125	1.94392	0.13661	0.17686	0.01211	0.975	1190	31	1096	46	1050	66	12.8	1190	31
NA010A-139	3	611665	0	0.07812	0.00089	1.92634	0.15427	0.17885	0.01418	0.990	1150	23	1090	52	1061	77	8.4	1150	23
NA010A-140	2	83965	0	0.07215	0.00096	1.50349	0.10289	0.15113	0.01014	0.981	990	27	932	41	907	57	9.0	990	27

Notes and calculations same as Table 1.

TABLE 3

Laser ablation U/Pb isotopic data for sample NA005A, Hayes Brook Formation

Hayes Brook Fm. (NA005A)	Morph.	Isotopic ratios									Ages (Ma)						disc.	reported age	
sample name		^{206}Pb (cps)	^{204}Pb (cps)	$\frac{^{207}Pb}{^{206}Pb}$	2σ	$\frac{^{207}Pb}{^{235}U}$	2σ	$\frac{^{206}Pb}{^{238}U}$	2σ	ρ	$\frac{^{207}Pb}{^{206}Pb}$	2σ	$\frac{^{207}Pb}{^{235}U}$	2σ	$\frac{^{206}Pb}{^{238}U}$	2σ	%	(Ma)	2σ
NA005A-001	1	35548	23	0.05711	0.00128	0.60882	0.03414	0.07732	0.00397	0.917	496	49	483	21	480	24	3.2	480	24
NA005A-002	1	28480	11	0.05631	0.00127	0.58114	0.03293	0.07485	0.00389	0.917	465	49	465	21	465	23	-0.1	465	23
NA005A-003	2	89974	11	0.05721	0.00083	0.61022	0.03327	0.07736	0.00407	0.964	500	32	484	21	480	24	4.0	480	24
NA005A-004	2	257277	14	0.05703	0.00073	0.64116	0.03319	0.08153	0.00409	0.969	493	28	503	20	505	24	-2.6	505	24
NA005A-005	2	201825	21	0.05749	0.00088	0.59012	0.03063	0.07445	0.00369	0.956	510	33	471	19	463	22	9.6	463	22
NA005A-006	2	183269	7	0.07025	0.00074	1.51758	0.07658	0.15667	0.00773	0.978	936	21	938	30	938	43	-0.3	936	21
NA005A-007	1	184695	9	0.05658	0.00084	0.61754	0.03291	0.07916	0.00405	0.960	475	33	488	20	491	24	-3.5	491	24
NA005A-008	2	152569	26	0.07162	0.00094	1.53598	0.11164	0.15555	0.01112	0.983	975	27	945	44	932	62	4.8	975	27
NA005A-009	2	80558	12	0.05656	0.00150	0.60973	0.03672	0.07819	0.00423	0.898	474	57	483	23	485	25	-2.4	485	25
NA005A-010	1	250181	7	0.05595	0.00074	0.60471	0.03176	0.07838	0.00398	0.967	451	29	480	20	486	24	-8.3	486	24
NA005A-011	1	74981	47	0.05760	0.00085	0.59715	0.03074	0.07519	0.00371	0.958	514	32	475	19	467	22	9.5	467	22
NA005A-012	1	111030	65	0.05871	0.00097	0.62450	0.03318	0.07715	0.00389	0.950	556	36	493	21	479	23	14.4	479	23
NA005A-013	2	167437	53	0.05714	0.00084	0.61214	0.03768	0.07770	0.00464	0.971	497	32	485	23	482	28	3.0	482	28
NA005A-014	1	136514	42	0.05716	0.00090	0.64060	0.03394	0.08129	0.00411	0.955	498	34	503	21	504	24	-1.3	504	24
NA005A-015	1	68858	38	0.05738	0.00098	0.60295	0.03542	0.07622	0.00428	0.957	506	37	479	22	473	26	6.7	473	26
NA005A-016	2	284284	47	0.07564	0.00080	1.88751	0.09842	0.18099	0.00924	0.979	1086	21	1077	34	1072	50	1.3	1086	21
NA005A-017	1	266937	101	0.05981	0.00131	0.59305	0.03325	0.07192	0.00371	0.920	597	47	473	21	448	22	25.8	448	22
NA005A-018	2	120318	39	0.05721	0.00105	0.58925	0.03454	0.07470	0.00416	0.950	500	40	470	22	464	25	7.3	464	25
NA005A-019	2	952316	54	0.08929	0.00093	2.97364	0.14527	0.24154	0.01153	0.977	1410	20	1401	36	1395	60	1.2	1410	20
NA005A-020	3	128513	52	0.07441	0.00093	1.74132	0.08681	0.16973	0.00819	0.968	1053	25	1024	32	1011	45	4.3	1053	25
NA005A-021	2	304802	33	0.05631	0.00071	0.61305	0.03183	0.07896	0.00398	0.970	464	28	485	20	490	24	-5.7	490	24
NA005A-022	2	84849	53	0.05595	0.00100	0.58953	0.03183	0.07642	0.00390	0.944	450	39	471	20	475	23	-5.6	475	23
NA005A-023	2	161813	25	0.09286	0.00098	3.21965	0.16639	0.25148	0.01272	0.979	1485	20	1462	39	1446	65	2.9	1485	20
NA005A-024	2	154588	49	0.05672	0.00082	0.60445	0.03231	0.07729	0.00398	0.962	481	32	480	20	480	24	0.2	480	24
NA005A-025	2	355630	56	0.08764	0.00091	2.88534	0.14167	0.23877	0.01146	0.977	1375	20	1378	36	1380	59	-0.5	1375	20
NA005A-026	2	242341	49	0.05595	0.00073	0.56935	0.02935	0.07380	0.00368	0.968	450	29	458	19	459	22	-2.0	459	22
NA005A-027	2	149982	61	0.05633	0.00078	0.55888	0.03081	0.07196	0.00384	0.968	465	30	451	20	448	23	3.8	448	23
NA005A-028	2	141139	76	0.07783	0.00088	2.03649	0.10085	0.18978	0.00915	0.974	1142	22	1128	33	1120	49	2.1	1142	22
NA005A-029	3	544164	93	0.09078	0.00095	3.04602	0.15793	0.24335	0.01236	0.980	1442	20	1419	39	1404	64	2.9	1442	20
NA005A-030	1	68414	292	0.10589	0.00713	1.12097	0.09240	0.07678	0.00365	0.577	1730	119	763	43	477	22	75.1	1730	119
NA005A-031	3	247380	369	0.10153	0.00520	3.15766	0.25337	0.22556	0.01393	0.770	1652	92	1447	60	1311	73	22.8	1652	92
NA005A-032	2	393786	31	0.05610	0.00071	0.60187	0.03018	0.07781	0.00378	0.968	456	28	478	19	483	23	-6.1	483	23
NA005A-033	1	43954	29	0.05286	0.00096	0.56261	0.03009	0.07720	0.00388	0.940	323	41	453	19	479	23	-50.4	479	23
NA005A-034	2	215147	24	0.05644	0.00077	0.57361	0.03034	0.07370	0.00377	0.966	470	30	460	19	458	23	2.5	458	23
NA005A-035	2	87320	22	0.07266	0.00085	1.60775	0.07802	0.16049	0.00756	0.971	1004	23	973	30	960	42	4.8	1004	23
NA005A-036	3	775037	31	0.07056	0.00098	1.37704	0.07505	0.14154	0.00746	0.967	945	28	879	32	853	42	10.3	945	28

TABLE 3
(continued)

Hayes Brook Fm. (NA005A)	Morph.	Isotopic ratios									Ages (Ma)						disc.	reported age	
sample name		^{206}Pb (cps)	^{204}Pb (cps)	$\frac{^{207}Pb}{^{206}Pb}$	2σ	$\frac{^{207}Pb}{^{235}U}$	2σ	$\frac{^{206}Pb}{^{238}U}$	2σ	ρ	$\frac{^{207}Pb}{^{206}Pb}$	2σ	$\frac{^{207}Pb}{^{235}U}$	2σ	$\frac{^{206}Pb}{^{238}U}$	2σ	%	(Ma)	2σ
NA005A-001	1	35548	23	0.05711	0.00128	0.60882	0.03414	0.07732	0.00397	0.917	496	49	483	21	480	24	3.2	480	24
NA005A-037	3	64531	11	0.05765	0.00088	0.60716	0.03294	0.07639	0.00398	0.960	516	33	482	21	475	24	8.4	475	24
NA005A-038	3	154948	18	0.05665	0.00077	0.57108	0.02952	0.07312	0.00365	0.965	478	30	459	19	455	22	5.0	455	22
NA005A-039	3	94732	32	0.07523	0.00124	1.75800	0.09046	0.16948	0.00826	0.948	1075	33	1030	33	1009	45	6.6	1075	33
NA005A-040	2	643166	25	0.10003	0.00103	3.57101	0.20817	0.25893	0.01485	0.984	1625	19	1543	45	1484	76	9.7	1625	19
NA005A-041	3	285909	5	0.08543	0.00096	2.27769	0.12508	0.19337	0.01039	0.979	1325	22	1205	38	1140	56	15.3	1325	22
NA005A-042	2	77603	12	0.05560	0.00089	0.53738	0.02866	0.07010	0.00356	0.954	436	35	437	19	437	21	-0.1	437	21
NA005A-043	2	73578	8	0.05802	0.00181	0.57533	0.03618	0.07192	0.00393	0.869	530	67	461	23	448	24	16.1	448	24
NA005A-044	1	165172	96	0.07102	0.00174	0.80086	0.05487	0.08178	0.00523	0.934	958	49	597	30	507	31	49.0	958	49
NA005A-045	1	514302	51	0.05724	0.00076	0.59979	0.03142	0.07599	0.00385	0.968	501	29	477	20	472	23	5.9	472	23
NA005A-046	2	66962	8	0.05622	0.00110	0.56673	0.03030	0.07311	0.00364	0.930	461	43	456	19	455	22	1.4	455	22
NA005A-047	2	763713	6	0.09275	0.00095	3.00065	0.14726	0.23464	0.01126	0.978	1483	19	1408	37	1359	59	9.3	1483	19
NA005A-048	2	262020	3	0.08630	0.00090	2.07032	0.10314	0.17399	0.00848	0.978	1345	20	1139	34	1034	46	25.0	1345	20
NA005A-049	2	103189	4	0.05564	0.00090	0.55967	0.02968	0.07296	0.00369	0.953	438	35	451	19	454	22	-3.8	454	22
NA005A-050	1	191104	4	0.15607	0.00163	9.12672	0.50001	0.42412	0.02281	0.982	2414	18	2351	49	2279	102	6.6	2414	18
NA005A-051	2	125783	2	0.08274	0.00090	2.31863	0.11236	0.20324	0.00960	0.974	1263	21	1218	34	1193	51	6.1	1263	21
NA005A-052	3	92668	17	0.09712	0.00134	2.01561	0.10799	0.15051	0.00779	0.966	1570	26	1121	36	904	44	45.4	1570	26
NA005A-053	2	533771	2	0.05577	0.00071	0.53874	0.02845	0.07006	0.00359	0.971	443	28	438	19	437	22	1.6	437	22
NA005A-054	2	438010	3	0.19778	0.00201	13.55700	0.66074	0.49715	0.02370	0.978	2808	17	2719	45	2602	101	8.9	2808	17
NA005A-055	2	920981	19	0.07613	0.00115	1.80829	0.10027	0.17228	0.00919	0.962	1098	30	1048	36	1025	50	7.3	1098	30
NA005A-056	1	84627	4	0.05380	0.00082	0.54637	0.02857	0.07366	0.00368	0.956	363	34	443	19	458	22	-27.3	458	22
NA005A-057	1	65265	1	0.05311	0.00095	0.51273	0.02811	0.07002	0.00363	0.945	333	40	420	19	436	22	-31.9	436	22
NA005A-058	2	29333	4	0.06441	0.00144	1.35252	0.07826	0.15230	0.00813	0.922	755	47	869	33	914	45	-22.6	914	45
NA005A-059	1	1171289	10	0.09799	0.00103	3.39877	0.16292	0.25155	0.01177	0.976	1586	19	1504	37	1446	60	9.8	1586	19
NA005A-060	2	199114	47	0.06120	0.00174	0.62472	0.03587	0.07403	0.00369	0.869	646	60	493	22	460	22	29.8	460	22
NA005A-061	2	389032	38	0.05671	0.00072	0.57501	0.03047	0.07353	0.00378	0.970	480	28	461	19	457	23	5.0	457	23
NA005A-062	2	2210728	67	0.05643	0.00070	0.57358	0.02918	0.07372	0.00364	0.970	469	27	460	19	459	22	2.4	459	22
NA005A-063	3	28857	45	0.06021	0.00156	0.73469	0.04384	0.08849	0.00476	0.901	611	55	559	25	547	28	11.0	547	28
NA005A-064	1	112395	40	0.05922	0.00121	0.59882	0.03372	0.07334	0.00385	0.931	575	44	476	21	456	23	21.4	456	23
NA005A-065	2	555433	55	0.05692	0.00072	0.59948	0.03150	0.07639	0.00390	0.971	488	28	477	20	475	23	2.9	475	23
NA005A-066	3	21017	36	0.07323	0.00142	1.44903	0.07940	0.14351	0.00735	0.935	1020	39	909	32	864	41	16.3	1020	39
NA005A-067	2	49834	36	0.05734	0.00108	0.55399	0.03019	0.07007	0.00358	0.939	505	41	448	20	437	22	14.0	437	22
NA005A-068	2	69681	48	0.05708	0.00088	0.59315	0.03125	0.07537	0.00380	0.956	495	34	473	20	468	23	5.5	468	23
NA005A-069	2	67601	49	0.05654	0.00101	0.58493	0.03052	0.07503	0.00368	0.939	474	39	468	19	466	22	1.6	466	22
NA005A-070	2	77747	47	0.07586	0.00094	1.80443	0.09560	0.17252	0.00888	0.972	1091	25	1047	34	1026	49	6.5	1091	25
NA005A-071	3	73861	37	0.07546	0.00138	1.67067	0.08548	0.16057	0.00767	0.934	1081	36	997	32	960	42	12.0	1081	36

TABLE 3
(continued)

Hayes Brook Fm. (NA005A)	Morph.	Isotopic ratios									Ages (Ma)						disc.	reported age	
sample name		^{206}Pb (cps)	^{204}Pb (cps)	$\frac{^{207}Pb}{^{206}Pb}$	2σ	$\frac{^{207}Pb}{^{235}U}$	2σ	$\frac{^{206}Pb}{^{238}U}$	2σ	ρ	$\frac{^{207}Pb}{^{206}Pb}$	2σ	$\frac{^{207}Pb}{^{235}U}$	2σ	$\frac{^{206}Pb}{^{238}U}$	2σ	%	(Ma)	2σ
NA005A-077	2	560691	255	0.06395	0.00091	0.70965	0.04244	0.08048	0.00468	0.971	740	30	545	25	499	28	33.9	499	28
NA005A-078	3	591686	8	0.07290	0.00077	1.58054	0.08348	0.15724	0.00814	0.980	1011	21	963	32	941	45	7.4	1011	21
NA005A-079	2	52725	43	0.05937	0.00341	0.59882	0.04521	0.07315	0.00358	0.648	581	120	476	28	455	21	22.4	455	21
NA005A-080	1	241334	1	0.05645	0.00079	0.57819	0.02968	0.07428	0.00367	0.962	470	31	463	19	462	22	1.8	462	22
NA005A-081	2	141642	11	0.05605	0.00079	0.56556	0.02894	0.07319	0.00360	0.961	454	31	455	19	455	22	-0.2	455	22
NA005A-082	3	1472376	6	0.11085	0.00112	4.82462	0.24168	0.31568	0.01549	0.979	1813	18	1789	41	1769	75	2.8	1813	18
NA005A-083	2	93690	12	0.05884	0.00094	0.60760	0.03098	0.07490	0.00363	0.949	561	35	482	19	466	22	17.6	466	22
NA005A-084	3	255758	18	0.11119	0.00127	5.06831	0.26310	0.33060	0.01674	0.976	1819	21	1831	43	1841	81	-1.4	1819	21
NA005A-085	2	81418	11	0.05538	0.00092	0.57362	0.03107	0.07513	0.00387	0.952	427	37	460	20	467	23	-9.6	467	23
NA005A-086A	2	95927	15	0.05531	0.00094	0.57017	0.03073	0.07477	0.00383	0.949	425	37	458	20	465	23	-9.8	465	23
NA005A-086B	2	21771	5	0.05073	0.00148	0.50354	0.02930	0.07198	0.00362	0.865	229	66	414	20	448	22	-99.3	448	22
NA005A-087	3	301449	4	0.08940	0.00096	2.90089	0.15057	0.23534	0.01195	0.978	1413	20	1382	38	1362	62	4.0	1413	20
NA005A-088	2	113054	4	0.05656	0.00104	0.57360	0.03148	0.07355	0.00380	0.943	475	40	460	20	458	23	3.7	458	23
NA005A-089	2	281736	5	0.05610	0.00075	0.57343	0.03079	0.07413	0.00386	0.969	456	29	460	20	461	23	-1.0	461	23
NA005A-090	1	39383	2	0.05530	0.00210	0.58011	0.03902	0.07608	0.00423	0.826	424	82	465	25	473	25	-11.8	473	25
NA005A-091	2	51741	2	0.05399	0.00097	0.53370	0.03062	0.07169	0.00391	0.950	371	40	434	20	446	23	-21.1	446	23
NA005A-092	2	393321	43	0.05926	0.00094	0.60271	0.03163	0.07377	0.00369	0.954	577	34	479	20	459	22	21.1	459	22
NA005A-093	3	149993	2	0.19031	0.00196	13.28314	0.63638	0.50623	0.02369	0.977	2745	17	2700	44	2641	101	4.6	2745	17
NA005A-094	2	204179	3	0.07708	0.00082	1.93246	0.09711	0.18184	0.00893	0.977	1123	21	1092	33	1077	49	4.5	1123	21
NA005A-095	2	257359	1	0.07301	0.00076	1.67985	0.08490	0.16688	0.00825	0.979	1014	21	1001	32	995	45	2.0	1014	21
NA005A-096	3	155287	12	0.10194	0.00143	3.89377	0.19531	0.27702	0.01334	0.960	1660	26	1612	40	1576	67	5.7	1660	26
NA005A-097	1	37164	4	0.05264	0.00193	0.54297	0.03704	0.07481	0.00430	0.843	313	81	440	24	465	26	-50.1	465	26
NA005A-098	2	240428	8	0.05659	0.00075	0.56124	0.02911	0.07193	0.00361	0.967	476	29	452	19	448	22	6.1	448	22
NA005A-099	2	49596	2	0.05385	0.00105	0.54571	0.02969	0.07350	0.00373	0.934	365	43	442	19	457	22	-26.2	457	22
NA005A-100	2	67181	17	0.06360	0.00219	0.65801	0.04003	0.07504	0.00376	0.824	728	71	513	24	466	23	37.3	466	23
NA005A-101	2	456343	205	0.06132	0.00122	0.66131	0.03656	0.07822	0.00404	0.933	651	42	515	22	485	24	26.3	485	24
NA005A-102	3	103666	88	0.05804	0.00098	0.62151	0.03350	0.07766	0.00398	0.950	531	37	491	21	482	24	9.6	482	24
NA005A-103	2	328885	67	0.08028	0.00084	2.17581	0.10639	0.19657	0.00939	0.977	1204	20	1173	33	1157	50	4.3	1204	20
NA005A-104	2	264433	125	0.05971	0.00133	0.60402	0.03314	0.07337	0.00368	0.914	593	48	480	21	456	22	23.9	456	22
NA005A-105	3	231104	71	0.10071	0.00108	3.99496	0.21346	0.28770	0.01506	0.979	1637	20	1633	42	1630	75	0.5	1637	20
NA005A-106	2	272400	37	0.07815	0.00083	1.95920	0.09729	0.18181	0.00882	0.977	1151	21	1102	33	1077	48	7.0	1151	21
NA005A-107	3	172538	39	0.07516	0.00088	1.81698	0.09005	0.17533	0.00844	0.972	1073	23	1052	32	1041	46	3.2	1073	23
NA005A-108	2	185511	37	0.05622	0.00075	0.56192	0.03015	0.07249	0.00377	0.968	461	29	453	19	451	23	2.3	451	23
NA005A-109	2	109348	39	0.05672	0.00089	0.56200	0.02816	0.07187	0.00342	0.950	480	34	453	18	447	21	7.1	447	21
NA005A-110	2	122250	50	0.05760	0.00090	0.58702	0.03146	0.07392	0.00379	0.956	515	34	469	20	460	23	11.0	460	23
NA005A-111	3	123253	17	0.05702	0.00083	0.56539	0.03054	0.07192	0.00374	0.963	492	32	455	20	448	22	9.4	448	22

TABLE 3
(continued)

Hayes Brook Fm. (NA005A)	Morph.	Isotopic ratios									Ages (Ma)						disc.	reported age	
sample name		^{206}Pb (cps)	^{204}Pb (cps)	$\frac{^{207}Pb}{^{206}Pb}$	2σ	$\frac{^{207}Pb}{^{235}U}$	2σ	$\frac{^{206}Pb}{^{238}U}$	2σ	ρ	$\frac{^{207}Pb}{^{206}Pb}$	2σ	$\frac{^{207}Pb}{^{235}U}$	2σ	$\frac{^{206}Pb}{^{238}U}$	2σ	%	(Ma)	2σ
NA005A-112	2	168000	37	0.05684	0.00076	0.54474	0.02811	0.06950	0.00346	0.965	485	29	442	18	433	21	11.1	433	21
NA005A-113	2	1237313	110	0.07338	0.00085	1.57467	0.07601	0.15564	0.00729	0.971	1024	23	960	30	933	41	9.6	1024	23
NA005A-114	2	73044	66	0.07621	0.00142	1.74641	0.11980	0.16619	0.01097	0.963	1101	37	1026	43	991	60	10.7	1101	37
NA005A-115	2	334422	24	0.08931	0.00094	2.81561	0.14359	0.22866	0.01141	0.979	1411	20	1360	38	1327	60	6.5	1411	20
NA005A-116	2	50776	20	0.08670	0.00145	2.45497	0.12304	0.20536	0.00970	0.943	1354	32	1259	36	1204	52	12.1	1354	32
NA005A-117	2	98541	16	0.05572	0.00079	0.53513	0.02795	0.06966	0.00350	0.963	441	31	435	18	434	21	1.7	434	21
NA005A-118	3	69240	9	0.06992	0.00088	1.36894	0.06847	0.14201	0.00687	0.968	926	26	876	29	856	39	8.1	926	26
NA005A-119	2	182399	21	0.05813	0.00088	0.56894	0.02908	0.07098	0.00347	0.955	535	33	457	19	442	21	17.9	442	21
NA005A-120	1	71953	18	0.05906	0.00175	0.57690	0.03251	0.07084	0.00339	0.850	569	63	462	21	441	20	23.3	441	20
NA005A-121	2	1569333	272	0.17277	0.00181	9.31759	0.50443	0.39115	0.02078	0.981	2585	17	2370	48	2128	96	20.7	2585	17
NA005A-122	2	275222	19	0.05623	0.00071	0.56797	0.02876	0.07326	0.00359	0.968	461	28	457	18	456	22	1.2	456	22
NA005A-123	2	469960	12	0.09154	0.00095	3.03208	0.15361	0.24023	0.01191	0.979	1458	20	1416	38	1388	62	5.3	1458	20
NA005A-124	2	118739	9	0.07294	0.00080	1.62809	0.08114	0.16189	0.00787	0.975	1012	22	981	31	967	44	4.8	1012	22
NA005A-125	2	228791	103	0.06466	0.00101	0.65408	0.03415	0.07337	0.00366	0.954	763	33	511	21	456	22	41.6	456	22
NA005A-126	2	49712	13	0.05570	0.00097	0.55122	0.02987	0.07177	0.00368	0.947	441	38	446	19	447	22	-1.5	447	22
NA005A-127	2	70848	12	0.05554	0.00100	0.55400	0.03069	0.07235	0.00379	0.945	434	40	448	20	450	23	-3.9	450	23
NA005A-128	2	183598	21	0.18830	0.00197	13.19534	0.66755	0.50824	0.02516	0.978	2727	17	2694	47	2649	107	3.5	2727	17
NA005A-129	2	242530	28	0.05896	0.00106	0.59195	0.03050	0.07281	0.00352	0.937	566	39	472	19	453	21	20.6	453	21
NA005A-130	1	42501	6	0.05467	0.00087	0.53776	0.02824	0.07134	0.00357	0.953	399	35	437	18	444	21	-11.8	444	21

Notes and calculations as Table 1.

TABLE 4

Laser ablation U/Pb isotopic data for sample NA001A, Burtts Corner Formation

Burtts Corner Fm. (NA001A)	Morph.	Isotopic ratios									Ages (Ma)						disc.	reported age	
sample name		^{206}Pb (cps)	^{204}Pb (cps)	$\frac{^{207}Pb}{^{206}Pb}$	2σ	$\frac{^{207}Pb}{^{235}U}$	2σ	$\frac{^{206}Pb}{^{238}U}$	2σ	ρ	$\frac{^{207}Pb}{^{206}Pb}$	2σ	$\frac{^{207}Pb}{^{235}U}$	2σ	$\frac{^{206}Pb}{^{238}U}$	2σ	%	(Ma)	2σ
NA001A-001	1	161231	56	0.06486	0.00160	0.94860	0.05799	0.10608	0.00594	0.915	770	51	677	30	650	35	16.3	650	35
NA001A-002	2	86915	32	0.07371	0.00093	1.54231	0.08498	0.15175	0.00814	0.973	1034	25	947	33	911	45	12.7	1034	25
NA001A-003	3	235024	36	0.06173	0.00123	0.85774	0.04658	0.10077	0.00509	0.930	665	42	629	25	619	30	7.2	619	30
NA001A-004	2	272467	7152	0.40895	0.03892	7.49725	0.97810	0.13296	0.01186	0.684	3942	136	2173	111	805	67	84.2	3942	136
NA001A-005	3	69125	79	0.06383	0.00145	1.06075	0.06050	0.12052	0.00631	0.917	736	47	734	29	734	36	0.4	734	36
NA001A-006	2	31906	70	0.07293	0.00134	1.70842	0.09394	0.16989	0.00880	0.942	1012	37	1012	35	1011	48	0.1	1012	37
NA001A-007	2	242104	106	0.07518	0.00132	1.55112	0.09788	0.14965	0.00907	0.961	1073	35	951	38	899	51	17.4	1073	35
NA001A-008	2	139034	102	0.10085	0.00114	3.98138	0.22056	0.28631	0.01553	0.979	1640	21	1630	44	1623	77	1.2	1640	21
NA001A-009	2	66206	64	0.05604	0.00128	0.59012	0.03584	0.07638	0.00430	0.926	454	50	471	23	474	26	-4.7	474	26
NA001A-010	2	166800	79	0.08654	0.00094	2.71653	0.14476	0.22766	0.01188	0.979	1350	21	1333	39	1322	62	2.3	1350	21
NA001A-011	2	266175	34	0.05753	0.00114	0.64071	0.03478	0.08077	0.00408	0.931	512	43	503	21	501	24	2.3	501	24
NA001A-012	2	12355	37	0.06847	0.00223	1.58962	0.09762	0.16839	0.00877	0.848	883	66	966	38	1003	48	-14.7	883	66
NA001A-013	2	653476	70	0.09259	0.00098	2.71900	0.15981	0.21297	0.01231	0.984	1480	20	1334	43	1245	65	17.5	1480	20
NA001A-014	1	26383	40	0.05229	0.00196	0.48982	0.03231	0.06794	0.00368	0.822	298	83	405	22	424	22	-43.6	424	22
NA001A-015	2	57551	41	0.07979	0.00102	2.13634	0.11915	0.19418	0.01054	0.973	1192	25	1161	38	1144	57	4.4	1192	25
NA001A-016	2	324743	61	0.10975	0.00135	3.04297	0.23846	0.20108	0.01556	0.988	1795	22	1418	58	1181	83	37.4	1795	22
NA001A-017	2	246187	59	0.11225	0.00117	4.82753	0.25945	0.31193	0.01645	0.981	1836	19	1790	44	1750	80	5.3	1836	19
NA001A-018	2	98382	44	0.08018	0.00100	2.16004	0.11659	0.19538	0.01026	0.973	1201	24	1168	37	1150	55	4.6	1201	24
NA001A-019	2	148966	60	0.06966	0.00080	1.49896	0.08048	0.15606	0.00818	0.977	918	24	930	32	935	45	-1.9	918	24
NA001A-020	2	241907	58	0.12832	0.00132	6.57839	0.36375	0.37181	0.02020	0.982	2075	18	2056	48	2038	94	2.1	2075	18
NA001A-021	2	68449	39	0.05845	0.00127	0.61774	0.03305	0.07665	0.00375	0.914	547	47	488	21	476	22	13.4	476	22
NA001A-022	2	145851	112	0.10006	0.00259	3.39424	0.20779	0.24602	0.01365	0.906	1625	47	1503	47	1418	70	14.2	1625	47
NA001A-023	2	55324	66	0.06408	0.00151	0.86057	0.04876	0.09740	0.00502	0.909	744	49	630	26	599	29	20.4	599	29
NA001A-024	2	783096	43	0.07791	0.00080	2.12882	0.11484	0.19818	0.01049	0.982	1144	20	1158	37	1166	56	-2.0	1144	20
NA001A-025	2	49528	42	0.05795	0.00132	0.62994	0.03597	0.07884	0.00413	0.917	528	49	496	22	489	25	7.6	489	25
NA001A-026	3	136968	81	0.11620	0.00128	5.28256	0.29560	0.32973	0.01809	0.980	1898	20	1866	47	1837	87	3.7	1898	20
NA001A-027	1	64117	40	0.05856	0.00134	0.64813	0.03786	0.08027	0.00432	0.921	551	49	507	23	498	26	10.0	498	26
NA001A-028	2	52629	68	0.05979	0.00155	0.64683	0.03513	0.07846	0.00375	0.879	596	55	507	21	487	22	19.0	487	22
NA001A-029	2	142554	49	0.10489	0.00114	4.15142	0.22126	0.28705	0.01498	0.979	1712	20	1664	43	1627	75	5.7	1712	20
NA001A-030	2	705819	72	0.06115	0.00121	0.88099	0.04651	0.10450	0.00512	0.927	644	42	642	25	641	30	0.6	641	30
NA001A-031	2	156214	115	0.13260	0.00142	6.72387	0.39733	0.36776	0.02137	0.983	2133	19	2076	51	2019	100	6.2	2133	19
NA001A-032	2	570090	210	0.06372	0.00135	0.94139	0.05407	0.10715	0.00572	0.929	732	44	674	28	656	33	10.9	656	33
NA001A-033	2	55811	129	0.07642	0.00101	1.88147	0.10416	0.17857	0.00960	0.971	1106	26	1075	36	1059	52	4.6	1106	26
NA001A-034	2	14125	119	0.08004	0.00238	1.74298	0.11341	0.15794	0.00914	0.890	1198	58	1025	41	945	51	22.7	1198	58
NA001A-035	2	71425	141	0.05945	0.00126	0.67128	0.03741	0.08189	0.00422	0.925	584	45	521	22	507	25	13.6	507	25
NA001A-036	2	195703	178	0.07230	0.00082	1.62299	0.09720	0.16281	0.00957	0.982	994	23	979	37	972	53	2.4	994	23

TABLE 4
(continued)

Burtts Corner Fm. (NA001A)	Morph.	Isotopic ratios									Ages (Ma)						disc.	reported age	
sample name		^{206}Pb (cps)	^{204}Pb (cps)	$\frac{^{207}Pb}{^{206}Pb}$	2σ	$\frac{^{207}Pb}{^{235}U}$	2σ	$\frac{^{206}Pb}{^{238}U}$	2σ	ρ	$\frac{^{207}Pb}{^{206}Pb}$	2σ	$\frac{^{207}Pb}{^{235}U}$	2σ	$\frac{^{206}Pb}{^{238}U}$	2σ	%	(Ma)	2σ
NA001A-037	2	222612	137	0.07823	0.00083	2.09941	0.11445	0.19465	0.01041	0.981	1153	21	1149	37	1146	56	0.6	1153	21
NA001A-038	2	394252	135	0.06459	0.00128	1.18341	0.05880	0.13288	0.00606	0.917	761	41	793	27	804	34	-6.0	804	34
NA001A-039	2	274946	118	0.07381	0.00079	1.82609	0.10363	0.17944	0.01000	0.982	1036	22	1055	37	1064	54	-2.9	1036	22
NA001A-040	2	141324	113	0.07785	0.00086	2.04997	0.10553	0.19097	0.00960	0.977	1143	22	1132	35	1127	52	1.6	1143	22
NA001A-041	2	282157	55	0.09389	0.00099	3.33289	0.18458	0.25746	0.01400	0.982	1506	20	1489	42	1477	71	2.2	1506	20
NA001A-042	2	47607	68	0.05632	0.00143	0.59826	0.03592	0.07704	0.00419	0.906	465	55	476	23	478	25	-3.0	478	25
NA001A-043	2	60207	53	0.05603	0.00129	0.56477	0.03378	0.07311	0.00404	0.923	453	50	455	22	455	24	-0.3	455	24
NA001A-044	2	48249	52	0.07971	0.00108	2.16543	0.11295	0.19703	0.00993	0.966	1190	26	1170	36	1159	53	2.8	1190	26
NA001A-045	2	29547	30	0.05582	0.00180	0.61604	0.04192	0.08005	0.00479	0.880	445	70	487	26	496	29	-12.0	496	29
NA001A-046	2	21422	34	0.05257	0.00154	0.56244	0.03311	0.07760	0.00396	0.867	310	65	453	21	482	24	-57.4	482	24
NA001A-047	2	33722	29	0.06769	0.00133	1.40389	0.07872	0.15042	0.00790	0.936	859	40	891	33	903	44	-5.5	859	40
NA001A-048	2	280159	9	0.10792	0.00113	4.55803	0.26544	0.30633	0.01755	0.984	1765	19	1742	47	1723	86	2.7	1765	19
NA001A-049	2	824725	49	0.09904	0.00104	3.52285	0.21475	0.25797	0.01549	0.985	1606	20	1532	47	1479	79	8.8	1606	20
NA001A-050	2	304338	26	0.07532	0.00083	1.86906	0.10267	0.17997	0.00969	0.980	1077	22	1070	36	1067	53	1.0	1077	22
NA001A-051	2	156048	1	0.07529	0.00088	1.79116	0.09836	0.17254	0.00926	0.977	1076	23	1042	35	1026	51	5.0	1076	23
NA001A-052	2	265459	0	0.10033	0.00103	3.89627	0.20984	0.28166	0.01489	0.982	1630	19	1613	43	1600	74	2.1	1630	19
NA001A-053	2	179799	4	0.05733	0.00121	0.59379	0.03084	0.07511	0.00356	0.913	504	46	473	19	467	21	7.7	467	21
NA001A-054	2	60731	119	0.05670	0.00153	0.58420	0.03680	0.07473	0.00425	0.903	480	59	467	23	465	25	3.3	465	25
NA001A-055	2	363070	170	0.09999	0.00118	3.81121	0.21063	0.27644	0.01493	0.977	1624	22	1595	44	1573	75	3.5	1624	22
NA001A-056	2	366090	151	0.05695	0.00118	0.60235	0.03872	0.07671	0.00467	0.947	490	45	479	24	476	28	2.8	476	28
NA001A-057	2	395223	136	0.09836	0.00108	3.56699	0.23783	0.26301	0.01730	0.986	1593	20	1542	52	1505	88	6.2	1593	20
NA001A-058	2	121438	99	0.05677	0.00116	0.57483	0.03455	0.07343	0.00415	0.940	483	45	461	22	457	25	5.6	457	25
NA001A-059	2	218791	78	0.09141	0.00249	2.94897	0.21544	0.23398	0.01586	0.928	1455	51	1395	54	1355	82	7.6	1455	51
NA001A-060	3	375351	79	0.11241	0.00118	4.89718	0.29747	0.31596	0.01890	0.985	1839	19	1802	50	1770	92	4.3	1839	19
NA001A-061	3	287070	33	0.08656	0.00091	2.67460	0.16630	0.22410	0.01373	0.985	1351	20	1321	45	1304	72	3.9	1351	20
NA001A-062	2	786279	43	0.08581	0.00095	2.64849	0.15509	0.22385	0.01287	0.982	1334	21	1314	42	1302	67	2.6	1334	21
NA001A-063	3	364332	24	0.07323	0.00077	1.64905	0.08863	0.16332	0.00861	0.981	1020	21	989	33	975	48	4.8	1020	21
NA001A-064	1	127034	21	0.05532	0.00117	0.54984	0.03264	0.07208	0.00400	0.935	425	46	445	21	449	24	-5.7	449	24
NA001A-065	2	190825	25	0.13261	0.00139	6.79370	0.40166	0.37157	0.02162	0.984	2133	18	2085	51	2037	101	5.2	2133	18
NA001A-066	2	150682	35	0.07458	0.00094	1.81015	0.10705	0.17603	0.01017	0.977	1057	25	1049	38	1045	56	1.2	1057	25
NA001A-066-B	2	400697	34	0.05631	0.00113	0.61437	0.03720	0.07913	0.00452	0.944	465	44	486	23	491	27	-5.9	491	27
NA001A-067	2	94125	32	0.05427	0.00119	0.51732	0.03234	0.06913	0.00405	0.936	382	49	423	21	431	24	-13.1	431	24
NA001A-068	2	151701	39	0.06008	0.00125	0.88421	0.04793	0.10674	0.00535	0.924	606	44	643	26	654	31	-8.2	654	31
NA001A-069	3	5436	36	0.02396	0.01199	0.33431	0.16870	0.10121	0.00638	0.125	-1912	1278	293	121	621	37	139.4	621	37
NA001A-070	2	138509	50	0.06229	0.00126	0.95566	0.05289	0.11127	0.00573	0.931	684	43	681	27	680	33	0.6	680	33

TABLE 4
(continued)

Burtts Corner Fm. (NA001A)	Morph.	Isotopic ratios									Ages (Ma)						disc.	reported age	
sample name		^{206}Pb (cps)	^{204}Pb (cps)	$\frac{^{207}Pb}{^{206}Pb}$	2σ	$\frac{^{207}Pb}{^{235}U}$	2σ	$\frac{^{206}Pb}{^{238}U}$	2σ	ρ	$\frac{^{207}Pb}{^{206}Pb}$	2σ	$\frac{^{207}Pb}{^{235}U}$	2σ	$\frac{^{206}Pb}{^{238}U}$	2σ	%	(Ma)	2σ
NA001A-071	2	95934	44	0.05543	0.00121	0.57510	0.03157	0.07525	0.00379	0.918	430	48	461	20	468	23	-9.2	468	23
NA001A-072	2	166508	38	0.10341	0.00110	4.02909	0.22007	0.28259	0.01514	0.981	1686	19	1640	43	1604	76	5.5	1686	19
NA001A-073	2	71706	28	0.05256	0.00121	0.51395	0.03640	0.07092	0.00475	0.946	310	51	421	24	442	29	-44.0	442	29
NA001A-074	3	71105	25	0.06838	0.00110	1.39815	0.08519	0.14829	0.00872	0.965	880	33	888	35	891	49	-1.4	880	33
NA001A-075	1	87070	46	0.05254	0.00119	0.50665	0.03055	0.06993	0.00391	0.927	309	51	416	20	436	24	-42.3	436	24
NA001A-076	2	392298	13	0.10169	0.00106	3.92633	0.27583	0.28003	0.01946	0.989	1655	19	1619	55	1592	97	4.3	1655	19
NA001A-077	2	946428	44	0.07179	0.00073	1.60132	0.09868	0.16177	0.00983	0.986	980	21	971	38	967	54	1.5	980	21
NA001A-078A	2	136859	17	0.05853	0.00122	0.80640	0.05041	0.09992	0.00589	0.942	550	45	600	28	614	34	-12.2	614	34
NA001A-078B	2	87908	25	0.05714	0.00125	0.81140	0.04861	0.10299	0.00574	0.931	497	48	603	27	632	33	-28.5	632	33
NA001A-079	2	246492	19	0.07410	0.00084	1.85248	0.10221	0.18130	0.00979	0.979	1044	23	1064	36	1074	53	-3.1	1044	23
NA001A-080	2	159138	110	0.06266	0.00167	0.67316	0.04244	0.07792	0.00445	0.906	697	56	523	25	484	27	31.7	484	27
NA001A-081	2	70726	10	0.06023	0.00126	0.82126	0.04909	0.09890	0.00554	0.937	612	45	609	27	608	32	0.7	608	32
NA001A-082	2	221241	23	0.05659	0.00118	0.62054	0.03391	0.07953	0.00402	0.925	476	45	490	21	493	24	-3.8	493	24
NA001A-083	1	129081	37	0.06015	0.00150	0.73524	0.04452	0.08865	0.00489	0.911	609	53	560	26	548	29	10.5	548	29
NA001A-084	2	48921	41	0.07622	0.00117	1.94444	0.11547	0.18503	0.01061	0.966	1101	30	1097	39	1094	57	0.6	1101	30
NA001A-085	2	62615	59	0.05764	0.00179	0.64023	0.04036	0.08056	0.00442	0.870	516	67	502	25	499	26	3.4	499	26
NA001A-086	2	459751	35	0.07585	0.00077	1.86573	0.11245	0.17840	0.01060	0.986	1091	20	1069	39	1058	58	3.3	1091	20
NA001A-087	2	416914	16	0.08089	0.00083	2.28078	0.12373	0.20449	0.01089	0.982	1219	20	1206	38	1199	58	1.7	1219	20
NA001A-088	2	329512	30	0.10102	0.00107	3.87635	0.19829	0.27829	0.01393	0.978	1643	20	1609	40	1583	70	4.1	1643	20
NA001A-089	2	170933	21	0.21210	0.00219	15.89050	0.91925	0.54338	0.03093	0.984	2922	17	2870	54	2798	128	5.2	2922	17
NA001A-090	2	380547	22	0.06073	0.00120	0.89546	0.05263	0.10694	0.00592	0.942	630	42	649	28	655	34	-4.2	655	34
NA001A-091	2	94081	14	0.07366	0.00091	1.67117	0.09766	0.16454	0.00940	0.977	1032	25	998	36	982	52	5.3	1032	25
NA001A-092	2	374724	14	0.09849	0.00102	3.72485	0.21698	0.27430	0.01573	0.984	1596	19	1577	46	1563	79	2.3	1596	19
NA001A-093	2	996156	6	0.08788	0.00090	2.89534	0.17576	0.23894	0.01430	0.986	1380	20	1381	45	1381	74	-0.1	1380	20
NA001A-094	3	539507	7	0.11654	0.00119	5.40098	0.30453	0.33613	0.01864	0.983	1904	18	1885	47	1868	89	2.2	1904	18
NA001A-095	2	584145	23	0.07584	0.00083	1.95887	0.12578	0.18734	0.01185	0.985	1091	22	1101	42	1107	64	-1.6	1091	22
NA001A-096	3	281946	24	0.06228	0.00129	0.93118	0.05291	0.10843	0.00574	0.931	684	44	668	27	664	33	3.1	664	33
NA001A-097	2	405625	6	0.07759	0.00080	2.01005	0.12065	0.18789	0.01111	0.985	1136	20	1119	40	1110	60	2.5	1136	20
NA001A-098	2	46453	6	0.05496	0.00142	0.60187	0.03763	0.07942	0.00452	0.911	411	57	478	24	493	27	-20.7	493	27
NA001A-099	2	2167303	225	0.09993	0.00103	3.19930	0.17610	0.23220	0.01256	0.982	1623	19	1457	42	1346	65	18.9	1623	19
NA001A-100	2	321964	13	0.08599	0.00089	2.69988	0.14212	0.22772	0.01175	0.981	1338	20	1328	38	1323	61	1.3	1338	20
NA001A-101	2	439308	21	0.11526	0.00128	5.19969	0.28811	0.32717	0.01776	0.980	1884	20	1853	46	1825	86	3.6	1884	20
NA001A-102	2	34211	24	0.05549	0.00177	0.58020	0.03721	0.07583	0.00422	0.867	432	70	465	24	471	25	-9.4	471	25
NA001A-103	2	190834	32	0.10148	0.00112	3.75327	0.21543	0.26824	0.01511	0.981	1651	20	1583	45	1532	76	8.1	1651	20
NA001A-104	2	204884	71	0.08769	0.00096	2.78408	0.15416	0.23026	0.01250	0.980	1376	21	1351	41	1336	65	3.2	1376	21
NA001A-105	2	188353	31	0.08817	0.00099	2.56821	0.17357	0.21126	0.01408	0.986	1386	21	1292	48	1236	75	11.9	1386	21

TABLE 4
(continued)

Burtts Corner Fm. (NA001A)	Morph.	Isotopic ratios									Ages (Ma)						disc.	reported age	
sample name		^{206}Pb (cps)	^{204}Pb (cps)	$\frac{^{207}Pb}{^{206}Pb}$	2σ	$\frac{^{207}Pb}{^{235}U}$	2σ	$\frac{^{206}Pb}{^{238}U}$	2σ	ρ	$\frac{^{207}Pb}{^{206}Pb}$	2σ	$\frac{^{207}Pb}{^{235}U}$	2σ	$\frac{^{206}Pb}{^{238}U}$	2σ	%	(Ma)	2σ
NA001A-106	2	1166414	33	0.18568	0.00188	12.17228	0.61194	0.47546	0.02341	0.979	2704	17	2618	46	2507	101	8.8	2704	17
NA001A-107	2	130697	30	0.08639	0.00098	2.75083	0.16220	0.23094	0.01336	0.981	1347	22	1342	43	1339	70	0.6	1347	22
NA001A-108	2	284767	35	0.08983	0.00098	2.98299	0.18758	0.24083	0.01492	0.985	1422	21	1403	47	1391	77	2.4	1422	21
NA001A-109	2	338222	56	0.07924	0.00092	1.95692	0.11014	0.17911	0.00986	0.978	1178	23	1101	37	1062	54	10.7	1178	23
NA001A-110	2	189813	61	0.07361	0.00103	1.72991	0.09402	0.17044	0.00895	0.966	1031	28	1020	34	1015	49	1.7	1031	28
NA001A-111	2	284964	15	0.07488	0.00079	1.77778	0.10055	0.17220	0.00957	0.982	1065	21	1037	36	1024	52	4.2	1065	21
NA001A-112	2	63308	43	0.06211	0.00180	0.74446	0.04561	0.08694	0.00469	0.880	678	61	565	26	537	28	21.6	537	28
NA001A-113	2	60966	58	0.05788	0.00123	0.70457	0.04083	0.08828	0.00476	0.931	525	46	542	24	545	28	-4.0	545	28
NA001A-114	2	108860	103	0.10206	0.00120	3.52020	0.21529	0.25016	0.01502	0.981	1662	22	1532	47	1439	77	14.9	1662	22
NA001A-115	2	191106	60	0.07067	0.00083	1.42078	0.08018	0.14581	0.00805	0.978	948	24	898	33	877	45	8.0	948	24
NA001A-116	3	314282	63	0.09533	0.00099	3.48306	0.18845	0.26500	0.01407	0.982	1535	19	1523	42	1515	71	1.4	1535	19
NA001A-117	2	725460	60	0.07872	0.00081	2.14760	0.12428	0.19786	0.01127	0.984	1165	20	1164	39	1164	60	0.1	1165	20
NA001A-118	2	301064	210	0.07561	0.00082	1.80754	0.10013	0.17338	0.00942	0.981	1085	22	1048	36	1031	52	5.4	1085	22
NA001A-119	3	95350	173	0.06245	0.00135	0.95984	0.06094	0.11146	0.00666	0.941	690	45	683	31	681	38	1.3	681	38
NA001A-120	2	603633	97	0.11061	0.00116	4.84937	0.24305	0.31797	0.01558	0.978	1809	19	1794	41	1780	76	1.9	1809	19
NA001A-121	2	53489	30	0.05724	0.00126	0.67654	0.04247	0.08572	0.00504	0.937	501	48	525	25	530	30	-6.1	530	30
NA001A-122	2	111329	34	0.07747	0.00084	1.98381	0.10922	0.18572	0.01003	0.981	1133	21	1110	37	1098	54	3.4	1133	21
NA001A-123	2	129686	141	0.05741	0.00126	0.60983	0.03332	0.07704	0.00386	0.916	507	47	483	21	478	23	5.9	478	23
NA001A-124	2	103721	65	0.07959	0.00101	2.16625	0.12036	0.19740	0.01068	0.973	1187	25	1170	38	1161	57	2.4	1187	25
NA001A-125	2	28228	41	0.06641	0.00185	1.37977	0.09244	0.15068	0.00918	0.909	819	57	880	39	905	51	-11.2	819	57
NA001A-126	2	179325	35	0.08953	0.00098	2.91410	0.16571	0.23606	0.01317	0.981	1416	21	1386	42	1366	68	3.9	1416	21
NA001A-127	2	65458	83	0.07436	0.00107	1.81137	0.10059	0.17667	0.00947	0.966	1051	29	1050	36	1049	52	0.3	1051	29
NA001A-128	2	358777	59	0.07797	0.00082	2.01462	0.10799	0.18741	0.00985	0.981	1146	21	1120	36	1107	53	3.7	1146	21
NA001A-129	2	1252270	643	0.10442	0.00128	3.47331	0.19714	0.24124	0.01337	0.976	1704	22	1521	44	1393	69	20.3	1704	22
NA001A-130	2	107530	180	0.07593	0.00112	1.84658	0.09941	0.17638	0.00913	0.962	1093	29	1062	35	1047	50	4.6	1093	29
NA001A-131	2	220137	7	0.06072	0.00122	0.85493	0.04733	0.10212	0.00527	0.932	629	43	627	26	627	31	0.4	627	31
NA001A-132	2	48007	5	0.05665	0.00130	0.67549	0.04011	0.08648	0.00473	0.922	478	50	524	24	535	28	-12.4	535	28
NA001A-133	2	7550	12	0.06117	0.00527	1.42939	0.14953	0.16947	0.01007	0.568	645	175	901	61	1009	55	-61.0	1009	55
NA001A-134	2	219892	12	0.07707	0.00083	1.79424	0.11703	0.16884	0.01086	0.986	1123	21	1043	42	1006	60	11.3	1123	21
NA001A-135	2	106509	5	0.08071	0.00096	2.20762	0.13664	0.19837	0.01205	0.981	1214	23	1183	42	1167	64	4.3	1214	23
NA001A-136	2	163315	34	0.05894	0.00120	0.73239	0.04244	0.09012	0.00489	0.936	565	44	558	25	556	29	1.6	556	29
NA001A-137	2	709777	901	0.11566	0.00298	4.31133	0.26942	0.27035	0.01539	0.911	1890	46	1696	50	1543	78	20.7	1890	46
NA001A-138	2	403826	55	0.10903	0.00113	4.51907	0.23996	0.30062	0.01566	0.981	1783	19	1734	43	1694	77	5.7	1783	19
NA001A-139	2	79015	12	0.05566	0.00136	0.53051	0.03347	0.06913	0.00402	0.922	439	54	432	22	431	24	1.8	431	24
NA001A-140	2	231477	13	0.05615	0.00115	0.60207	0.03266	0.07777	0.00391	0.926	458	45	479	20	483	23	-5.5	483	23
NA001A-141	1	129546	12	0.06090	0.00126	0.83194	0.05521	0.09908	0.00625	0.950	636	44	615	30	609	37	4.4	609	37

TABLE 4
(continued)

Burtts Corner Fm. (NA001A)	Morph.	Isotopic ratios									Ages (Ma)						disc.	reported age	
sample name		^{206}Pb (cps)	^{204}Pb (cps)	$\frac{^{207}Pb}{^{206}Pb}$	2σ	$\frac{^{207}Pb}{^{235}U}$	2σ	$\frac{^{206}Pb}{^{238}U}$	2σ	ρ	$\frac{^{207}Pb}{^{206}Pb}$	2σ	$\frac{^{207}Pb}{^{235}U}$	2σ	$\frac{^{206}Pb}{^{238}U}$	2σ	%	(Ma)	2σ
NA001A-106	2	1166414	33	0.18568	0.00188	12.17228	0.61194	0.47546	0.02341	0.979	2704	17	2618	46	2507	101	8.8	2704	17
NA001A-142	2	235366	17	0.07752	0.00082	1.97181	0.10317	0.18448	0.00945	0.980	1135	21	1106	35	1091	51	4.1	1135	21
NA001A-143	2	136898	11	0.08198	0.00090	2.28067	0.13437	0.20176	0.01168	0.982	1245	21	1206	41	1185	62	5.3	1245	21
NA001A-144	2	472020	7	0.06400	0.00127	1.06492	0.05816	0.12068	0.00614	0.932	742	41	736	28	734	35	1.0	734	35
NA001A-145	2	387002	30	0.09547	0.00101	3.44538	0.18468	0.26175	0.01375	0.980	1537	20	1515	41	1499	70	2.8	1537	20
NA001A-146	2	100872	23	0.07780	0.00096	2.02353	0.11815	0.18864	0.01076	0.977	1142	24	1123	39	1114	58	2.6	1142	24
NA001A-147	2	105668	63	0.08691	0.00130	2.09578	0.11599	0.17489	0.00932	0.963	1359	29	1147	37	1039	51	25.4	1359	29
NA001A-148	2	36331	8	0.07199	0.00162	1.61484	0.10329	0.16269	0.00974	0.936	986	45	976	39	972	54	1.5	986	45
NA001A-149	2	181463	12	0.07290	0.00080	1.60343	0.08349	0.15953	0.00812	0.978	1011	22	972	32	954	45	6.1	1011	22
NA001A-150	2	692730	14	0.11620	0.00119	5.17133	0.28730	0.32278	0.01762	0.983	1899	18	1848	46	1803	85	5.7	1899	18

Notes and calculations as Table 1.

0.5 ppb Tl solution (NIST SRM 997), utilizing an exponential mass fractionation law and assuming a natural $^{205}Tl/^{203}Tl$ of 2.3871. Data were reduced using an offline Excel-based spreadsheet, in which sample (unknown) isotopic ratios were corrected based on standard analyses, using a cutoff value of $^{207}Pb/^{206}Pb = 0.0658$ (800 Ma): young grains were normalized to GJ1-32, and old grains to LH94-15. This method of normalization allows unknowns to be corrected based on standards of a similar age; natural gaps in our data typically occur at 800 Ma, making this a convenient cutoff. Uncertainties were reported using a quadratic combination of the standard error of the measured isotopic ratio, and the standard deviation of the standard means. Reproducibility of the zircon standards is estimated at ~1 percent ($^{207}Pb/^{206}Pb$) and 2 percent ($^{206}Pb/^{238}U$) (2σ). Sample measurements were discarded in the case of obvious inclusions that contributed to analysis (and could not be isolated), an extreme common Pb component, or analysis of non-zircons. Common Pb corrections after Simonetti and others (2005) were typically applied when measured ^{204}Pb exceeded ~400 cps. The software Isoplot (version 3.75: Ludwig, 2012) was employed to produce relative probability density plots for zircons 90 percent concordant or better. Concordia diagrams, weighted means, MSWD calculations, and other statistical analyses were prepared with the same software. Cumulative probability plots and Kolmogorov-Smirnov tests were calculated using analysis tools from the Arizona LaserChron Center (Gehrels and others, 2006).

RESULTS

Sampled Units

Lithological and petrographic observations (and classification after Dott, 1964) from each of the four sampled formations bear broadly similar characteristics (see below), and are consistent with their interpretation as polydeformed, turbiditic material deposited in a narrowing seaway. Zircon grains from each of the four formations share similar characteristics (fig. 4). They vary from rounded, abraded shapes to euhedral. Older zircons more commonly show rounded forms, and young zircons (< ~800 Ma) demonstrate more euhedral outlines. Each morphology occurs in a range of grain sizes, but the largest zircons tend to be both more rounded and older. Fractured zircon shapes are uncommon, but occur in grains that are otherwise either angular or rounded. Occurrences of rounded zircons with sharp, cross-cutting fractures suggest that fracturing occurred late in their history, possibly during the mineral separation process. Common internal textures include oscillatory zoning (with or without inherited cores), overgrowths, and various textures related to metasomatism, metamictization, or recrystallization.

Digdeguash Formation.—The Digdeguash Formation was examined in the Digdeguash river where outcrops exhibit three generations of structures. The earliest fabric is a bedding-parallel S1 cleavage. F1 folds are not observed at outcrop scale. F2 folds gently plunge eastward and exhibit parasitic folding, and are refolded by F3 folds. These latest folds are open, with axial traces trending NNE-SSW.

Because of the lack of fossils in the type section, the Digdeguash Formation was sampled at a known fossil locality (Upper Rhuddanian *Coronograptus cyphus* zone; Fyffe and Riva, 2001) in a discontinuous exposure in woodland southwest of Otter Lake (fig. 2). Thin section analysis (fig. 5) using optical and electron microprobe methods indicates the rock is a feldspathic wacke, with a relatively high amount of matrix (~40%). However, it is likely that this high matrix proportion conceals an amount of fine-grained rock fragments, modified by diagenesis, metamorphism and deformation. Recognizable framework grains consist of quartz (~50%, approximately normalized to total QFL components; subgrain boundaries and polycrystalline quartz are particularly common) with a large amount of feldspar (~40%, mainly plagioclase) and some lithic

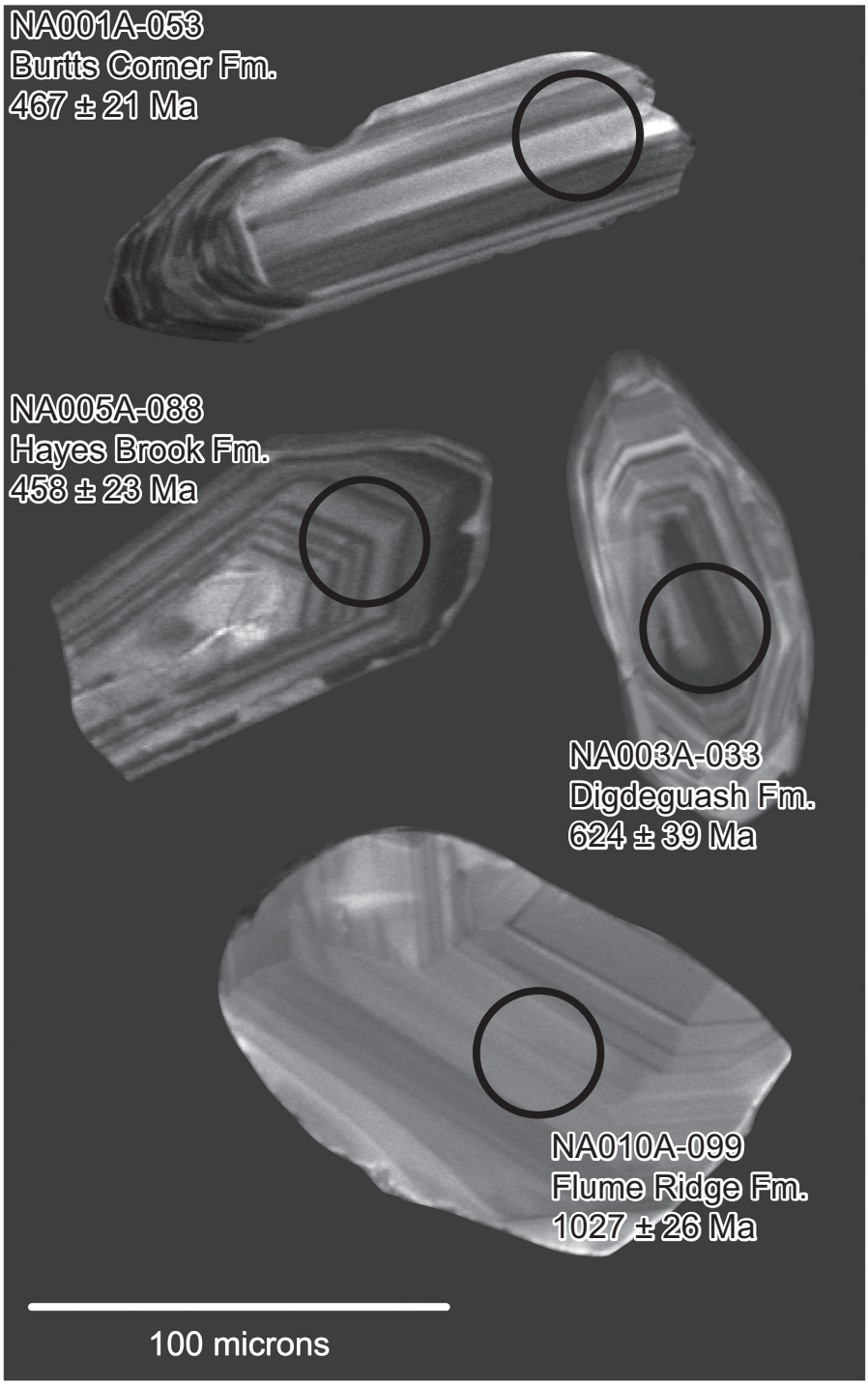

Fig. 4. CL (cathodoluminescence) images of selected zircons from four formations of the Fredericton Trough. Circles, marked during the ablation process, show size and location of 30 micron laser ablation pits.

Fig. 5. Representative thin section photomicrographs from sampled units of four formations of the Fredericton Trough. PPL: plane polarized light, XPL: cross polarized light. (A) Digdeguash Formation, NA003A, PPL. (B) Digdeguash Formation, NA003A, XPL. (C) Flume Ridge Formation, NA010A, PPL. (D) Flume Ridge Formation, NA010A, XPL. (E) Hayes Brook Formation, NA005A, PPL. (F) Hayes Brook Formation, NA005A, XPL. (G) Burtts Corner Formation, NA001A, PPL. (H) Burtts Corner Formation, NA001A, XPL.

fragments (~5%). Accessory phases include mainly biotite and opaque minerals with rare zircon and apatite. Framework grains are mainly subangular, and typically show evidence of strain. Biotite comprises most of the matrix, along with a small amount of quartz and feldspar, and uncommon heavy minerals and opaques. A persistent foliation is present, approximately 60° to bedding, and is defined mainly by biotite, and to a lesser extent lath-shaped feldspars. Because of the discontinuous nature of the outcrop, it is not possible to place this fabric into the structural overprinting history defined at the type section. Detrital zircon morphologies in the Digdeguash Formation (table 1; fig. 4) include mainly subhedral, subangular forms. Young zircons (< ~800 Ma) are commonly more angular, with high aspect ratios. Older zircons, in contrast, are more rounded, equant, and anhedral.

Flume Ridge Formation.—The Flume Ridge Formation contains multiple generations of mapped folds (for example, Smith, 2005), though these structures are commonly obscured in outcrop by abundant brittle fractures. The sampled section (fig. 2) is largely overturned, alternating with shorter intervals of upright beds, but the corresponding outcrop-scale fold closures themselves were not observed. Discrete, highly sheared intervals typically divide upright from overturned sections, and contain small folds, rare axial planar cleavage, and small duplexes (< 20 cm width).

The sampled rock (fig. 5) is a lithic wacke, including ~60 percent matrix, although much of this may represent modified rock fragments and possibly highly altered feldspar. Approximate QFL proportions include mainly quartz (~75%), and lithic fragments (~25%). Detrital accessory minerals include mainly muscovite, and smaller amounts of carbonate lithoclasts, chlorite, opaques, and rare zircon. The morphologies of the separated zircons (table 2; fig. 4) include proportionally more rounded, subhedral to anhedral grains than in the underlying Digdeguash Formation. These rounded, abraded and equant grains typically show ages older than 800 Ma, whereas younger zircons (< ~800 Ma) are, as previously observed, more angular and euhedral. The matrix is composed mainly of calcite, muscovite, and fine quartz, with less common chlorite, opaques, and heavy minerals. Alteration is common, particularly of the matrix, and products include sericite, iron carbonate, and other iron-rich phases. A prominent foliation is defined by mostly muscovite and strained or recrystallized phases, and is about 60° to bedding.

Hayes Brook Formation.—The Hayes Brook Formation shows multiple generations of map-scale folds (for example, Smith and Fyffe, 2006), but may appear less deformed on outcrop scale relative to other sections of the Fredericton Trough. The sampled section, at a Coronograptus cyphus fossil locality (fig. 2; Cumming, 1960; Fyffe, 1995), contains consistently upright, steeply dipping beds striking NE (for example, 045/80). Visible cleavage in outcrop is at a low angle to bedding, and is strictly limited to thin finer-grained beds between thickly bedded sandstones.

Thin section analysis (fig. 5) indicates the rock is a feldspathic wacke, comprising ~45 percent matrix. Approximate framework grain proportions include quartz (~50%), feldspar (40%, mainly albite), and lithic fragments (~10%, including chert, volcanics, and granitoids). Epidote and titanite make up a small portion of the detrital components. Framework grains are mainly subrounded to subangular. The matrix fraction of the rock includes quartz and feldspar, calcite, muscovite, and chlorite. There is no obvious or persistent fabric in thin section, despite the presence of orientable phases, in contrast to outcrop observations of bedding in coarser sandstone layers and cleavage in finer-grained siltstone and mudstone. Detrital zircons in the Hayes Brook Formation (table 3; fig. 4) include mostly subhedral, subangular morphologies. Relatively young zircons (< ~800 Ma) continue to correlate strongly with angular and euhedral shapes. Older grains include proportionally more rounded, anhedral forms.

Burtts Corner Formation.—Three distinct generations of folds have been identified in turbidites of the Burtts Corner Formation by Park and Whitehead (2003). The most prominent are chevron-type, F2 folds locally exhibiting a well-developed axial planar cleavage. Interlimb angles tighten, from open to tight, with increasing proximity to the Fredericton Fault, while fold hinges become more curvilinear. These F2 folds plunge gently NE and SW, roughly parallel to the strike of the nearby Fredericton Fault. F1 fold closures have not been observed in outcrop, but limited occurrence is suggested by Park and Whitehead (2003). F3 structures reported by the same authors include kink bands, and chevron folds with sub-horizontal axial planes and poorly developed axial planar cleavage. The sampled section (fig. 2), consisting of gray lithic wacke interbedded with dark gray siltstone and shale, bore graptolites of the *Cyrtograptus linnarssoni (rigidus)* zone (Fyffe, 1995).

Thin section analysis (fig. 5) indicates the rock is a feldspathic wacke with a high proportion of matrix (~55%), again possibly including altered rock fragments. Framework grains consist of quartz (~75%) with a significant amount of feldspar (~20%, mainly albite), and minor recognizable lithic fragments (~3%). Major components are mainly subangular, and irregular grain boundaries are particularly common in quartz. Common accessories include muscovite, tourmaline and opaque minerals. Identifiable matrix consists mainly of calcite and white mica, with a small amount of chlorite. A strong foliation is defined primarily by white mica, and is about 50° to 60° from bedding. Zircons separated from the Burtts Corner Formation (table 4; fig. 4) show subequal amounts of angular and rounded morphologies. Angular and elongate forms continue to be more common in young zircons (< ~800 Ma). Older zircons, in contrast, are commonly more rounded and equant.

Detrital Zircon Geochronology

South of the Fredericton Fault.—Detrital zircon concordia plots and probability density distributions are shown in figures 6 and 7 for the four analyzed formations of the Kingsclear Group. To the south of the Fredericton Fault, the upper Rhuddanian Digdeguash Formation (fig. 7; table 1) shows a dominant statistical peak at *ca.* 615 Ma, consistent with sources in the peri-Gondwanan terranes of Ganderia and Avalonia. A scatter of other Proterozoic zircons range from 1.0 to 2.0 Ga, and a minor Cambrian peak (488.9 ± 7.1 Ma; MSWD of 0.63, probability of fit 0.71) is also observed.

The overlying Flume Ridge Formation (fig. 7; table 2) shows a distinctly different zircon signature. A strong asymmetric latest Mesoproterozoic ("Grenville") peak, at about 1.0 Ga, is accompanied by a range of Proterozoic zircons up to 1.9 Ga, – a distribution closely resembling those from the Laurentian margin (Cawood and Nemchin, 2001; Waldron and others, 2008, 2014a) indicating Laurentian provenance. It bears a strong peak in the Ordovician (*ca.* 465 Ma), probably derived from an arc associated with Iapetan subduction. It contains only a single Neoproterozoic zircon (grain NA010A-130, 582 ± 49 Ma), in contrast to the abundant population in the underlying Digdeguash Formation, suggesting that peri-Gondwanan sources are minor. Rare zircons from 2.1 to 2.8 Ga could also represent a combination of Laurentian and minor peri-Gondwanan sources.

North of the Fredericton Fault.—North of the fault, the upper Rhuddanian Hayes Brook Formation (fig. 7; table 3) displays a strong Ordovician peak (*ca.* 465 Ma), probably representing an arc source. The majority of the remaining zircon is contained in an asymmetric "Grenville" peak at 1.0 Ga, accompanied by a range of Proterozoic zircons to 1.8 Ga, and a scatter of zircons from 2.4 to 2.8 Ga, indicating Laurentian sediment input. There are no zircons in the "Eburnean" (2.0–2.2 Ga) range, nor *circa* 600 Ma that would indicate peri-Gondwanan sources.

The Burtts Corner Formation (fig. 7; table 4), sampled at a mid-Wenlock fossil locality, similarly displays an asymmetric "Grenville" peak at 1.0 to 1.1 Ga, suggesting

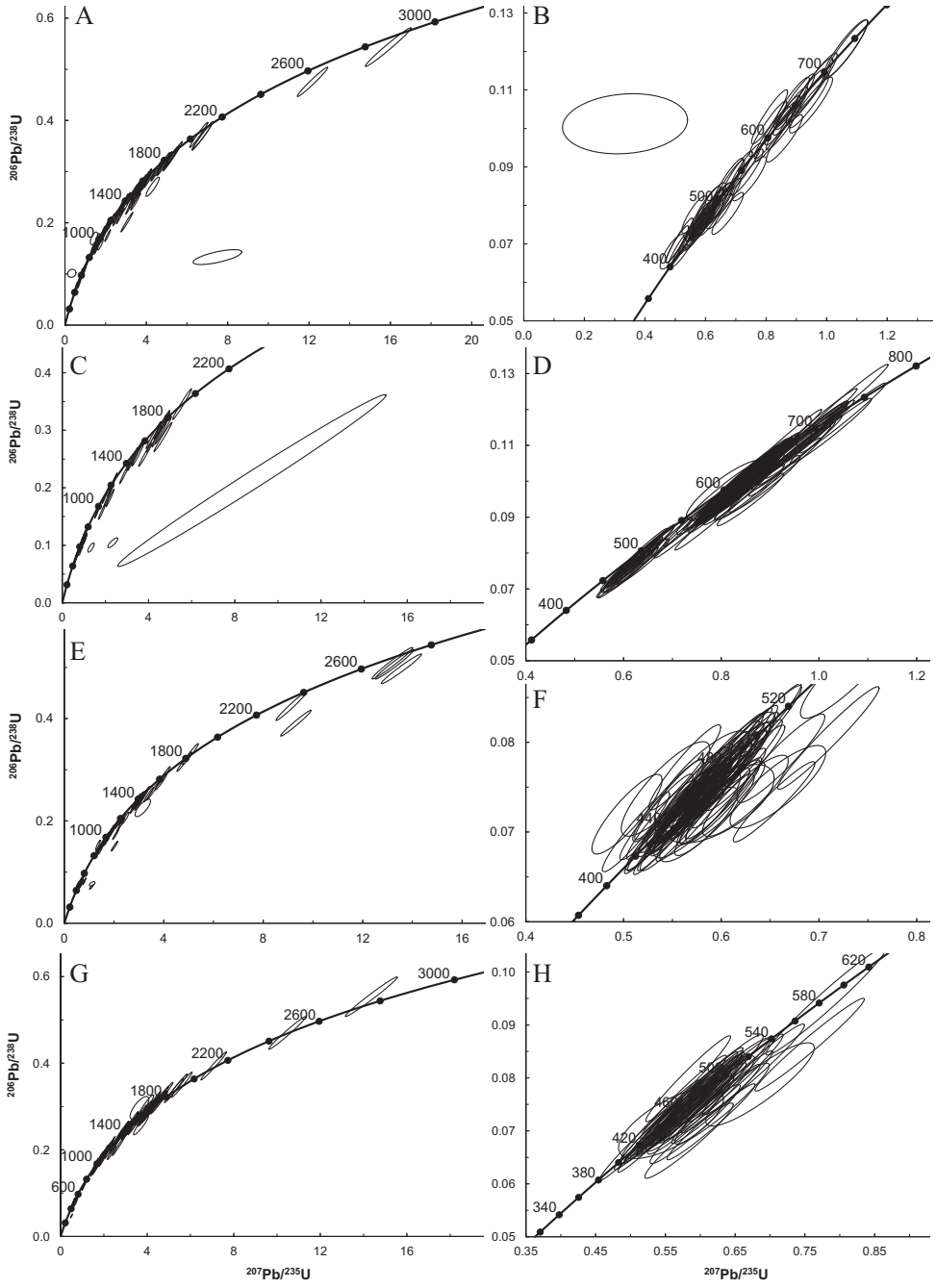

Fig. 6. Concordia plots showing analytical results for Silurian samples from the Fredericton Trough. Data point error ellipses are 2σ. Plots show all grains analyzed, including highly discordant results that are disregarded in subsequent plots. Left-hand plots show full range of results; right-hand plots show enlarged view of younger populations. (A, B) Digdeguash Formation NA003A. (C, D) Flume Ridge Formation NA010A. (E, F) Hayes Brook Formation NA005A. (G, H) Burtts Corner Formation NA001A.

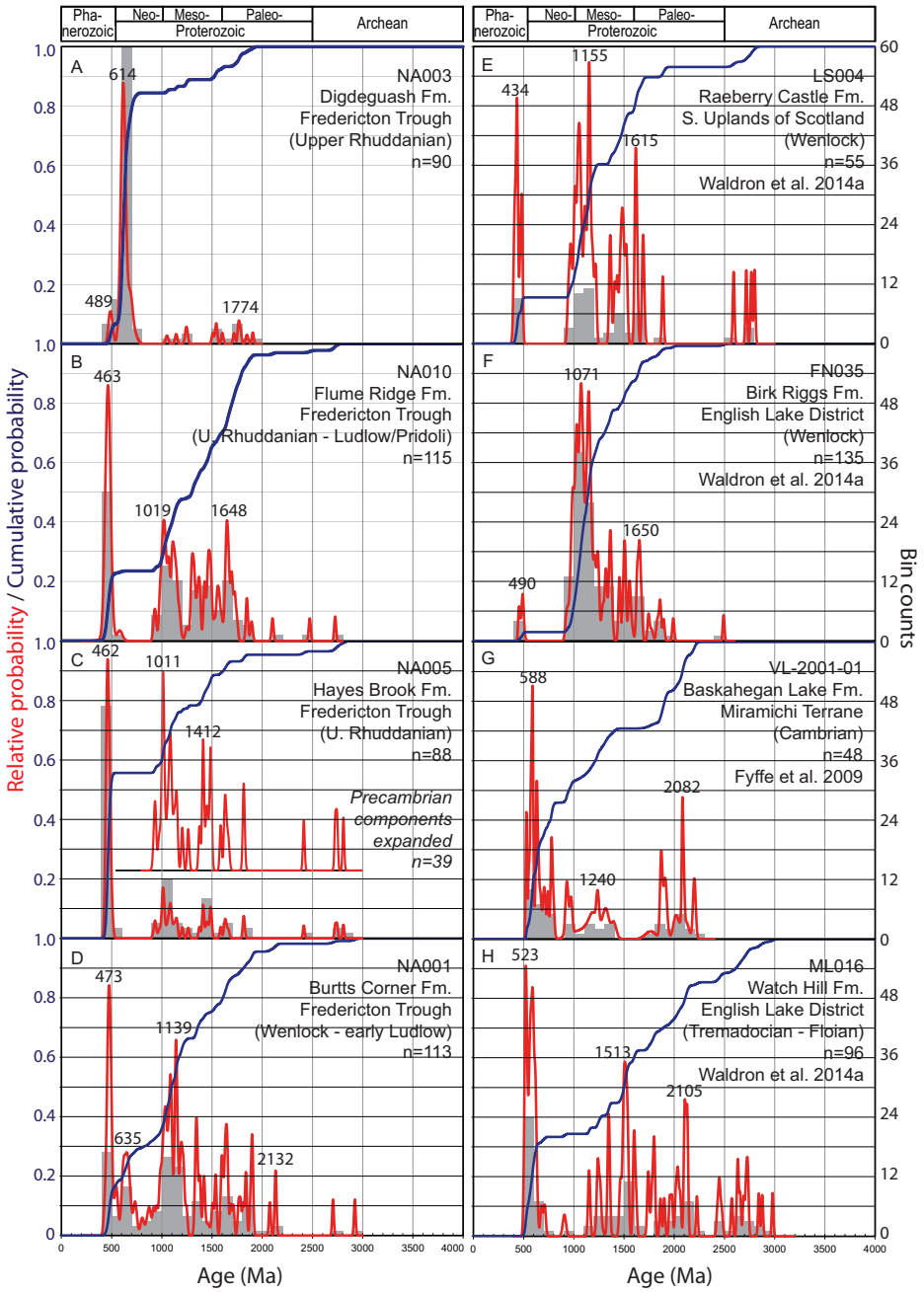

Fig. 7. Detrital zircon probability density plots (PDP), cumulative probability distributions (CPD), and histograms. Horizontal axes from 0 to 4000 Ma; histogram bin width 100 Ma. Vertical scales arbitrary (PDP), from 0.0 to 1.0 (CPD). All data <10% discordant. Analyses with $^{207}Pb/^{206}Pb$ ratios of less than 0.0658 are reported as $^{206}Pb/^{238}U$ ages; $^{207}Pb/^{206}Pb$ ages are reported otherwise. (A) Digdeguash Formation. (B) Flume Ridge Formation. (C) Hayes Brook Formation. (D) Burtts Corner Formation. Comparative data from Laurentia: (E) Raeberry Castle Formation, Southern Uplands of Scotland (Waldron and others, 2014a). (F) Birk Riggs Formation, English Lake District (Waldron and others, 2014a). Comparative data from Ganderia: (G) Baskahegan Lake Formation, Miramichi Terrane (Fyffe and others, 2009). (H) Watch Hill Formation, English Lake District (Waldron and others, 2014a).

Laurentian sources. However, the range of Mesoproterozoic and Paleoproterozoic zircons extends back to 2.2 Ga, overlapping the Eburnean range. In addition, it displays a strong Neoproterozoic (~640 Ma) peak. These observations suggest a mixture of Laurentian and peri-Gondwanan sources. A peak in the Paleozoic (480 Ma) is similar in age to the youngest Penobscot volcanics in Central Newfoundland (487 ± 3 Ma: Fyffe and others, 2011), volcanism in the Annidale terrane (from 493 ± 2 Ma: McLeod and others, 1992; Ruitenberg and others, 1993; to 481 ± 1.7 Ma: Johnson and others, 2012), and comparable volcanics from the Penobscot Formation in Maine (489.8 ± 1.2 Ma and 487.1 ± 1.2 Ma: Burke and others, 2016). This zircon peak probably indicates a contribution from Ordovician arc sources, as in the samples from the Flume Ridge and Hayes Brook Formations.

DISCUSSION

Provenance of Zircon

South of the Fredericton Fault our results show a distinct change in provenance through time. Although the early Llandovery Digdeguash Formation lacks the 2.0 to 2.2 Ga Eburnean zircons frequently present in peri-Gondwanan rocks (Pollock and others, 2007; Waldron and others, 2014a), its dominant late Neoproterozoic peak, and the scatter of Mesoproterozoic zircons without a strong concentration at 1.0 Ga, are characteristic of peri-Gondwanan provenance (Fyffe and others, 2009; Waldron and others, 2014a). In contrast, the overlying Flume Ridge Formation shows a distinctive large and asymmetric Mesoproterozoic "Grenville" peak at 1.0 Ga, with a positive tail of older zircon extending to 1.9 Ga. These features indicate that by the time of deposition of the Flume Ridge Formation, Laurentian sources had overwhelmed Gondwanan sources in this part of the Fredericton Trough. Minor peaks in the Neoproterozoic and early Proterozoic suggest only a minor contribution of the peri-Gondwanan zircon that dominates the underlying Digdeguash Formation, or that might suggest exhumation of the Miramichi terrane to the north. Given our depositional age constraints for these formations, this brackets the arrival of Laurentian detritus in the southern Fredericton Trough between the late Rhuddanian (~441 Ma: Melchin and others, 2012) deposition of the Digdeguash Formation and intrusion of the Pocomoonshine pluton at 422.7 ±3 Ma (West and others, 1992), close to the Ludlow-Pridoli boundary (Melchin and others, 2012). Furthermore, the absence of material consistent with exhumed Miramichi terrane sources (seen in the Burtt Corner Formation by mid-Wenlock), suggests that the Flume Ridge sample predates this event: It is likely that the arrival of Laurentian detritus occurred no later than mid-Wenlock.

North of the fault, in the Hayes Brook Formation (contemporaneous with the Digdeguash Formation at the resolution of graptolite biostratigraphy; see Melchin and others, 2012), we record Laurentian detritus in the upper Rhuddanian, indicated by an asymmetric "Grenville" peak and tail similar to that in the Flume Ridge Formation. The conspicuous absence of peri-Gondwanan material suggests that the Miramichi terrane had not been exhumed at this time. The younger Burtts Corner Formation, in contrast, has a mixed zircon signature of both Laurentian and peri-Gondwanan elements, bearing both an asymmetric 1.0 Ga peak and tail, in addition to Neoproterozoic (*ca.* 660 Ma) and Eburnean (2.0–2.2 Ga) zircons typical of peri-Gondwanan terranes. Both samples indicate the presence of a significant Laurentian source; the additional components in the Burtts Corner Formation probably record exhumation of the peri-Gondwanan Miramichi terrane to the north, following its Late Ordovician to Llandovery metamorphism under high P/T conditions in the Brunswick Subduction Complex (van Staal and others, 2008). Exhumation must have occurred by the Wenlock, consistent with the history proposed by van Staal and others (2008).

Large Ordovician (~465–480 Ma) peaks are characteristic of each of the three formations showing Laurentian zircon signatures, comprising 15 to 55 percent of their detrital zircon populations. The association of these young zircons with Laurentian detritus suggests that they almost certainly represent peri-Laurentian arcs associated with Iapetan subduction.

Tectonic Implications

McKerrow (1982) argued that the Iapetan suture in New Brunswick lies along the Fredericton Trough, the trough itself representing the floor of the Iapetus Ocean (McKerrow and Ziegler, 1971). However, Williams (1979) regarded the Iapetus suture as an Ordovician feature and interpreted the Fredericton Trough as a successor basin. Subsequent work (for example, van Staal and de Roo, 1995 and references therein) confirmed peri-Gondwanan material north of the trough, and identified the main Iapetan suture along the Red Indian Line (van Staal and others, 1998), largely concealed as it passes through northwest New Brunswick. The Fredericton Trough was interpreted (for example, van Staal and others, 2009) to record a part of the Tetagouche-Exploits backarc basin, which closed during Salinic orogenesis, with the Kendall Mountain Formation of the St. Croix terrane recording its south-eastern passive margin. The terminal Salinic suture, marking the final closure of this seaway, was determined to lie along the Bamford Brook – Hainesville fault in New Brunswick (Pollock and others, 2007; Reusch and van Staal, 2012), which bounds the northern margin of the Fredericton Trough against rocks of the Miramichi terrane (fig. 2). The Tetagouche-Exploits seaway, though originating as a backarc basin, evolved into a seaway of significant width (van Staal and others, 2012), showing scarce volcanic input in its later (Silurian) history (van Staal and others, 2009). Recent reconstructions (Waldron and others, 2014a, 2014b) suggest that the Iapetus Ocean formed a large system comprising a number of seas separated by arcs and microcontinents. The Fredericton Trough, regarded as a part of this larger system, records a remnant of the Iapetus Ocean in the New Brunswick Appalachians.

Contrasting detrital zircon signatures across the Fredericton Fault suggest that it marks the position of an earlier structure (for example, a suture or terrane boundary) (McKerrow and Ziegler, 1971; McKerrow, 1982) dividing two distinct slices of the Fredericton foredeep as they were accreted to a composite Laurentia (fig. 8). An alternative hypothesis, that provenance differences could be produced from variable paleoflows in a small successor basin bounded by contrasting margins, is unlikely in the case of the Fredericton Trough. Previous work (for example, Waldron and others, 2008, 2012, 2014a) shows that Laurentian detritus is abundant in Silurian deepwater basins along the Laurentian margin in the Caledonides and Newfoundland, regardless of spatial and temporal fluctuations in paleocurrent direction. Thus, it is unlikely that interleaving turbiditic fans from different sources could preserve as clear a separation of distinct sediment sources as is seen in the contemporary Hayes Brook and Digdeguash Formations; reworking of sediment, and mixing of detrital zircon signatures, would be expected. It is therefore likely that provenance differences seen in the Fredericton Trough result from tectonic closure of a wider basin.

Structural observations (Park and Whitehead, 2003) indicate that the portion of the Fredericton Trough to the north of the Fredericton Fault overrode those sediments to the south, juxtaposing the northern and southern portions of the basin. Because fabrics and structures in the Kingsclear Group are overprinted by the Pocomoonshine pluton, dated at 422.7 ± 3 Ma, this juxtaposition is interpreted to have occurred during the Silurian, well before the strike-slip motion (Ludman and West, 1999; Ludman and others, 1999) that brought the two sides of the trough into approximately their present configuration. The division of provenance across the fault, between Laurentian and Gondwanan sources, is unlikely to have resulted from

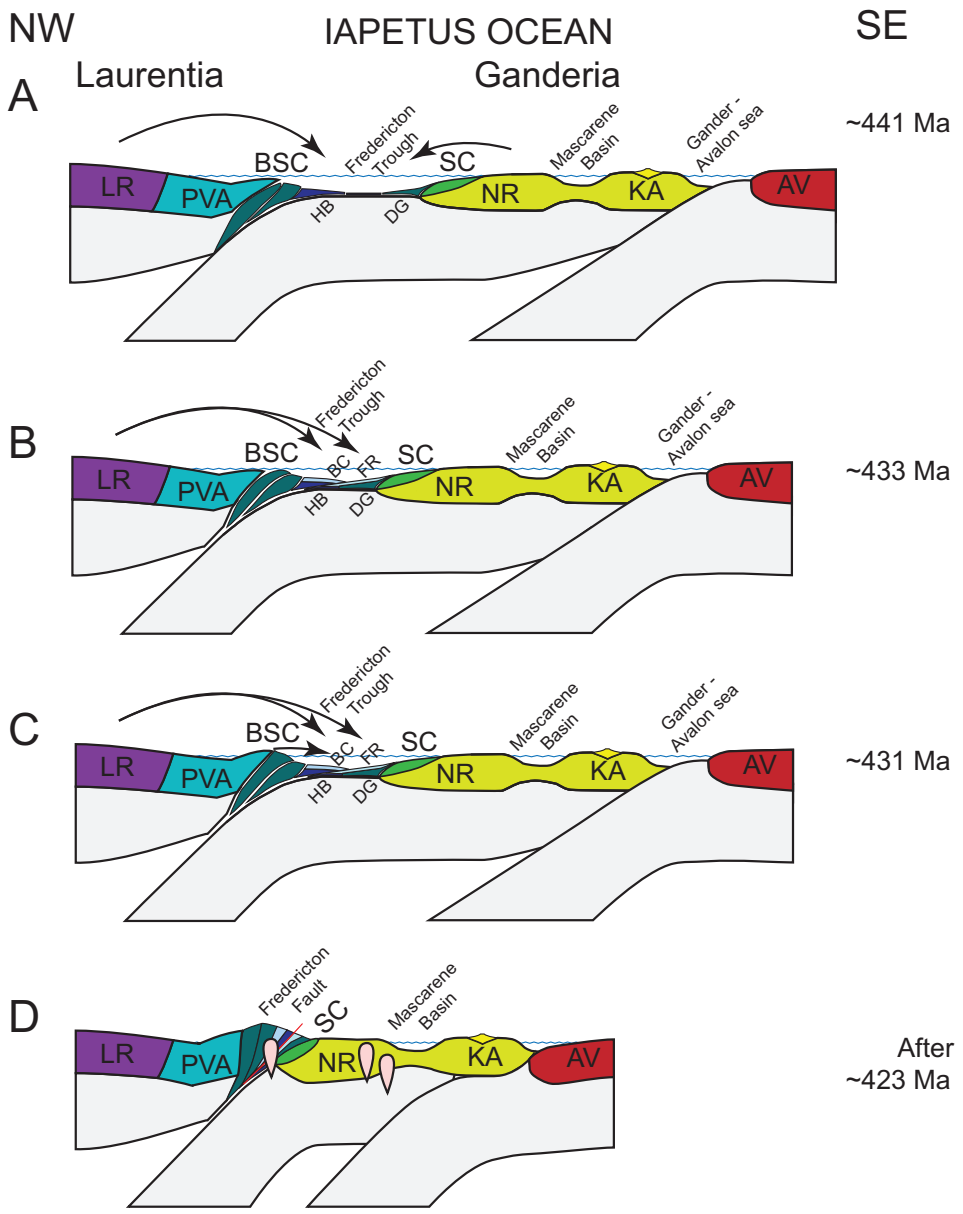

Fig. 8. Schematic evolution of the Fredericton Trough and adjacent terranes during the Silurian Period. (A) Late Llandovery; (B) Early Wenlock (before exhumation of the Brunswick subduction complex); (C) Mid-Wenlock (after exhumation of the Brunswick subduction complex); (D) Devonian, post-accretion. AV: Avalonia, BC: Burtts Corner Formation, BSC: Brunswick subduction complex, DG: Digdeguash Formation, FR: Flume Ridge Formation, HB: Hayes Brook Formation, KA: Kingston arc, LR: Laurentia, NR: New River terrane, PVA: Popelogan-Victoria arc, SC: St. Croix terrane. Arrows indicate the provenance of detritus.

purely strike-slip offset. We therefore interpret that these contrasts record a seaway of significant width — a barrier to sedimentation—during deposition of the Hayes Brook and Digdeguash Formations, which are constrained to be approximately of the same

late Rhuddanian depositional age. Contrasts in provenance between the Burtts Corner and Flume Ridge Formations may result from localization of exhumed Miramichi terrane sources along the Laurentian margin, either in time or space, or may indicate deposition of the Flume Ridge Formation sample prior to the exhumation of the Miramichi terrane, recorded in the Burtts Corner Formation sample. The seaway which divided the older Hayes Brook and Digdeguash Formations cannot have persisted after 422.7 ± 3 Ma, because by this time Laurentian detritus is clearly seen in the Flume Ridge Formation.

Several locations have been proposed for the placement of the Salinic suture in New Brunswick. A position along the Bamford Brook – Hainesville faults (fig. 2; Reusch and van Staal, 2012) is not consistent with our results, particularly the evidence of Laurentian detritus in the late Rhuddanian Hayes Brook Formation, south of this proposed suture, prior to the closure of the Tetagouche-Exploits seaway. Based on detrital zircon provenance, the Fredericton Fault itself, though a later feature, approximates the position of the terminal Salinic suture in the New Brunswick Appalachians between the late Rhuddanian and 422.7 ± 3 Ma (late Ludlow - early Pridoli; West and others, 1992).

Traced to the northeast, this boundary corresponds to the Dog Bay Line in Newfoundland (Williams and others, 1993), where detrital zircon data and other work (Pollock and others, 2007) are consistent with a Silurian closure of the last vestige of Iapetus Ocean. Farther northeast, in the British Isles, the equivalent Solway Line is commonly regarded as the Iapetan suture (Phillips and others, 1976; Leggett and others, 1983; Bluck and others, 1992), bounding the southern margin of the Southern Uplands terrane. Detrital zircon geochronology in the Caledonides (Waldron and others, 2014a) provides evidence for Ganderia-Laurentia collision in the Wenlock; however, there is no evidence for earlier Ordovician accretion of Ganderian fragments, as in the equivalent Canadian Appalachians and New England.

Relationships in Maine are summarized by Ludman and others (2017). The Fredericton Trough is typically correlated southwestwards with the Bucksport belt of coastal Maine and the Merrimack Trough of southern New England (Hibbard and others, 2006). Because of the lack of fossil control it is difficult to unambiguously match units in these belts with those in New Brunswick. Waldron and others (2018) speculatively trace the boundary represented by the Fredericton Trough into these areas. Verifying this hypothesis would require additional constraints on depositional ages and provenance.

The timing and nature of Ganderia-Avalonia juxtaposition is unclear (for example, Landing, 1996; van Staal and others, 1996, 2009), and is not further clarified by our detrital zircon data. However, work from Pothier and others (2015) in Wales has suggested that a portion of Ganderia was juxtaposed with Avalonia in the Early Ordovician Monian/Penobscot orogenic event, associated with sinistral movement along the Menai Strait Fault System. A similar scenario is possible in the New Brunswick Appalachians between southern Ganderian terranes and Avalonia, represented by the Caledonia terrane.

CONCLUSIONS

Detrital zircon U-Pb data from four formations of the Fredericton Trough contribute to resolving several longstanding controversies in Appalachian geology:

1. A remnant of the Iapetus Ocean persisted into the mid-Silurian, and is recorded by the Fredericton Trough.
2. The closure of this seaway, and terminal Salinic convergence between northern and southern Ganderian components, is constrained by the arrival of Laurentian detritus within the Flume Ridge Formation: after the late Rhuddanian depositional age of the Digdeguash Formation, before intrusion of the

Pocomoonshine pluton at 422.7 ± 3 Ma, and probably prior to the mid-Wenlock deposition of the Burtts Corner Formation.

3. The Brunswick subduction complex, incorporating the Miramichi terrane, was exhumed by the mid-Silurian and shed detritus into the adjacent Fredericton Trough. Exhumation occurred after the late Rhuddanian Hayes Brook Formation, and had occurred by the mid-Wenlock deposition of the Burtts Corner Formation at the sampled locality.
4. The terminal Salinic suture in New Brunswick may be located close to the trace of the Fredericton Fault.

Acknowledgments

Les Fyffe, Adrian Park, and Susan Johnson aided in field work and sample collection by identifying fossil localities, providing field maps, assisting with field work in-person, and otherwise sharing their knowledge of New Brunswick geology. Nathan Gerein and Richard Stern facilitated sample imaging. Allan Ludman has provided helpful insights into related geological puzzles in Maine. Cees van Staal has provided encouragement and constructive feedback. Graham Pearson read an earlier version of the manuscript and provided helpful suggestions. Reviews by Doug Reusch and Gregory Dunning were indispensable, along with assistance and review by editorial staff at the American Journal of Science. Funding was provided through a Natural Sciences and Engineering Research Council of Canada Discovery Grant to Dr. John Waldron.

References

Ashton, K. E., Heaman, L. M., Lewry, J. F., Hartlaub, R. P., and Shi, R., 1999, Age and origin of the Jan Lake Complex: A glimpse at the buried Archean craton of the Trans-Hudson Orogen: Canadian Journal of Earth Sciences, v. 36, n. 2, p. 185–208, https://doi.org/10.1139/e98-038

Barr, S. M., and White, C. E., 1996, Contrasts in late Precambrian–early Paleozoic tectonothermal history between Avalon composite terrane *sensu stricto* and other possible peri-Gondwanan terranes in southern New Brunswick and Cape Breton Island, Canada, *in* Nance, R. D., and Thompson, M. D., editors, Avalonian and related peri-Gondwanan terranes of the Circum-North Atlantic: Geological Society of America, Special Papers, v. 304, p. 95–108, https://doi.org/10.1130/0-8137-2304-3.95

Barr, S. M., Davis, D. W., Kamo, S., and White, C. E., 2003, Significance of U–Pb detrital zircon ages in quartzite from peri-Gondwanan terranes, New Brunswick and Nova Scotia, Canada: Precambrian Research, v. 126, n. 1–2, p. 123–145, https://doi.org/10.1016/S0301-9268(03)00192-X

Bluck, B. J., Gibbons, W., and Ingham, J. K., 1992, Terranes, *in* Cope, J. C. W., Ingham, J. K., and Rawson, P. F., editors, Atlas of Palaeogeography and Lithofacies: United Kingdom, Geological Society, London, Memoirs, v. 13, p. 1–4, https://doi.org/10.1144/GSL.MEM.1992.013.01.03

Bradley, D. C., and O'Sullivan, P., 2017, Detrital zircon geochronology of pre- and syncollisional strata, Acadian orogen, Maine Appalachians: Basin Research, v. 29, n. 5, p. 571–590, https://doi.org/10.1111/bre.12188

Burke, W., West, D. P., Jr., and Coish, R., 2016, Late Cambrian to Early Ordovician (Penobscot) peri-Gondwanan arc volcanism in south-central Maine: evidence from U-Pb ages and whole rock geochemistry from the St. Croix Belt: Geological Society of America, Abstracts with Programs, v. 48, n. 7, 1 p.

Cawood, P. A., and Nemchin, A. A., 2001, Paleogeographic development of the East Laurentian margin: Constraints from U-Pb dating of detrital zircons in the Newfoundland Appalachians: Geological Society of America Bulletin, v. 113, n. 9, p. 1234–1246, https://doi.org/10.1130/0016-7606(2001)113<1234:PDOTEL>2.0.CO;2

Cawood, P. A., McCausland, P. J. A., and Dunning, G. R., 2001, Opening Iapetus: Constraints from the Laurentian margin in Newfoundland: Geological Society of America Bulletin, v. 113, n. 4, p. 443–453, https://doi.org/10.1130/0016-7606(2001)113<0443:OÍCFTL>2.0.CO;2

Cawood, P. A., Nemchin, A. A., Smith, M., and Loewy, S., 2003, Source of the Dalradian Supergroup constrained by U-Pb dating of detrital zircon and implications for the East Laurentian margin: Journal of the Geological Society, London, v. 160, n. 2, p. 231–246, https://doi.org/10.1144/0016-764902-039

Cawood, P. A., Nemchin, A. A., Strachan, R. A., Kinny, P. D., and Loewy, S., 2004, Laurentian provenance and an intracratonic tectonic setting for the Moine Supergroup, Scotland, constrained by detrital zircons from the Loch Eil and Glen Urquhart successions: Journal of the Geological Society, London, v. 161, n. 5, p. 861–874, https://doi.org/10.1144/16-764903-117

Cooper, R. A., and Sadler, P. M., 2012, The Ordovician Period, *in* Gradstein, F. M., Ogg, J. G., Schmitz, M. D., and Ogg, G. M., editors, The geologic time scale 2012: Oxford, Elsevier, p. 489–523, https://doi.org/10.1016/B978-0-444-59425-9.00020-2

Cumming, L. M., 1960, Report on fossils from the Hayesville and adjacent areas, New Brunswick, submitted by Dr. W.H. Poole: Geological Survey of Canada, Report O-S-1-60/61-LMC, 2 p.

Dorais, M. J., Wintsch, R. P., Nelson, W. R., and Tubrett, M., 2009, Insights into the Acadian orogeny, New England Appalachians: A provenance study of the Carrabassett and Kittery formations, Maine: Atlantic Geology, v. 45, p. 50–71, https://doi.org/10.4138/atlgeol.2009.002

Dorais, M. J., Wintsch, R. P., Kunk, M. J., Aleinikoff, J., Burton, W., Underdown, C., and Kerwin, C. M., 2012, P-T-t conditions, Nd and Pb isotopic compositions and detrital zircon geochronology of the Massabesic Gneiss Complex, New Hampshire: Isotopic and metamorphic evidence for the identification of Gander basement, central New England: American Journal of Science, v. 312, n. 10, p. 1049–1097, https://doi.org/10.2475/10.2012.01

Dott, R. H., 1964, Wacke, graywacke and matrix—What approach to immature sandstone classification?: Journal of Sedimentary Research, v. 34, n. 3, p. 625–632, https://doi.org/10.1306/74D71109-2B21-11D7-8648000102C1865D

Dunning, G. R., O'Brien, S. J., Colman-Sadd, S. P., Blackwood, R. F., Dickson, W. L., O'Neill, P. P., and Krogh, T. E., 1990, Silurian Orogeny in the Newfoundland Appalachians: The Journal of Geology, v. 98, n. 6, p. 895–913, https://doi.org/10.1086/629460

Elhlou, S., Belousova, E., Griffin, W. L., Pearson, N. J., and O'Reilly, S. Y., 2006, Trace element and isotopic composition of GJ-red zircon standard by laser ablation: Geochimica et Cosmochimica Acta, v. 70, n. 18, supplement, p. A158, https://doi.org/10.1016/j.gca.2006.06.1383

Fyffe, L. R., 1991, Geology of the Flume Ridge-Kedron Stream map areas, Charlotte County, New Brunswick, *in* Abbott, S. A., editor, Project summaries for 1991, sixteenth annual review of activities: New Brunswick Department of Natural Resources and Energy, Mineral Resources, Information Circular 91–2, p. 12–20.

——— 1995, Fredericton Belt, *in* Williams, H., editor, Geology of the Appalachian-Caledonian Orogen in Canada and Greenland: Geological Survey of Canada, Geology of Canada, v. 6, p. 351–354.

Fyffe, L. R., and Riva, J., 1990, Revised stratigraphy of the Cookson Group of southwestern New Brunswick and adjacent Maine: Atlantic Geology, v. 26, n. 3, p. 271–275, https://doi.org/10.4138/1709

——— 2001, Regional significance of graptolites from the Digdeguash Formation of southwestern New Brunswick, *in* Carroll, B. M. W., editor, Current Research 2000: New Brunswick Department of Natural Resources and Energy, Minerals and Energy Division, Mineral Resource Report 2001-4, p. 47–54.

Fyffe, L. R., Barr, S. M., Johnson, S. C., McLeod, M. J., McNicoll, V. J., Valverde-Vaquero, P., van Staal, C. R., and White, C. E., 2009, Detrital zircon ages from Neoproterozoic and Early Paleozoic conglomerate and sandstone units of New Brunswick and coastal Maine: Implications for the tectonic evolution of Ganderia: Atlantic Geology, v. 45, p. 110–144, https://doi.org/10.4138/atlgeol.2009.006

Fyffe, L. R., Johnson, S. C., and van Staal, C. R., 2011, A review of Proterozoic to Early Paleozoic lithotectonic terranes in New Brunswick, Canada and their tectonic evolution during Penobscot, Taconic, Salinic, and Acadian orogenesis: Atlantic Geology, v. 47, p. 211–248, https://doi.org/10.4138/atlgeol.2011.010

Gehrels, G., Valencia, V., and Pullen, A., 2006, Detrital zircon geochronology by laser-ablation multicollector ICPMS at the Arizona LaserChron Center, *in* Olszewski, T. D., editor, Geochronology: Emerging Opportunities: The Paleontological Society Papers, v. 12, p. 67–76, https://doi.org/10.1017/S1089332600001352

Ghanem, H., Kunk, M. J., Ludman, A., Bish, D. L., and Wintsch, R. P., 2016, Dating slate belts using $^{40}Ar/^{39}Ar$ geochronology and zircon ages from crosscutting plutons: A case study from east-central Maine, USA: Journal of Structural Geology, v. 93, p. 51–66, https://doi.org/10.1016/j.jsg.2016.10.004

Hibbard, J. P., van Staal, C. R., Rankin, D. W., and Williams, H., 2006, Lithotectonic map of the Appalachian Orogen, Canada-United States of America: Geological Survey of Canada, Map 2096A, scale 1:1,500,000.

Hibbard, J. P., van Staal, C. R., and Rankin, D. W., 2007, A comparative analysis of pre-Silurian crustal building blocks of the northern and the southern Appalachian Orogen: American Journal of Science, v. 307, n. 1, p. 23–45, https://doi.org/10.2475/01.2007.02

Jackson, S. E., Pearson, N. J., Griffin, W. L., and Belousova, E. A., 2004, The application of laser ablation-inductively coupled plasma-mass spectrometry to *in situ* U–Pb zircon geochronology: Chemical Geology, v. 211, n. 1–2, p. 47–69, https://doi.org/10.1016/j.chemgeo.2004.06.017

Johnson, S. C., and McLeod, M. J., 1996, The New River Belt: A unique segment along the western margin of the Avalon composite terrane, southern New Brunswick, Canada, *in* Nance, R. D., and Thompson, M. D., editors, Avalonian and related peri-Gondwanan terranes of the Circum-North Atlantic: Geological Society of America, Special Papers, v. 304, p. 149–164, https://doi.org/10.1130/0-8137-2304-3.149

Johnson, S. C., McLeod, M. J., Fyffe, L. R., and Dunning, G. R., 2009, Stratigraphy, geochemistry, and geochronology of the Annidale and New River Belts, and the development of the Penobscot Arc in southern New Brunswick, *in* Martin, G. L., editor, Geological investigations in New Brunswick for 2008: New Brunswick Department of Natural Resources, Minerals, Policy, and Planning Division, Mineral Resource Report 2009-2, p. 141–218.

Johnson, S. C., Fyffe, L. R., McLeod, M. J., and Dunning, G. R., 2012, U–Pb ages, geochemistry, and tectonomagmatic history of the Cambro-Ordovician Annidale Group: A remnant of the Penobscot arc system in southern New Brunswick?: Canadian Journal of Earth Sciences, v. 49, n. 1, p. 166–188, https://doi.org/10.1139/e11-031

Kerr, A., Jenner, G. A., and Fryer, B. J., 1995, Sm–Nd isotopic geochemistry of Precambrian to Paleozoic granitoid suites and the deep-crustal structure of the southeast margin of the Newfoundland Appalachians: Canadian Journal of Earth Sciences, v. 32, n. 2, p. 224–245, https://doi.org/10.1139/e95-019

Landing, E., 1996, Avalon: Insular continent by the latest Precambrian, *in* Nance, R. D., and Thompson, M. D., editors, Avalonian and related peri-Gondwanan terranes of the Circum-North Atlantic: Geological Society of America, Special Papers, v. 304, p. 29–63, https://doi.org/10.1130/0-8137-2304-3.29

Leggett, J. K., McKerrow, W. S., and Soper, N. J., 1983, A model for the crustal evolution of southern Scotland: Tectonics, v. 2, n. 2, p. 187–210, https://doi.org/10.1029/TC002i002p00187

Li, Z. X., Bogdanova, S. V., Collins, A. S., Davidson, A., De Waele, B., Ernst, R. E., Fitzsimons, I. C. W., Fuck, R. A., Gladkochub, D. P., Jacobs, J., Karlstrom, K. E., Lu, S., Natapov, L. M., Pease, V., Pisarevsky, S. A.,

Thrane, K., and Vernikovsky, V., 2008, Assembly, configuration, and breakup history of Rodinia: A synthesis, *in* Bogdanova, S. V., Li, Z. X., Moores, E. M., and Pisaresvky, S. A., editors, Testing the Rodinia hypothesis: Records in its building blocks: Precambrian Research, v. 160, n. 1–2, p. 179–210, https://doi.org/10.1016/j.precamres.2007.04.021

Ludman, A., 1987, Pre-Silurian stratigraphy and tectonic significance of the St. Croix Belt, southeastern Maine: Canadian Journal of Earth Sciences, v. 24, n. 12, p. 2459–2469, https://doi.org/10.1139/e87-230

——— 1991, Revised stratigraphy of the Cookson Group in eastern Maine and southwestern New Brunswick: An alternative view: Atlantic Geology, v. 27, n. 1, p. 49–55, https://doi.org/10.4138/1719

Ludman, A., and West, D. P., Jr., editors, 1999, Norumbega fault system of the Northern Appalachians: Geological Society of America, Special Papers, v. 331, 202 p., https://doi.org/10.1130/SPE331

Ludman, A., Hopeck, J. T., and Brock, P. C., 1993, Nature of the Acadian Orogeny in eastern Maine, *in* Roy, D. C., and Skehan, J. W., editors, The Acadian Orogeny: Recent studies in New England, Maritime Canada, and the autochthonous foreland: Geological Society of America, Special Papers, v. 275, p. 67–84, https://doi.org/10.1130/SPE275-p67

Ludman, A., Lanzirotti, A., Lux, D., and Wang, C., 1999, Constraints on timing and displacement of multistage shearing in the Norumbega fault system, eastern Maine, *in* Ludman, A., and West, D. P., Jr., editors, Norumbega fault system of the Northern Appalachians: Geological Society of America, Special Papers, v. 331, p. 179–194, https://doi.org/10.1130/0-8137-2331-0.179

Ludman, A., Hopeck, J. T., and Berry, H. N., IV., 2017, Provenance and paleogeography of post-Middle Ordovician, pre-Devonian sedimentary basins on the Gander composite terrane, eastern and east-central Maine: Implications for Silurian tectonics in the northern Appalachians: Atlantic Geology, v. 53, p. 63–85, https://doi.org/10.4138/atlgeol.2017.003

Ludwig, K. R., 2012, User's manual for Isoplot 3.75: Berkeley, California, Berkeley Geochronology Center Special Publication, 5, 75 p.

Macdonald, F. A., Ryan-Davis, J., Coish, R. A., Crowley, J. L., and Karabinos, P., 2014, A newly identified Gondwanan terrane in the northern Appalachian mountains: Implications for the Taconic orogeny and closure of the Iapetus Ocean: Geology, v. 42, n. 6, p. 539–542, https://doi.org/10.1130/G35659.1

McKerrow, W. S., 1982, The northwest margin of the Iapetus Ocean during the early Paleozoic, *in* Watkins, J. S., and Drake, C. L., editors, Studies in continental margin geology: American Association of Petroleum Geologists, Memoirs, v. 34, p. 521–533, https://doi.org/10.1306/M34430C27

McKerrow, W. S., and Ziegler, A. M., 1971, The lower Silurian paleogeography of New Brunswick and adjacent areas: Journal of Geology, v. 79, n. 6, p. 635–646, https://doi.org/10.1086/627695

McLeod, M. J., Ruitenburg, A. A., and Krogh, T. E., 1992, Geology and U-Pb geochronology of the Annidale Group, southern New Brunswick: Lower Ordovician volcanic and sedimentary rocks formed near the southeastern margin of Iapetus Ocean: Atlantic Geology, v. 28, n. 2, p. 181–192, https://doi.org/10.4138/1860

McNamara, A. K., Niocaill, C. M., van der Pluijm, B. A., and Van der Voo, R., 2001, West African proximity of the Avalon terrane in the latest Precambrian: Geological Society of America Bulletin, v. 113, n. 9, p. 1161–1170, https://doi.org/10.1130/0016-7606(2001)113<1161:WAPOTA>2.0.CO;2

McWilliams, C. K., Walsh, G. J., and Wintsch, R. P., 2010, Silurian-Devonian age and tectonic setting of the Connecticut Valley-Gaspé trough in Vermont based on U-Pb SHRIMP analyses of detrital zircons: American Journal of Science, v. 310, n. 5, p. 325–363, https://doi.org/10.2475/05.2010.01

Melchin, M. J., Sadler, P. M., and Cramer, B. D., 2012, The Silurian Period, *in* Gradstein, F. M., Ogg, J. G., Schmitz, M. D., and Ogg, G. M., editors, The geologic time scale 2012: Oxford, Elsevier, p. 525–558, https://doi.org/10.1016/B978-0-444-59425-9.00021-4

Murphy, J. B., Nance, R. D., and Keppie, J. D., 2002, Discussion and reply: West African proximity of the Avalon terrane in the latest Precambrian: Geological Society of America Bulletin, v. 114, n. 8, p. 1049–1050, https://doi.org/10.1130/0016-7606(2002)114<1049:DARWAP>2.0.CO;2

Murphy, J. B., Fernández-Suárez, J., Keppie, J. D., and Jeffries, T. E., 2004a, Contiguous rather than discrete Paleozoic histories for the Avalon and Meguma Terranes based on detrital zircon data: Geology, v. 32, n. 7, p. 585–588, https://doi.org/10.1130/G20351.1

Murphy, J. B., Pisarevsky, S. A., Nance, R. D., and Keppie, J. D., 2004b, Neoproterozoic—early Paleozoic evolution of peri-Gondwanan terranes: implications for Laurentia-Gondwana connections, *in* Doerr, W., Finger, F., Linnemann, U., and Zulauf, G., editors, The Avalonian-Cadomian Belt and related peri-Gondwanan terranes: International Journal of Earth Sciences, v. 93, n. 5, p. 659–682, https://doi.org/10.1007/s00531-004-0412-9

Nance, R. D., Murphy, J. B., and Keppie, J. D., 2002, A Cordilleran model for the evolution of Avalonia: Tectonophysics, v. 352, n. 1–2, p. 11–31, https://doi.org/10.1016/S0040-1951(02)00187-7

O'Brien, S. J., O'Brien, B. H., Dunning, G. R., and Tucker, R. D., 1996, Late Neoproterozoic Avalonian and related peri-Gondwanan rocks of the Newfoundland Appalachians, *in* Nance, R. D., and Thompson, M. D., editors, Avalonian and related peri-Gondwanan terranes of the Circum-North Atlantic: Geological Society of America, Special Papers, v. 304, p. 9–28, https://doi.org/10.1130/0-8137-2304-3.9

Park, A. F., and Whitehead, J., 2003, Structural transect through Silurian turbidites of the Fredericton Belt southwest of Fredericton, New Brunswick: The role of the Fredericton Fault in late Iapetus convergence: Atlantic Geology, v. 39, n. 3, p. 227–237, https://doi.org/10.4138/1183

Peng, S., Babcock, L. E., and Cooper, R. A., 2012, The Cambrian Period, *in* Gradstein, F. M., Ogg, J. G., Schmitz, M. D., and Ogg, G. M., editors, The geologic time scale 2012: Oxford, Elsevier, p. 437–488, https://doi.org/10.1016/B978-0-444-59425-9.00019-6

Phillips, E. R., Evans, J. A., Stone, P., Horstwood, M. S. A., Floyd, J. D., Smith, R. A., Akhurst, M. C., and Barron, H. F., 2003, Detrital Avalonian zircons in the Laurentian Southern Uplands terrane, Scotland: Geology, v. 31, n. 7, p. 625–628, https://doi.org/10.1130/0091-7613(2003)031<0625:DAZITL>2.0.CO;2

Phillips, W. E. A., Stillman, C. J., and Murphy, T., 1976, A Caledonian plate tectonic model: Journal of the Geological Society, London, v. 132, n. 6, p. 579–609, https://doi.org/10.1144/gsjgs.132.6.0579

Pollock, J. C., Wilton, D. H. C., van Staal, C. R., and Morrissey, K. D., 2007, U-Pb detrital zircon geochronological constraints on the Early Silurian collision of Ganderia and Laurentia along the Dog Bay Line: The terminal Iapetan suture in the Newfoundland Appalachians: American Journal of Science, v. 307, n. 2, p. 399–433, https://doi.org/10.2475/02.2007.04

Pollock, J. C., Hibbard, J. P., and Sylvester, P. J., 2009, Early Ordovician rifting of Avalonia and birth of the Rheic Ocean: U-Pb detrital zircon constraints from Newfoundland: Journal of the Geological Society, London, v. 166, n. 3, p. 501–515, https://doi.org/10.1144/0016-76492008-088

Pollock, J. C., Hibbard, J. P., and van Staal, C. R., 2012, A paleogeographical review of the peri-Gondwanan realm of the Appalachian Orogen: Canadian Journal of Earth Sciences, v. 49, n. 1, p. 259–288, https://doi.org/10.1139/e11-049

Poole, W. H., 1963, Geology, Hayesville, New Brunswick: Geological Survey of Canada, Map 6-1963, scale 1:63,360.

Pothier, H. D., Waldron, J. W. F., Schofield, D. I., and DuFrane, S. A., 2015, Peri-Gondwanan terrane interactions recorded in the Cambrian–Ordovician detrital zircon geochronology of North Wales: Gondwana Research, v. 28, n. 3, p. 987–1001, https://doi.org/10.1016/j.gr.2014.08.009

Prigmore, J. K., Butler, A. J., and Woodcock, N. H., 1997, Rifting during separation of Eastern Avalonia from Gondwana: Evidence from subsidence analysis: Geology, v. 25, n. 3, p. 203–206, https://doi.org/10.1130/0091-7613(1997)025<0203:RDSOEA>2.3.CO;2

Reusch, D. N., and van Staal, C. R., 2012, The Dog Bay-Liberty Line and its significance for Silurian tectonics of the Northern Appalachian Orogen: Canadian Journal of Earth Sciences, v. 49, n. 1, p. 239–258, https://doi.org/10.1139/e11-024

Rosenblum, S., and Brownfield, I. K., 2000, Magnetic susceptibilities of minerals: United States Geological Survey, Open-File Report 99-529, 37 p.

Ruitenberg, A. A., and Ludman, A., 1978, Stratigraphy and tectonic setting of early Paleozoic sedimentary rocks of the Wirral-Big Lake area, southwestern New Brunswick and southeastern Maine: Canadian Journal of Earth Sciences, v. 15, n. 1, p. 22–32, https://doi.org/10.1139/e78-002

Ruitenberg, A. A., McLeod, M. J., and Krogh, T. E., 1993, Comparative metallogeny of Ordovician volcanic and sedimentary rocks in the Annidale-Shannon (New Brunswick) and Harborside-Blue Hill (Maine) areas: Implications of new U-Pb age dates: Exploration and Mining Geology, v. 2, n. 4, p. 355–365.

Schulz, K. J., Stewart, D. B., Tucker, R. D., Pollock, J. C., and Ayuso, R. A., 2008, The Ellsworth terrane, coastal Maine: Geochronology, geochemistry, and Nd-Pb isotopic composition—Implications for the rifting of Ganderia: Geological Society of America Bulletin, v. 120, n. 9–10, p. 1134–1158, https://doi.org/10.1130/B26336.1

Simonetti, A., Heaman, L. M., Hartlaub, R. P., Creaser, R. A., MacHattie, T. C., and Bohm, C., 2005, U-Pb zircon dating by laser ablation-MC-ICP-MS using a new multiple ion counting Faraday collector array: Journal of Analytical Atomic Spectrometry, v. 20, n. 8, p. 677–686, https://doi.org/10.1039/b504465k

Smith, E. A., 2005, Bedrock geology of southwestern New Brunswick (NTS 21 G, part of 21 B): New Brunswick Department of Natural Resources, Minerals, Policy, and Planning Division, Map NR-5 (Second Edition), scale 1:250000.

Smith, E. A., and Fyffe, L. R., 2006, Bedrock geology of central New Brunswick (NTS 21 J): New Brunswick Department of Natural Resources, Minerals, Policy, and Planning Division, Map NR-4 (Second Edition), scale 1:250000.

van Staal, C. R., 1994, Brunswick subduction complex in the Canadian Appalachians: Record of the Late Ordovician to Late Silurian collision between Laurentia and the Gander margin of Avalon: Tectonics, v. 13, n. 4, p. 946–962, https://doi.org/10.1029/93TC03604

van Staal, C. R., and de Roo, J. A., 1995, Mid-Paleozoic tectonic evolution of the Appalachian Central mobile belt in northern New Brunswick, Canada: Collision, extensional collapse and dextral transpression, *in* Hibbard, J. P., van Staal, C.R., and Cawood, P. A., editors, Current perspectives in the Appalachian-Caledonian Orogen: Geological Association of Canada, Special Paper, v. 41, p. 367–389.

van Staal, C. R., Ravenhurst, C. E., Winchester, J. A., Roddick, J. C., and Langton, J. P., 1990, Post-Taconic blueschist suture in the Northern Appalachians of northern New Brunswick, Canada: Geology, v. 18, n. 11, p. 1073–1077, https://doi.org/10.1130/0091-7613(1990)018<1073:PTBSIT>2.3.CO;2

van Staal, C. R., Sullivan, R. W., and Whalen, J. B., 1996, Provenance of tectonic history of the Gander Zone in the Caledonian/Appalachian Orogen: Implications for the origin and assembly of Avalon, *in* Nance, R. D., and Thompson, M. D., editors, Avalonian and related peri-Gondwanan terranes of the Circum–North Atlantic: Geological Society of America, Special Papers, v. 304, p. 347–367, https://doi.org/10.1130/0-8137-2304-3.347

van Staal, C. R., Dewey, J. F., Mac Niocaill, C., and McKerrow, W. S., 1998, The Cambrian-Silurian tectonic evolution of the Northern Appalachians and British Caledonides: History of a complex, west and southwest Pacific-type segment of Iapetus, *in* Blundell, D. J., and Scott, A. C., editors, Lyell: the Past is the Key to the Present: Geological Society of London, Special Publications, v. 143, p. 199–242, https://doi.org/10.1144/GSL.SP.1998.143.01.17

van Staal, C. R., Currie, K. L., Rowbotham, G., Rogers, N., and Goodfellow, W., 2008, Pressure-temperature paths and exhumation of Late Ordovician-Early Silurian blueschists and associated metamorphic nappes of the Salinic Brunswick subduction complex, Northern Appalachians: Geological Society of America Bulletin, v. 120, n. 11–12, p. 1455–1477, https://doi.org/10.1130/B26324.1

van Staal, C. R., Whalen, J. B., Valverde-Vaquero, P., Zagorevski, A., and Rogers, N., 2009, Pre-Carboniferous, episodic accretion-related, orogenesis along the Laurentian margin of the Northern Appalachians, *in* Murphy, J. B., Keppie, J. D., and Hynes, A. J., editors, Ancient orogens and modern analogues:

Geological Society of London, Special Publications, v. 327, p. 271–316, https://doi.org/10.1144/SP327.13
van Staal, C. R., Barr, S. M., and Murphy, J. B., 2012, Provenance and tectonic evolution of Ganderia: Constraints on the evolution of the Iapetus and Rheic Oceans: Geology, v. 40, n. 11, p. 987–990, https://doi.org/10.1130/G33302.1
van Staal, C. R., Wilson, R. A., Kamo, S. L., McClelland, W. C., and McNicoll, V., 2016, Evolution of the Early to Middle Ordovician Popelogan Arc in New Brunswick, Canada, and adjacent Maine, USA: Record of arc-trench migration and multiple phases of rifting: Geological Society of America Bulletin, v. 128, n. 1–2, p. 122–146, https://doi.org/10.1130/B31253.1
Waldron, J. W. F., Floyd, J. D., Simonetti, A., and Heaman, L. M., 2008, Ancient Laurentian detrital zircon in the closing Iapetus Ocean, Southern Uplands terrane, Scotland: Geology, v. 36, n. 7, p. 527–530, https://doi.org/10.1130/G24763A.1
Waldron, J. W. F., White, C. E., Barr, S. M., Simonetti, A., and Heaman, L. M., 2009, Provenance of the Meguma Terrane, Nova Scotia: Rifted margin of early Paleozoic Gondwana: Canadian Journal of Earth Sciences, v. 46, n. 1, p. 1–8, https://doi.org/10.1139/E09-004
Waldron, J. W. F., Schofield, D. I., White, C. E., and Barr, S. M., 2011, Cambrian successions of the Meguma Terrane, Nova Scotia, and Harlech Dome, north Wales: Dispersed fragments of a peri-Gondwanan basin?: Journal of the Geological Society, London, v. 168, n. 1, p. 83–98, https://doi.org/10.1144/0016-76492010-068
Waldron, J. W. F., McNicoll, V. J., and van Staal, C. R., 2012, Laurentia-derived detritus in the Badger Group of central Newfoundland: Deposition during closing of the Iapetus Ocean: Canadian Journal of Earth Sciences, v. 49, n. 1, p. 207–221, https://doi.org/10.1139/e11-030
Waldron, J. W. F., Schofield, D. I., Dufrane, S. A., Floyd, J. D., Crowley, Q. G., Simonetti, A., Dokken, R. J., and Pothier, H. D., 2014a, Ganderia–Laurentia collision in the Caledonides of Great Britain and Ireland: Journal of the Geological Society, London, v. 171, n. 4, p. 555–569, https://doi.org/10.1144/jgs2013-131
Waldron, J. W. F., Schofield, D. I., Murphy, J. B., and Thomas, C. W., 2014b, How was the Iapetus Ocean infected with subduction?: Geology, v. 42, n. 12, p. 1095–1098, https://doi.org/10.1130/G36194.1
Waldron, J. W. F., Schofield, D. I., and Murphy, J. B., 2018, Diachronous Paleozoic accretion of peri-Gondwanan terranes at the Laurentian margin, *in* Wilson, R. W., Houseman, G. A., McCaffrey, K. J. W., Doré, A. G., and Buiter, S. J. H., editors, Fifty years of the Wilson cycle concept in plate tectonics: Geological Society of London, Special Publications, v. 470, https://doi.org/10.1144/SP470.11
West, D. P., Jr., Ludman, A., and Lux, D. R., 1992, Silurian age for the Pocomoonshine Gabbro-Diorite, southeastern Maine and its regional tectonic implications: American Journal of Science, v. 292, n. 4, p. 253–273, https://doi.org/10.2475/ajs.292.4.253
White, C. E., and Barr, S. M., 1996, Geology of the Brookville Terrane, southern New Brunswick, Canada, *in* Nance, R. D., and Thompson, M. D., editors, Avalonian and related peri-Gondwanan terranes of the Circum-North Atlantic: Geological Society of America, Special Papers, v. 304, p. 133–147, https://doi.org/10.1130/0-8137-2304-3.133
White, C. E., Barr, S. M., Bevier, M. L., and Kamo, S., 1994, A revised interpretation of Cambrian and Ordovician rocks in the Bourinot Belt of central Cape Breton Island, Nova Scotia: Atlantic Geology, v. 30, n. 2, p. 123–142, https://doi.org/10.4138/2125
Williams, H., 1979, Appalachian Orogen in Canada: Canadian Journal of Earth Sciences, v. 16, n. 3, p. 792–807, https://doi.org/10.1139/e79-070
Williams, H., and Hiscott, R. N., 1987, Definition of the Iapetus rift-drift transition in western Newfoundland: Geology, v. 15, n. 11, p. 1044–1047, https://doi.org/10.1130/0091-7613(1987)15<1044:DOTLRT>2.0.CO;2
Williams, H., Currie, K. L., and Piasecki, M. A. J., 1993, The Dog Bay Line: A major Silurian tectonic boundary in Northeast Newfoundland: Canadian Journal of Earth Sciences, v. 30, n. 12, p. 2481–2494, https://doi.org/10.1139/e93-215
Wilson, R. A., 2000, Geology of the Popelogan Lake-Lost Pine Lake area (NTS 21O/15a and b), Restigouche County, New Brunswick, *in* Carroll, B. M. W., editor, Current research 1999: New Brunswick Department of Natural Resources and Energy, Minerals and Energy Division, Mineral Resource Report 2000-4, p. 91–136.
——— 2003, Geochemistry and petrogenesis of Ordovician arc-related mafic volcanic rocks in the Popelogan Inlier, northern New Brunswick: Canadian Journal of Earth Sciences, v. 40, n. 9, p. 1171–1189, https://doi.org/10.1139/e03-034
Wilson, R. A., van Staal, C. R., and McClelland, W. C., 2015, Synaccretionary sedimentary and volcanic rocks in the Ordovician Tetagouche backarc basin, New Brunswick, Canada: Evidence for a transition from foredeep to forearc basin sedimentation: American Journal of Science, v. 315, n. 10, p. 958–1001, https://doi.org/10.2475/10.2015.03
Wintsch, R. P., Aleinikoff, J. N., Walsh, G. J., Bothner, W. A., Hussey, A. M., II., and Fanning, C. M., 2007, Shrimp U-Pb evidence for a Late Silurian age of metasedimentary rocks in the Merrimack and Putnam-Nashoba terranes, eastern New England: American Journal of Science, v. 307, n. 1, p. 119–167, https://doi.org/10.2475/01.2007.05
Zalasiewicz, J. A., Williams, M., and Akhurst, M., 2003, An unlikely evolutionary lineage: The Rhuddanian (Silurian, Llandovery) graptolites *Huttagraptus? praematurus* and *Coronograptus cyphus* re-examined: Scottish Journal of Geology, v. 39, n. 1, p. 89–96, https://doi.org/10.1144/sjg39010089
Zalasiewicz, J. A., Taylor, L., Rushton, A. W. A., Loydell, D. K., Rickards, R. B., and Williams, M., 2009, Graptolites in British stratigraphy: Geological Magazine, v. 146, n. 6, p. 785–850, https://doi.org/10.1017/S0016756809990434